

Martin Næss
Fredrik Selnes Patricksson

Production Planning for Atlantic Salmon under Uncertainty with Impact of Extensive Site Management

Master's thesis in Industrial Economics and Technology
Management

Supervisor: Peter Schütz

June 2019



Production Planning for Atlantic Salmon under Uncertainty with Impact of Extensive Site Management

Martin Næss and Fredrik Selnes Patricksson

TIØ4905 - Applied Economics and Optimization, Masters Thesis
Academic supervisor: Peter Schütz
Department of Industrial Economics and Technology Management
Norwegian University of Science and Technology
June 11, 2019

Preface

This master thesis is the final step of achieving a Master of Science at Norwegian University of Science and Technology (NTNU). The specialization of the degree is Applied Economics and Optimization at the Department of Industrial Economics and Technology Management. This masters thesis is written in cooperation with AquaGen AS, Eidsfjord Sjøfarm AS and Sisomar AS.

We would like to thank our supervisor and associate professor at NTNU, Peter Schütz, for helpful contributions to our work. Furthermore, we would like to thank Ingun Næve and her colleagues in AquaGen AS for taking a genuine interest in our work and for valuable information. Also, we would like to thank Rolf-Arne Reinholdtsen in Eidsfjord Sjøfarm for valuable information and for teaching us about the industry. Our work has greatly benefited from all mentioned above.

Trondheim, June 11, 2019

Martin Næss

Fredrik Selnes Patricksson

Abstract

Norwegian salmon production has expanded and then flattened over the past few years, due to strict regulatory requirements which limit the opportunity of increased production. However, new technological advances have contributed to increased production in the past, and might further increase production in the future. The option of using monosex smolt in salmon farming, in addition to traditional mixed-gender smolt is a new opportunity for increased salmon production. In this thesis, we have developed a two-stage stochastic optimization model with the main goal of maximizing total harvested biomass. The model is inspired by the work of Hæreid (2011) and Øveraas and Rynning-Tønnesen (2012). The way of modelling growth is the same, and the modelling of extensive site management has been developed based on the current regulatory framework.

The basis for this thesis is a long-term tactical planning problem in which plans for smolt ordering, smolt deployment, and harvesting of salmon are to be made. The problem scope is limited to the seawater part of the value chain. (, and growth is considered with uncertainty). We consider growth as an uncertain parameter. Relevant constraints applying to a salmon farmer is included, although with some simplifications to ensure solvability. We implement the model in two versions, a deterministic and a two-stage stochastic version. We implement both versions for a production system based on Eidsfjord Sjøfarm.

The results from the deterministic version of the model when including the option for monosex smolt deployments indicate an annual average production level on 19 203 tonnes. This result implies a 21.3 % increase in production compared to the result of only using traditional mixed-gender smolt. The increase in production output is due to faster growth for monosex smolt, which leads to more and shorter rearing cycles, and thus an increased number of harvested salmon over the planning horizon. The results from including growth uncertainty in the model indicate 4.2 % decrease in production compared to a deterministic approach with perfect information available.

Sammendrag

Norsk lakseproduksjon har ekspandert, og deretter flatet ut de siste årene, på grunn av strenge regulatoriske krav som begrenser muligheten for økt produksjon. Nye teknologiske fremskritt har imidlertid bidratt til økt produksjon i tidligere år, og kan ytterligere bidra til å øke lakseproduksjonen i fremtiden. En ny mulighet for potensiell økt lakseproduksjon er å ta i bruk kjønnsorterte smoltpopulasjoner i tillegg til tradisjonell smoltpopulasjoner av begge kjønn. I denne oppgaven har vi utviklet en to-trinns stokastisk optimeringsmodell med et formål om å maksimere total høstet biomasse. Modellen er inspirert av arbeidet til Hæreid (2011) og Øveraas og Rynning-Tønnesen (2012). Måten vi modellerer vekst er det samme, men modelleringen av den omfattende styringen av produksjonsstedene er utviklet basert på dagens gjeldende regelverk.

Utgangspunktet for denne oppgaven er et langsiktig taktisk planleggingsproblem der det skal planlegges for smoltbestilling, smoltusett og høsting av laks. Omfanget av problemet er begrenset til sjøvanddelen av verdikjeden, og tilvekst håndteres med usikkerhet. Vi inkluderer relevante begrensninger som gjelder for en laksebonde i modellen, men med noen forenklinger for å sikre løsbarehet av modellen. Modellen blir implementert i to versjoner, en deterministisk og en to-trinns stokastisk versjon, som begge er implementert for et produksjonssystem basert på Eidsfjord Sjøfarm.

Resultatene fra den deterministiske versjonen av modellen indikerer et årlig gjennomsnittlig produksjonsnivå på 19 203 tonn når muligheten for kjønnsorterte smoltusett er inkludert. Dette innebærer 21,3 % økning i produksjon sammenlignet med resultatet ved å bare bruke tradisjonelle smoltpopulasjoner av blandet kjønn. Økningen i produksjonen skyldes raskere tilvekst for kjønnsortert smolt, som fører til flere og kortere oppdrettssykluser, og dermed en økt mengde høstet laks over planleggingshorisonten. Resultatene fra å inkludere vekstusikkerhet i modellen indikerer 4.2 % reduksjon i produksjonen sammenlignet med en deterministisk tilnærming med perfekt informasjon tilgjengelig.

Contents

1	Introduction	1
2	Introduction to Salmon Farming	3
2.1	Salmon production	3
2.1.1	Broodstock and egg hatchery	3
2.1.2	Freshwater production	4
2.1.3	Seawater production	4
2.1.4	Harvesting and Market demand	5
2.2	Regulatory constraints and production level	6
2.2.1	Licences and maximum allowable biomass	6
2.2.2	Stagnation in salmon production	9
2.3	Uncertainties in seawater production	10
2.3.1	Growth	10
2.3.2	Loss in production	14
2.3.3	Importance of uncertainty in production planning	16
2.4	Gender-specific properties	16
3	Literature Review	19
3.1	Relevant literature from other industries	19
3.2	Growth modelling	19
3.3	Optimization in salmon farming	20
3.4	Our contribution	22
4	Model Introduction	23
4.1	Problem scope	23
4.2	Model aim	24
4.3	Planning horizon	25
4.4	Representation of time and information structure	25
4.5	Conceptual model	26
4.5.1	Model objective	27
4.5.2	Decisions	27
4.5.3	Constraints	27

4.6	Assumptions and simplifications	28
4.7	Modelling choices	30
4.7.1	Initial condition	30
4.7.2	End-of-horizon condition	30
4.7.3	Scenarios	31
4.7.4	Biomass development	31
4.8	Use of model	34
5	Mathematical Model	35
5.1	Formal definitions	35
5.2	Model formulation	38
5.2.1	Objective function	38
5.2.2	Constraints	38
5.3	The Complete Model	46
5.4	Compact model formulation	48
6	Case Study	49
6.1	Production system	49
6.2	Data sets	51
6.2.1	Planning horizon and time resolution	51
6.2.2	Biomass development	51
6.2.3	Seawater temperatures	53
6.2.4	Initial biomass	54
6.2.5	Additional parameters	55
7	Computational Study	57
7.1	Model implementation	57
7.2	Base case study	57
7.2.1	Base case instance	58
7.2.2	Technical results from the base case run	59
7.2.3	Total production level	60
7.2.4	Production plan	61
7.2.5	Smolt deployments	63
7.2.6	Contributions to increased production	65
7.3	Deterministic case study	65
7.3.1	Instances	66
7.3.2	Computational results from deterministic instances	66
7.3.3	Effects of monosex growth	67
7.3.4	Effects of different harvest limits	69
7.4	Stochastic study	71
7.4.1	Scenario generation	71
7.4.2	Stochastic instances	73
7.4.3	Deterministic benchmark	74

7.4.4	Sample Average Approximation	76
7.4.5	Effects of uncertainty	80
8	Concluding Remarks	83
9	Future Research	85
A	Appendix A - Results from the SAA analysis	I
A.0.1	SAA results	I
A.0.2	Evaluation results for candidate solution	I
B	Appendix B Confidence interval in seawater temperature for each re- gion	III
B.0.1	Vesterålen	IV
B.0.2	Senja	V
B.0.3	Nord-Troms	VI
C	Appendix C Growth Tables	VII
C.0.1	Monthly growth rates for mixed-gender salmon	VII
C.0.2	Monthly growth rates for monosex salmon	IX

Todo list

List of Figures

2.1	Illustration of the value chain in Atlantic salmon aquaculture	4
2.2	Average weekly NASDAQ Salmon Index (sales prices) (week 13, 2013 - week 18, 2019)	5
2.3	Illustration of how a company is organized with sites in different regions, and how the company and each site is subject to MAB restrictions	8
2.4	Norwegian salmon production (1994 - 2018)	9
2.5	Parameters affecting stock development (Asche and Bjørndal, 2011) . . .	10
2.6	Monthly mean seawater temperatures at Eidsfjord Sjøfarm's production sites in Vesterålen, 2013 - 2019 (Eidsfjord Sjøfarm, 2019).	12
2.7	Monthly mean seawater temperatures at Eidsfjord Sjøfarm's production sites in Senja, 2013 - 2019 (Eidsfjord Sjøfarm, 2019).	12
2.8	Monthly mean seawater temperatures at Eidsfjord Sjøfarm's production sites in Nord-Troms, 2014 - 2018 (Eidsfjord Sjøfarm, 2019).	13
2.9	Number of escaped salmon and Norwegian salmon production, 2001 - 2017 (Fiskeridirektoratet, 2019b).	15
2.10	Frequency of mature and immature female salmon in different weight classes in the batch of salmon counted in Chile December 2013 (AquaGen, 2018a).	17
2.11	Frequency of mature and immature male salmon in different weight classes in the batch of salmon counted in Chile December 2013 (AquaGen, 2018a).	17
4.1	The part of the value chain included in the problem scope	23
4.2	Illustration of the relation between decision-making and when information is revealed	26
4.3	Illustration of decision-making in a two-stage stochastic optimization model, and how the decisions in our problem	31
4.4	Illustration of how fish in one fish class are split into two fractions when growing from one period to another.	33
4.5	Illustration of how several fish classes contribute with a fraction each to the number of fish in a higher fish class when growing from one period to another.	33

6.1	Map of Eidsfjord Sjøfarm's production sites in Vesterålen (blue area), Senja (red area) and Nord-Troms (purple area)	49
6.2	All time periods (upper row) and release windows (bottom row)	51
6.3	Fish classes, smolt class, and harvest classes	52
6.4	Simulated development in growth for two separate population, with start in January	55
6.5	Logged temperature data for Eidsfjord Sjøfarm	56
7.1	Seawater temperature profile used as input to the deterministic instances	58
7.2	Optimality gap and objective value for each solution during base case model run	59
7.3	Annual and total salmon production from the base case run, compared to historical data from Eidsfjord Sjøfarm over a five-year period.	60
7.4	Production plan of all smolt deployments and salmon harvesting periods at all production sites from the deterministic base case run	62
7.5	Overview of all smolt deployment quantities and harvest amounts in the planning horizon at production site 8, Sandan SØ.	63
7.6	Comparison of all smolt deployments in the base case run and in Eidsfjord Sjøfarm's historical data, sorted by magnitude.	64
7.7	Comparison of all smolt deployments. on site level, in the base case run and in Eidsfjord Sjøfarm's historical data, sorted chronological and per half year.	65
7.8	Annual and total salmon production from base case and the Instance 2. .	67
7.9	Production plan of all smolt deployments and salmon harvesting periods at all production sites from the model run of Instance 2	68
7.10	Annual salmon production for different lower bounds on harvesting weights.	69
7.11	Confidence interval of monthly mean temperature for each region, with $\alpha = 0.05$	72
7.12	Scaled-down production system	74
7.13	Production plan of all smolt deployments and salmon harvesting periods at all production sites from the model run for the down-scaled instance. .	75

List of Tables

4.1	Conceptual model	26
5.1	Definition of sets, indices, parameters and variables	36
6.1	An overview of the production sites	50
6.2	Absolute monthly growth (kg) for Atlantic salmon in different fish classes f , depending on weight and seawater temperature, developed by Skretting and adjusted by Hæreid (2011)	53
6.3	Absolute monthly growth (kg) for Atlantic salmon of monosex type in different fish classes f , depending on weight and seawater temperature, calculated on basis from logging data from a batch of male salmon reared by AquaGen.	54
6.4	Initial biomass prior to planning horizon	54
6.5	Summarizing table describing input parameters	56
7.1	Deterministic base case instance	59
7.2	Deterministic base case result	59
7.3	Deterministic instances	66
7.4	Computational results from the deterministic runs	67
7.5	Computational results from the instances with different harvesting limits	69
7.6	Computational results from the small deterministic instance	75
7.7	First-stage solutions, $\hat{\delta}^m$ for each of the SAA problem	78
7.8	Statistical lower bound and upper bound	79
7.9	Estimated optimality gap and confidence interval with $\alpha = 0.05$ and $\alpha = 0.10$	79
A.1	Objective value v_N^m with corresponding optimality gap and Run time for each solution of the SAA problems	I

1. Introduction

Over the past 50 years, the world's consumption of seafood has more than doubled, from 10 kg per capita in 1965 to more than 20 kg per capita today (Food and Agriculture Organization of the United Nations, 2018). Salmon is a popular and healthy food choice, which contains proteins, Omega-3, fatty acids, vitamins, and minerals. Aquaculture production posed a relatively insignificant portion of the total production compared to wild salmon in the very beginning; however, today, 73 % of the world's salmon production is farmed. The majority of farmed salmon is produced in Norway, Chile, Scotland and Canada (Marine Harvest, 2018). Norway has a long coastline which is rich in maritime resources, and salmon has been an important livelihood for Norwegians for a long time. The emergence of the farmed salmon industry happened in the 1970s, as an attempt to counteract a decrease in the wild salmon fishing. The focus in the first years was to establish a sustainable farming industry. It did not take many years until the large scale commercial production of farmed salmon emerged in the 1980s (Liu et al., 2010). Farmed salmon have dominated the total supply of salmon produced in Norway since 1999, and the production volume has increased further since then (Marine Harvest, 2018).

Salmon production has increased until 2013, but in recent years the production has stagnated (Fiskeridirektoratet, 2017). This is due to salmon farming being subject to strict regulations which restrict the opportunity for an increase in production. The purpose of these regulations is to ensure a sustainable industry and prevent adverse environmental consequences, especially regarding the spread of sea lice (Nærings- og fiskeridepartementet, 2018b). It is essential for salmon farmers to exploit available production capacity.

Technological advances have contributed to increasing the production of farmed salmon over the past decades, and new technology might increase the production further in the upcoming years. Over the past few years, gender-specific differences between male and female salmon have been studied, and the results indicate that gender-sorted batches of male and female salmon grow faster than traditional mixed-gender populations (Aqua-Gen, 2018b). This result opens up a new opportunity in using gender-sorted batches of smolt in salmon farming in addition to mixed-gender smolt, in order to possibly obtain larger production volumes as a result of faster growth in monosex batches.

The scope of this thesis is limited to the seawater part of the value chain. The first goal of

this thesis is to give a brief introduction to the salmon farming industry and identify the uncertainties present in the seawater part of the value chain. Thereafter, we develop a two-stage stochastic optimization model with the main objective of maximizing harvested biomass. The model considers regulatory requirements and extensive production site management and handles uncertainty in biomass development. The purpose of the model is to provide decision support to a production planner regarding optimal smolt ordering, smolt deployment, and harvesting of salmon. Another purpose is to provide a basis for analyzing biomass production. The model is implemented and applied with a selection of Eidsfjord Sjøfarm's production sites. The option of using monosex smolt in addition to traditional mixed-gender smolt is also implemented. We implement the model in two versions, one deterministic and one stochastic version. We make use of a Sample Average Approximation, to obtain stochastic results for a sufficiently large amount of scenarios.

This thesis consists of nine chapters. After the introduction follows a description of relevant industry background and sources to uncertainty in the salmon farming industry in Chapter 2, followed by a summary of related literature and previous work on the field in Chapter 3. Thereafter follows an introduction to the two-stage stochastic optimization model in Chapter 4, which includes a description of the problem scope, representation of time and information, a conceptual model and necessary assumptions and modelling choices. Then, we present the mathematical formulation of the two-stage stochastic optimization model in Chapter 5. The relevant input data used in the implementation is presented in Chapter 6, followed by an analysis of the computational results in Chapter 7. Finally, we conclude the analyzes in Chapter 8 and discuss possibilities for future work in Chapter 9.

2. Introduction to Salmon Farming

This chapter gives an introduction to the salmon farming industry. The main focus is on describing the seawater part of the value chain. The freshwater and post-harvesting phases are also presented, however more briefly and with a focus on how they affect the seawater production phase. First, Section 2.1 describes the value chain, followed by a presentation of relevant regulations in the salmon farming industry and the historical development in production level in Section 2.2. Thereafter, sources to uncertainty in salmon farming are discussed in Section 2.3, and a review of relevant research on gender-specific differences in salmon is presented in Section 2.4.

2.1 Salmon production

The salmon production cycle is divided into multiple phases, summing up to total production time in about 3 years (Marine Harvest, 2018). The biological process in salmon aquaculture can be divided into the following steps: Production of broodstock, production of fry (hatcheries), production of smolt, and production of farmed salmon (Asche and Bjørndal, 2011). Thereafter salmon is sold in the market. An overview of the value chain is shown in Figure 2.1.

2.1.1 Broodstock and egg hatchery

During the first 10 - 16 months in the value chain, salmon grow in a freshwater environment. First, eggs from broodstock are fertilized and transported to a hatchery. After an incubation period of two months, the yolk-sack larvae are hatched. For the first weeks, the fry feed on content from the yolk-sack, followed by initial feeding from the first so-called starter diets. As the fry grows to about 5 g, they reach the fingerling phase and start to develop salmon characteristics (Asche and Bjørndal, 2011). Egg suppliers supply freshwater farmers with newly hatched fry. The egg suppliers might easily scale their production to match the demand from the freshwater farmers, by obtaining more or less salmon for breeding during the preceding season, and their market is international. (Marine Harvest, 2018).

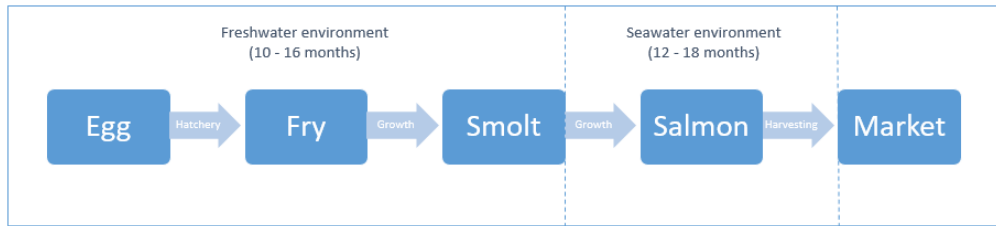


Figure 2.1: Illustration of the value chain in Atlantic salmon aquaculture

2.1.2 Freshwater production

Fry grow in freshwater tanks for about 6 - 12 months, up to reaching approximately 100 - 150 grams, until the smoltification process occurs (Marine Harvest, 2018). Smoltification is the physiological process whereby fish change their physiology, in order to adapt to a seawater environment. Hence, smolt producers transfer salmon to seawater farmers, when fry reach the smolt stage. In nature, the smoltification process occurs normally in between April and July. However, research on conditions controlling smoltification enables smolt producers to alter the timing of smoltification by making use of artificial light. Today, smolt producers thus can have smolt ready for transfer to seawater throughout the year (Laird, 2001).

2.1.3 Seawater production

Smolt is transferred to seawater production sites subsequent to the smoltification process. Combinations of seawater tolerance testing techniques and experience verify that the smoltification process is finished. For each rearing cycle, it is most common to put out all smolt at one single point of time. The seawater production sites consist of a multiple number of net pens, usually in between 6 - 14, in which salmon are placed for further growth. These are cages consisting of large nets anchored to the seabed, and several cages are grouped together in a site. Net pens might be either circular or square shaped and come in various sizes (Food and Agriculture Organization of the United Nations, 2019).

The seawater production sites are placed in locations having suitable seawater characteristics, such as water temperature, salinity, and flow rates. Distance to the nearby production sites and compliance with local farming license regulations also impact the choice of locations. In terms of seawater temperature, salmon grow best in the range 6 - 16 °C, and salinity close to oceanic levels (33 - 34 ‰) (Food and Agriculture Organization of the United Nations, 2019). The production sites must be suitable for a good living environment for salmon at the time of smolt deployment into seawater (Nærings- og fiskeridepartementet, 2018b). Thus, salmon are released during the warmer half of the year (April - September), due to warmer months having the most ideally growth conditions. Exceptionally, salmon farmers also deploy smolt in January (Eidsfjord Sjøfarm, 2018). From here on we denote these months as the "release windows" in a year.

Salmon grow in seawater for up to 2 years prior to harvesting and reach weights in between 2 - 8 kg. Usually, salmon stay in seawater for 12 - 18 months, and reach weights around 3 - 5 kg (Asche and Bjørndal, 2011). These relatively wide weight intervals are due to local variations and uncertainties regarding salmon growth, which we describe in Subsection 2.3.1.

Smolt availability is obviously a key input parameter in the seawater production phase, and the potential lack of availability might limit the production. In most years, however, the smolt production seems to be sufficiently large to comply with demand from the salmon farmers, and thus make this concern irrelevant (Asche and Bjørndal, 2011). The smolt sizes in the deployments are usually in between 60 - 150 grams (Fiskeridirektoratet, 2018).

2.1.4 Harvesting and Market demand

When salmon reach their desired weight and are ready to be harvested, they are either pumped up and transported alive to a slaughterhouse by well boats, or slaughtered on the side of the net pens (Food and Agriculture Organization of the United Nations, 2019). Transportation of salmon to a slaughterhouse is most common, where at they are slaughtered and gutted. Harvesting might be done in all months throughout a year, although harvesting during the last half of a year is most common when the growth conditions are best (Marine Harvest, 2018).

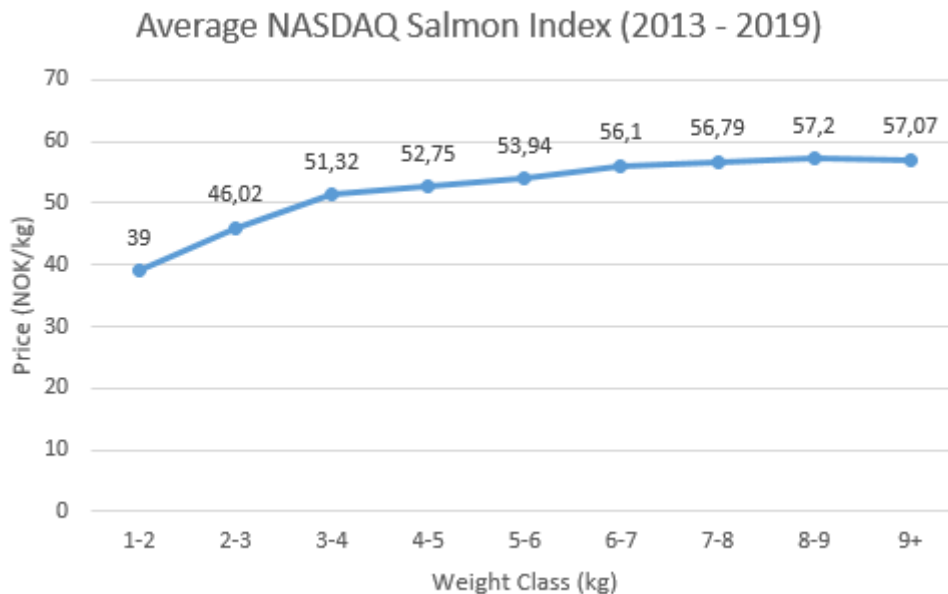


Figure 2.2: Average weekly NASDAQ Salmon Index (sales prices) (week 13, 2013 - week 18, 2019)

Subsequent to slaughtering, salmon are sold in the market. Historically, the market demand for Atlantic salmon has been, and still are, larger than the deliveries supplied by the salmon farmers. Salmon larger than 3 kilograms are those who are demanded in the market, thus harvesting of salmon smaller than 3 kilograms is not performed by the salmon farmers. There is little variation in salmon prices due to salmon weight, and the average salmon prices in terms of weight class in the period 2013 - 2019 are shown in Figure 2.2. The sales prices increase up to 3 kilograms, beyond which it flattens out. Since salmon price is almost independent of salmon weights beyond 3 kilograms, harvesting amount is the central parameter for salmon farmers in order to create the largest possible values.

2.2 Regulatory constraints and production level

Aquaculture in Norway is governed by the Ministry of Fisheries and Coastal Affairs and is primarily administrated by the Directorate of Fisheries. The Aquaculture Act gives the overall regulations, by which all salmon farmers must abide (Liu et al., 2010). The Aquaculture Act aims to promote profitability, competitiveness, and sustainability in the aquaculture industry, in addition, to promote good fish health (Nærings- og fiskeridepartementet, 2018b). The Food Safety Authority is responsible for animal health, food safety, and quality (Liu et al., 2010). In this section, we describe the most relevant regulations which affect the production level at the production sites, and we refer the reader to "Forskrift om drift av akvakulturanlegg" for a complete list of all regulations concerning the operation of aquaculture production sites.

2.2.1 Licences and maximum allowable biomass

Salmon farming is a permission-based industry. Reporting of production data from aquaculture started in 1996, as the authorities introduced feeding quotas to regulate salmon production. In 2005, the authorities changed from feeding regulation to a regulatory framework called Laksetildelingsforskriften (2005). This framework regulates biomass through licenses (Fiskeridirektoratet, 2016), and is still in use. Today, 1129 licenses exist and permit for salmon farming in Norway (Statistisk sentralbyrå, 2017). Those who are operating in the industry, or want to enter the industry, need one or more licenses to do so. Each license regulates biomass and gives an upper bound for the total salmon weight which the license owner can hold in seawater at all times, called maximum allowable biomass (MAB). A standard production license permits to hold 780 tonnes of salmon in seawater, except in the counties Troms and Finnmark where the standard is 945 tonnes (Fiskeridirektoratet, 2016).

MAB regulates the industry at two levels; production site level and company level. At company level, one specific salmon farming company disposes several farming licenses. The sum of biomass from all of those constitutes the company-specific MAB, and cannot

be exceeded. At production site level, every production site has an associated production site-specific MAB which cannot be exceeded (Nærings- og fiskeridepartementet, 2018b). An illustration of how a typical salmon farming company is organized with production sites in different regions, and how these sites and the company in total, are subject to MAB restrictions, are shown in Figure 2.3. The total production site specific MAB aggregated from all sites to a particular company usually exceeds the company-specific MAB. Thus, a salmon farming company cannot use all of its production sites at once, and all of the sites being in use cannot reach their MAB limits simultaneously, in order to comply with the company-specific MAB limit. Hence, it is important for the salmon farmer carefully to choose which production sites to use in what time periods, in order to exploit the company-specific MAB as much as possible throughout a year. However, uncertain growth conditions and seasonal variations make it hard to exploit the MAB capacity to its maximum throughout a year, which we describe in more detail in Subsection 2.3.1. The MAB regulations are hard constraints, meaning that salmon farmers cannot break them under any circumstances, although there is uncertainty present in salmon growth. It is e.g. not allowed to spread out biomass over time, such that the mean biomass fulfills the MAB constraints. Available biomass capacity in one period cannot be compensated by a surplus of biomass in a later period. Finally, there also are restrictions regarding biomass in individual net pens. The density of salmon in the net pens must not exceed 25 kg/m^3 , and the number of salmon in a net pen should regardless not exceed 200 000.



Figure 2.3: Illustration of how a company is organized with sites in different regions, and how the company and each site is subject to MAB restrictions

Salmon farmers must furthermore abide by regulations regarding fallowing. Production sites in seawater must be emptied and fallowed for at least two months subsequent to a production cycle. The Food Safety Authority can make decisions on extended fallowing periods, and coordinated fallowing of all sites in the same region, due to fish health concerns (Nærings- og fiskeridepartementet, 2018b). Furthermore, a production site cannot be fallowed for more than two years. That might lead to revocation of the permission for having production at the site.

Salmon farmers must prepare an operational plan for the upcoming two years. It must be stated in the operation plan which production sites the company plans to release smolt at, in which time period, and the number of smolts. Periods of fallowing, and which sites are not being in use, should also be stated in the operation plan. Violation of the Aquaculture Act might result in sanctions and other reactions (Nærings- og fiskeridepartementet, 2018b).

Salmon farmers must also abide by the Regulation on Combating Sea Lice in Aquaculture Facilities. The regulation requires that all production sites have a sea lice treatment plan for efficient control and combating sea lice. The plan must be coordinated with other sites in the region and must annually be submitted to The Food Safety Authority. If the

plans are not considered to be sufficient for sea lice treatment in specific areas, or sea lice zones, the Food Safety Authority might demand additional fallowing and treatment in these zones (Nærings- og fiskeridepartementet, 2018a). The regulation furthermore defines upper bounds for the occurrence of sea lice in different parts of Norway, at different times of the year. Violations of these limits can result in implementation requirement of actions to combat sea lice.

2.2.2 Stagnation in salmon production

The Aquaculture Act demands salmon farmers to make operation plans for salmon production in the upcoming two years. Many salmon farmers, however, also choose to make five-year plans, due to the long production time of salmon. Production planning can be challenging, and decision makers are in a need for decision support to make good plans. The model we develop in this thesis gives decision support to salmon farmers in their decision making regarding these five-year operation plans.

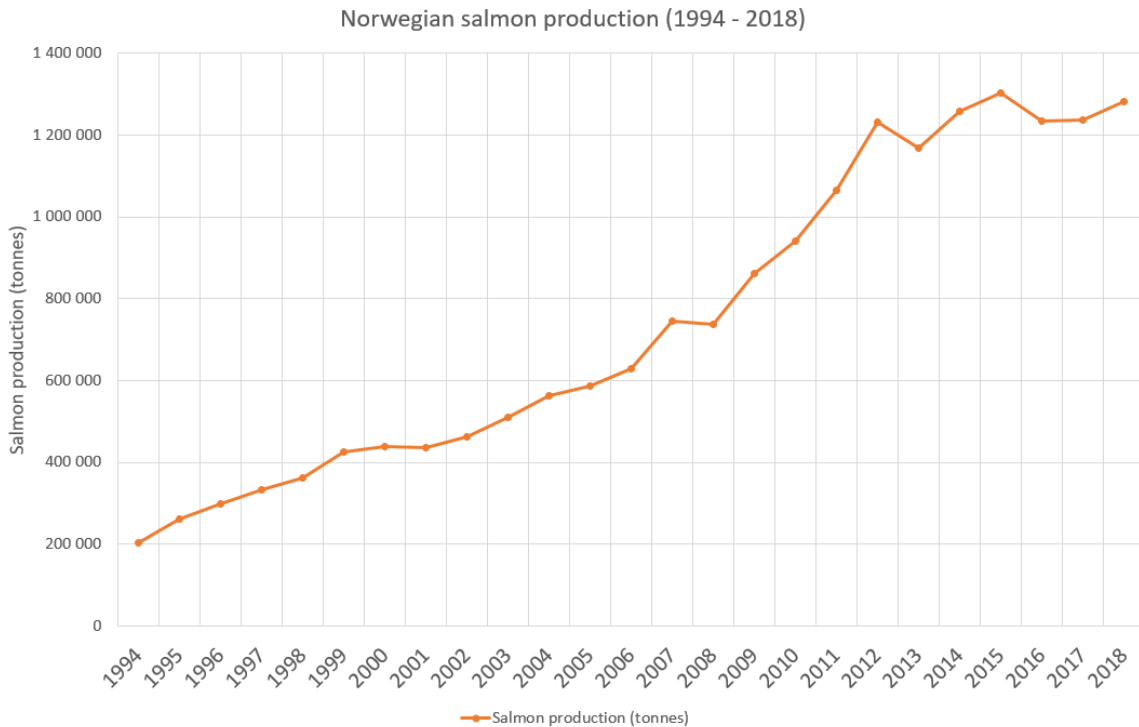


Figure 2.4: Norwegian salmon production (1994 - 2018)

The market demand for Atlantic salmon is larger than the deliveries from the salmon producers, as we pointed out in Subsection 2.1.4. The main task for a salmon farmer consequently is to produce as much salmon biomass as possible, in order to face the market demand. Salmon farmers have streamlined their production over the years, in

order to increase biomass production and exploit their farming licenses to the fullest. However, the hard restrictions concerning maximum allowable biomass, in combination with the lack of new farming licenses, limit the opportunity of further increasing biomass production. In recent years, there has been a stagnation in the total level of produced biomass, as shown in Figure 2.4. The MAB regulations only restrict the level of biomass allowed to hold in seawater, not the biomass allowed to produce. Thereby, producing as much salmon as possible in a short amount of time is important to the salmon farmers, in order to fully utilize their licenses, which we address and analyze in this thesis.

2.3 Uncertainties in seawater production

Stock development in salmon farming can be viewed as a combination of decisions regarding smolt deployment and harvesting of salmon, in combination with influencing parameters, growth, and loss in production, which is indicated in Figure 2.5. Growth and losses are both dependent on salmon age, and they are consequently important in decisions concerning the timing of the smolt deployment and harvesting. In this section, we discuss uncertainties present in seawater production, whereby growth and production losses are the two most central parameters.



Figure 2.5: Parameters affecting stock development (Asche and Bjørndal, 2011)

2.3.1 Growth

Salmon growth can be viewed both at single fish level and batch level. First, at single fish level, growth over time can be represented as a function of abiotic factors such as time, light, net pen density, water quality and seawater temperature, and biotic factors such as fish size (Aunsmo, 2014). Local variations in environment, management, nutrition, and diseases also affect growth. All of these growth factors can be either classified as controllable or non-controllable. Controllable growth factors can be held within acceptable values, according to achieve stable and optimal growth, while non-controllable factors represent an uncertainty in salmon growth. Thus, growth represents an uncertainty in seawater production. In this subsection, we discuss how different growth factors affect salmon growth, and whether they function as a driver for uncertainty in growth or not.

On the other hand, at batch level, there is uncertainty regarding the development of the weight distribution in a batch over time, which is also discussed in this subsection.

Salmon growth is mainly dependent on water quality and how it varies over time. Wild salmon have the opportunity to swim away from areas they do not prefer, while farmed salmon at any time must cope with the water flowing through the net pens. The most critical water quality parameters which affect growth are seawater temperature, oxygen concentration, pH, salinity, ammonia concentration, and carbon dioxide concentration. All these parameters, except seawater temperature, usually are within acceptable values in net pens in seawater, and hence they do not cause any growth uncertainty (Torgersen et al., 2009).

The seawater temperature must be above 0 °C, and not more than 18 - 20 °C (Marine Harvest, 2018). Higher temperatures increase the risk for disease outbreaks, and lower temperatures increase the risk for mass mortality, implying that very high or low temperatures are not preferable. Thus, the optimal temperature range is between 6 - 16 °C. Within this interval, experiments indicate that the growth rate increases from low temperatures up to a maximum at approximately 14 °C, beyond which it decreases.

The seawater temperature in a net pen is determined by the location of the production site, combined with water flow and local weather, and the annual temperature curves follow a clear seasonal pattern, which can be seen in Figures 2.6 - 2.8. The curves take the highest values in the warmer half of the year, with a temperature maximum occurring in late summer or early autumn. This is also the period of the year when there is relatively most daylight. The cold half of the year has correspondingly low temperature values, with a temperature minimum occurring in late winter or early spring (Asche and Bjørndal, 2011). The seawater temperature curves follow the same annual pattern as air temperature curves; however, they are shifted to the right. That is due to water having high heat capacity. The property of high heat capacity also means that daily variations in local weather will not make a significant impact on the seawater temperature in a short-term perspective.

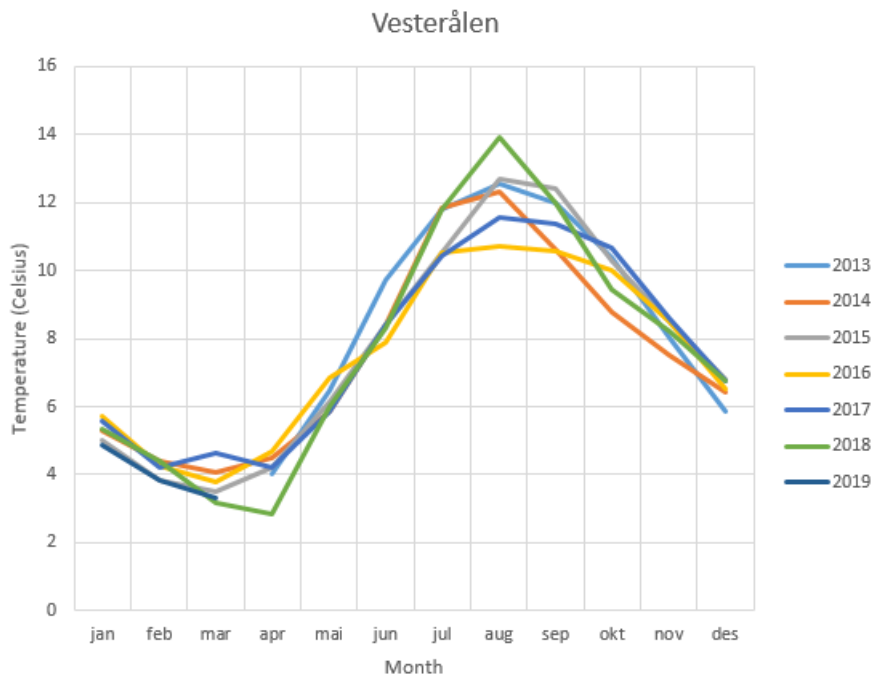


Figure 2.6: Monthly mean seawater temperatures at Eidsfjord Sjøfarm's production sites in Vesterålen, 2013 - 2019 (Eidsfjord Sjøfarm, 2019).

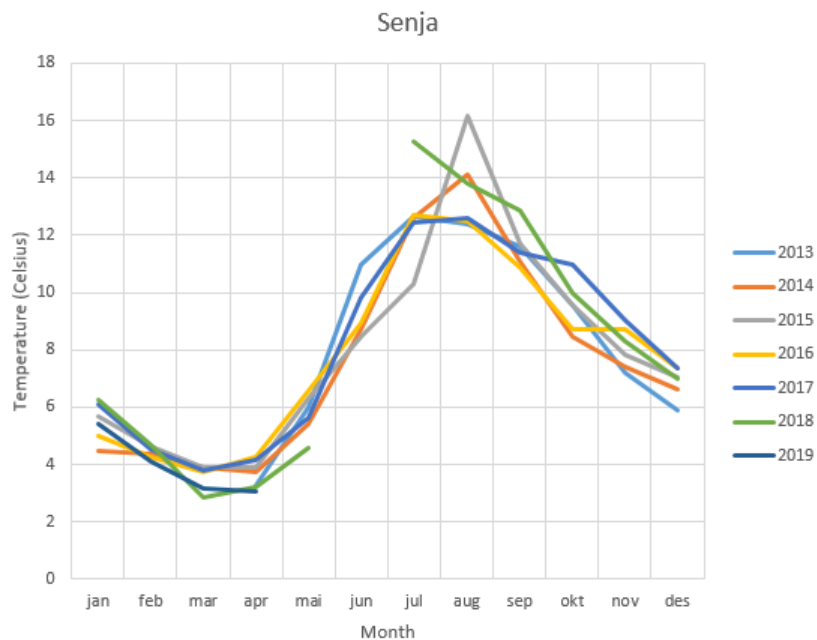


Figure 2.7: Monthly mean seawater temperatures at Eidsfjord Sjøfarm's production sites in Senja, 2013 - 2019 (Eidsfjord Sjøfarm, 2019).

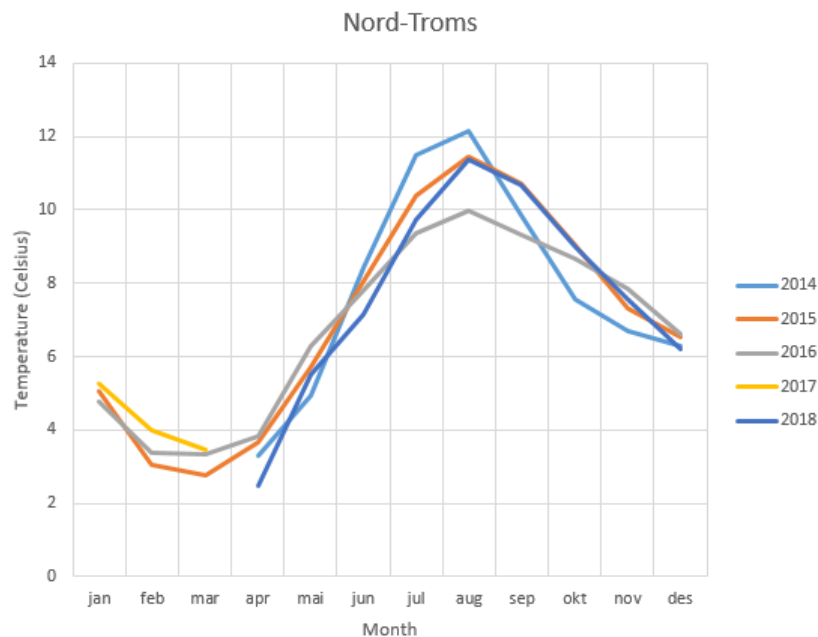


Figure 2.8: Monthly mean seawater temperatures at Eidsfjord Sjøfarm's production sites in Nord-Troms, 2014 - 2018 (Eidsfjord Sjøfarm, 2019).

Although the seawater temperature curves follow a seasonal pattern, Figures 2.6 - 2.8 show that there are variations in the monthly mean temperature from one year to another. The figures indicate that the variance is most significant in the warmest months. This will also cause seasonal differences in salmon growth because seawater temperature is a dominating characteristic of salmon growth.

In addition to water quality, salmon growth is dependent on density, light conditions, and feeding, as we pointed out initially. These factors are all to a large extent, controllable. Density values up to 80 kg/m^3 do not limit the growth or survival of Atlantic salmon, given that the water quality is provided within acceptable limits (Thorarensen and Farrell, 2010). In practical applications, however, the maximum density is limited by the upper bound of 25 kg/m^3 , which was pointed out as a regulatory limit in Subsection 2.2.1, hence salmon density will not be a restricting factor in salmon growth. Regarding light conditions, the application of artificial light might be made to stabilize or increase salmon growth. Exposure to continuous light instead of natural light results in increased growth during spring and decreased growth in late summer (Nordgarden et al., 2003). Regarding feeding, salmon are often fed with feed which is rich in fish oil and is efficiently consumed by the salmon with a feed transfer ratio (i.e. feed quantity per kilogram of growth) close to 1.26 for salmon in commercial farms (Thorarensen and Farrell, 2010). In the early days, unconsumed feed sank through the net pens and caused environmental problems, unnecessary costs and represented an uncertainty regarding salmon growth. (Asche and

Bjørndal, 2011). The feeding methods have undergone a technological development for the last decades towards automatic feeding systems with video surveillance, which report back to the control office when the salmon are fed up and stop eating. This makes it possible to stop feeding at the moment the salmon are satisfied, and it eliminates the risk for overfeeding and loss of feed (Food and Agriculture Organization of the United Nations, 2019). A number of studies show that other diets than "feeding to saturation" will increase the feed conversion ratio (Asche and Bjørndal, 2011). Hence, there is little variation in feeding patterns, and therefore, feeding does not represent an uncertain variable in growth development.

2.3.2 Loss in production

Mortality, out-throws, and escapes are the main categories causing a loss in salmon production. Regarding mortality, the production losses have increased in line with production growth over the years. The number of salmon lost due to mortality was e.g. 35.7 and 53.0 million individuals in 2008 and 2018, respectively (Fiskeridirektoratet, 2019c). Mortality can be divided into natural mortality and mortality due to disease outbreaks. Regarding natural mortality, the highest mortality rate occurs in the first two months after placing smolt into seawater, due to problems in the adaptation to the seawater environment. Subsequent stages usually will face a lower mortality rate (Marine Harvest, 2018). Elevated mortality rates in later stages will be due to exceptional circumstances like predator attack, disease outbreak, or treatment of sea lice. The annual percentage mortality rate has been approximately $15 \pm 1\%$ in the period 2014 - 2018 (Hjeltnes et al., 2019).

Disease outbreaks increase the risk of mortality in a batch of salmon, and there is a higher risk for diseases to spread among farmed fish rather than wild fish, due to high density of fish in the net pens (Asche and Bjørndal, 2011). The risk of disease outbreaks represents uncertainty in salmon farming.

For Atlantic salmon, sexual maturity occurs about 28 months after smoltification. Maturation leads to a quality degradation in salmon meat. Matured salmon are counted as waste for the salmon farmer. Thus harvesting must be done before maturation. It should be noted that the time of maturation varies greatly for salmon within the same batch or generation, and a relative proportion of all fish in the batch mature already after one year. This means that a small percentage of all harvested salmon must be out-thrown due to maturity. There are substantial differences in time for maturation due to environmental conditions such as seawater temperature and light conditions. Over the years, the industry has achieved better control over the timing of smoltification and sexual maturity, and can, to a more considerable extent delay the process, for example by making use of artificial light (Asche and Bjørndal, 2011). The ability to control the maturity process ensures that it does represent a minor uncertainty compared to growth uncertainty.

Escape of salmon is another source to loss in production, and the main reasons for

accidental escapes of salmon are winter storms, propeller damage, and wear and tear on equipment (Asche and Bjørndal, 2011). The total salmon production and the number of escaped salmon in Norway from 2001 - 2017 are shown in Figure 2.9. The figure shows that salmon production has increased and then flattened since 2012. Increased salmon production implies an increased risk regarding escapes, and it is thereby expected that accidents leading to escapees will involve a larger number of salmon than before, due to larger production sites and net pens. However, Figure 2.9 shows a decreasing trend in the number of escapees. This indicates that salmon farmers have gained better control in order to avoid escapes. There are seasonal variations in the number of escaped salmon, which is due to coincidences regarding the size of the sites and net pens being exposed to an accident. Furthermore, there is a small number of escapes that account for the main contribution to the total number of escapes salmon. In 2018, there were two cases of escapes which accounted for 90 % av all escapees (Hjeltnes et al., 2019).

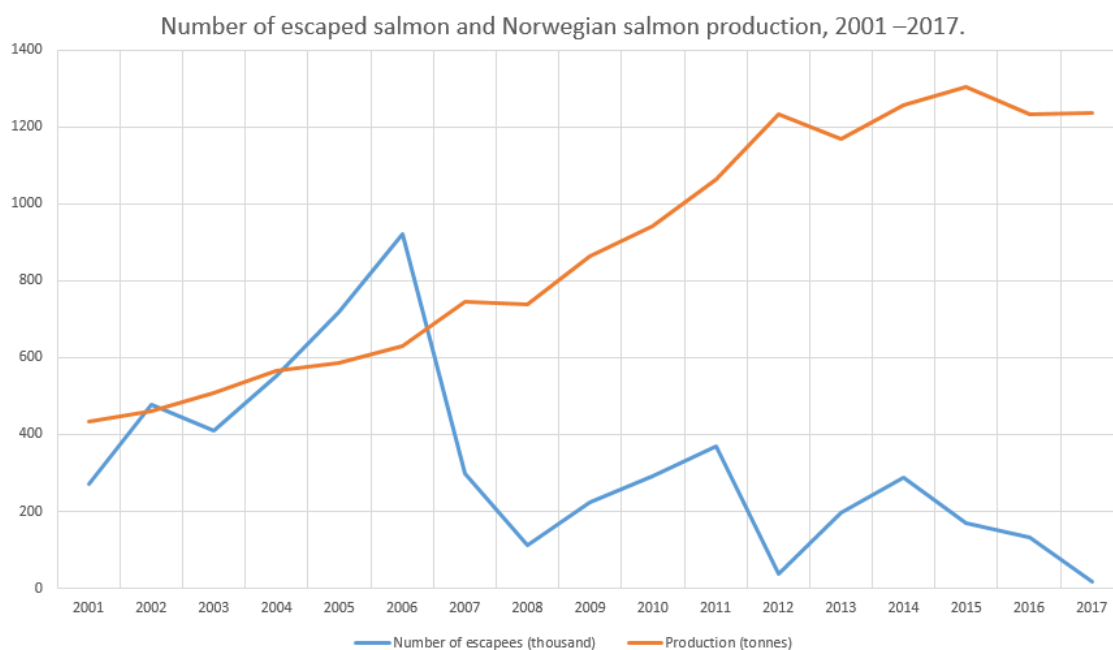


Figure 2.9: Number of escaped salmon and Norwegian salmon production, 2001 - 2017 (Fiskeridirektoratet, 2019b).

In 2017, there was reported a loss of 57.6 million individuals, and the total salmon production was 1.24 million tonnes. The mean weight of harvested salmon was 4 - 5 kilograms, and calculation with a mean weight of 4.5 kilograms gives a total production of approximately 276 million individuals, or 333 million individuals after adding the lost individuals, which implies a production loss of 17 %. The production losses were distributed on 91.0 % due to mortality, 5.7 % due to out-throw, 0.03 % due to escapes, and 6.6 % due to other reasons (Fiskeridirektoratet, 2019c). Mortality clearly contributes

most to the largest production losses, and this distribution confirms the mortality rate of 15 ± 1 %. The percentage distribution within these four loss categories is approximately the same from one year to another, and the loss rate is approximately the same from one month to another, unless a production site is exposed to a larger disease outbreak, or is forced to treat for sea lice.

2.3.3 Importance of uncertainty in production planning

We have discussed the main sources of uncertainty regarding biomass development in seawater production in this section. These uncertainties affect salmon farmers and complicate production planning. It is challenging for salmon farmers to exactly predict growth, and they must hence account for uncertainty when they make their production plans. They must assess how much smolt they can order and deploy at their production sites, knowing that growth is uncertain, and for certainty not break with the regulatory restrictions regarding maximum allowable biomass in the future. A similar assessment applies to harvesting. They must also assess the timing of smolt ordering, deployment and salmon harvesting among the different production sites, and continuously consider which production sites to use and fallow, respectively. It is essential for the farmers to deploy as much smolt as possible to fully exploit their farming licenses and at the same time, not break with the MAB constraints. Therefore, getting decision support based on the analysis of uncertain parameters is useful to them in their production planning.

2.4 Gender-specific properties

Over the past ten years, research concerning gender-specific differences on male and female salmon has been carried out. AquaGen Chile has reared a batch of salmon which, in December 2013, was counted and analyzed in terms of gender and maturity. The outcome in terms of weight distributions among female and male salmon in the batch are shown in Figure 2.10 and 2.11, respectively. As can be seen from the figures, the two genders developed significantly different weight distributions. During the rearing cycle, male fish grew to reach a mean weight on 7.4 kilograms, while female fish grew to reach a mean weight on 5.7 kilograms. These results indicate a faster growth for male compared to female salmon.

Differences in growth rates between males and females open up new opportunities regarding the separation of smolt into pure male or female batches, which might be reared at the seawater production sites, in addition to traditional mixed-gender batches. Such a sorting process might be done shortly after egg hatchery, as one then might identify the gender of the fry, and the smolt producer might then procreate and offer three types of gender composition to the seawater farmers: male, female or mixed-gender (AquaGen, 2018b). Advantages in terms of customized feeding programs with better feed exploitation can be achieved from this. Furthermore, differences in growth rates might lead to

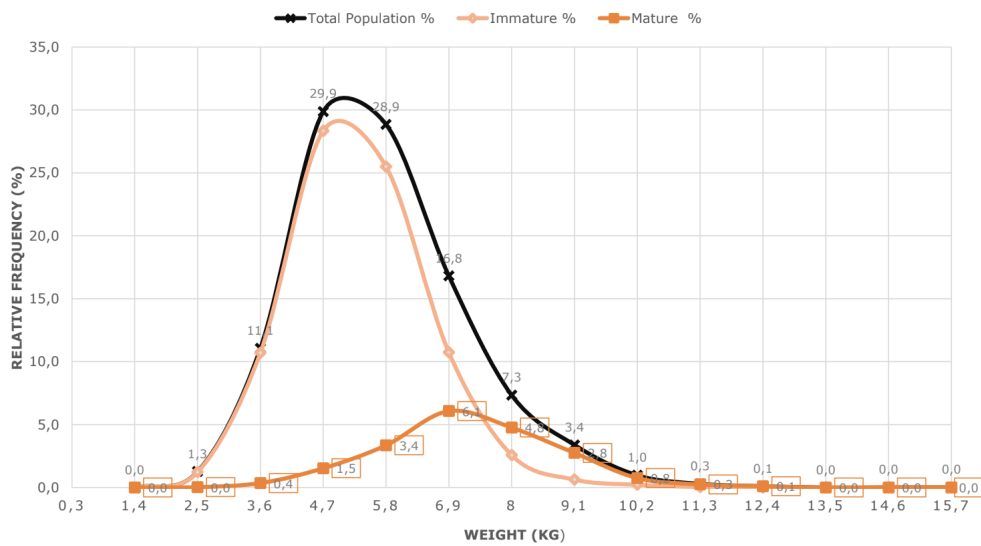


Figure 2.10: Frequency of mature and immature female salmon in different weight classes in the batch of salmon counted in Chile December 2013 (AquaGen, 2018a).

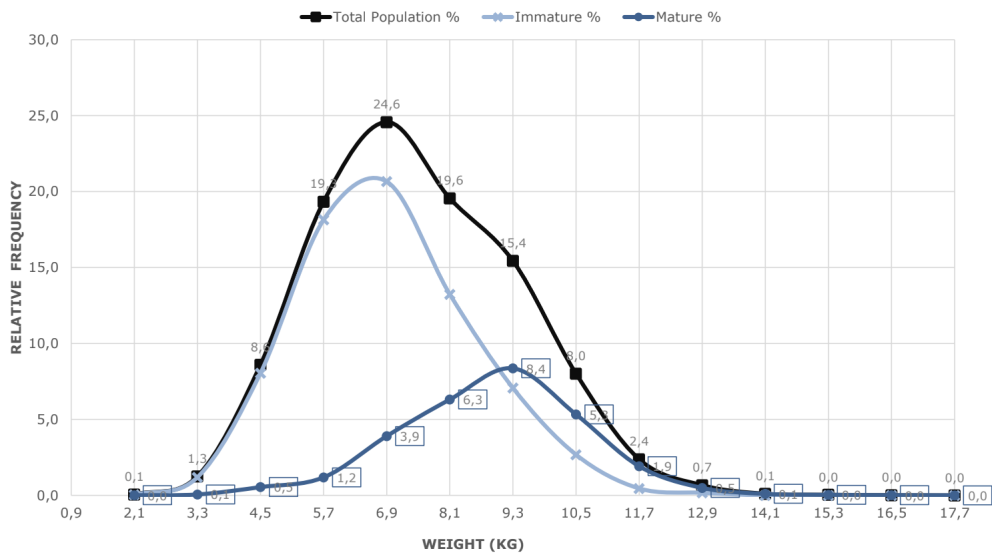


Figure 2.11: Frequency of mature and immature male salmon in different weight classes in the batch of salmon counted in Chile December 2013 (AquaGen, 2018a).

less variance in the growth distribution within a batch of salmon, and consequently less salmon being in adverse weight classes in time of harvesting, which in worst case scenario must be discarded. Different growth rates might also lead to male salmon reaching the targeted harvesting weight more rapidly than female salmon, and can hence be harvested earlier than if the batch consisted of a traditional mixed-gender population. This leads to an acceleration in commencing the fallowing period and thereby also deployment of a new generation of smolt. The effect of shortening down the production time in seawater might be quite beneficial, because the existing MAB regulations prevent the farmers from deploying a larger amount of salmon into seawater, and the only way to increase the production volume further is therefore by completing more rearing cycles within a given time window.

In January 2017, AquaGen AS sorted eggs into batches of pure male and female smolt, which both were deployed in seawater, in addition to a batch of mixed-gender smolt, and they were all exposed to the same growth conditions during the rearing cycle. Although the batch of salmon which was analyzed in Chile indicated that males grow faster than females, these pure male and female batches resulted in the same mean weight. This result suggests that there are biological factors present when rearing males and females together, which creates a gender imbalance in terms of growth, which is not present when males and females are separated. However, the growth rates of the monosex populations were slightly higher compared to the mixed-gender population, indicating that there is an opportunity for smolt producers in offering two types: monosex and mixed-gender (AquaGen, 2018b). Summarized, males grow faster than females when they are reared in the same net pen, while they grow equally fast when they are reared in separate net pens.

These gender-specific differences open up new opportunities in applying modern breeding technology to optimize and increase production in large-scale commercial aquaculture. An important attention is whether the deployment of sorted batches of pure male and female smolt, in addition to traditional mixed-gender smolt will provide gains in terms of customized feeding, and thus increased exploitation of feed and increased biomass production. In this thesis, we analyze whether monosex batches of smolt contribute to faster growth, hence an opportunity of increasing total salmon production due to reduced production time in seawater. A shortened production time in seawater means that a salmon farmer can expedite the fallowing period at a production site, and hence deployment of a new generation of smolt. Over a longer time horizon, a salmon farmer then might complete more rearing cycles than before in a shorter amount of time, which consequently gives increased biomass production.

3. Literature Review

Two complementary focuses on modelling salmon culture exist in the literature (Bravo et al., 2013). On one side, the biological approach consists of topics such as growth, mortality, environmental conditions, feeding, and diseases. On the other side, the operational approach focuses on operational concerns, such as facility location, harvesting, smolt deployment, optimal farming conditions, costs, and profitability. The merger of these two approaches has produced models for appraising different farming strategies and decision support. In this chapter, we present some relevant literature from other industries in Section 3.1, followed by literature on growth modelling of salmon in Section 3.2. Thereafter follows a presentation of optimization in salmon farming in Section 3.3, and finally we present our contribution from this thesis in Section 3.4.

3.1 Relevant literature from other industries

Salmon farming industry can adapt knowledge from other industries, to obtain further growth in production. Asche et al. (2018) state that salmon farming is one of the most efficient seafood supply chains, however, the industry still has much to learn from other food producing industries, such as the (asc). They claim that salmon farming remains semi-automated with less control over the production processes and has a more limited product specter than poultry.

3.2 Growth modelling

In the biological approach, growth modelling is a central topic in which there have been done several studies. Representation of growth through a model is also a central element in production planning in the salmon farming industry. Managing fish growth, however, is complex, and includes aspects such as identification of growth factors, future prediction of growth, and benchmarking of growth between net pens, sites, genetic strains, and companies (Aunsmo, 2014). Aunsmo et al. (2014) compared and validated four growth models that are used in salmon farming by varying the input biotic and abiotic factors. Their results indicate that no growth model is perfect in representing the real world, however some growth models are more robust, and thus better suited for predicting growth

than others. Their study also states that growth models can be improved by accounting for more non-linear effects on growth and include abiotic factors. Growth is also subject to local variations. Thyholdt (2014) developed an aggregated growth function for three different regions in Norway, motivated by the range of different environmental and biological conditions along the Norwegian coast. Although salmon growth is a function of several factors, he represents growth as a function seawater temperature as the only variable input to the model. The results indicated that an increase in sea temperature positively affects the growth in the regions of Northern and Central Norway, while an increase in sea temperatures negatively affect the growth in the Southern region.

3.3 Optimization in salmon farming

Although the salmon farming industry emerged in the 1970s, it took some time until the first literature with a bioeconomic approach was written. Lillestøl (1986) was among the first ones to do so by analyzing optimal feeding and harvesting and the relation between them (Lillestøl, 1986). Bjørndal (1988) also studied optimal harvesting, and made an optimization model in a microeconomic approach (Bjørndal, 1988). He models salmon growth as a function of age, density, and feed quantity. Arnason (1992) further developed Bjørndal's growth model by establishing mutual dependence between optimal feeding and harvesting. Arnason stated that optimal feeding is dependent on the growth model used in the growth model so that there cannot exist any general optimal feeding schedule. Bjørndal's work was also extended by Hean (1994) who studied optimal management strategy in aquaculture as a combination of releasing an optimal number of smolt, in addition to harvesting of those at the optimal harvesting time (Hean, 1994). This work is to our knowledge among the first to not just include harvesting and feeding, but also include smolt deployment as a factor in developing an optimal farming strategy. Forsberg (1999) considered two management strategies for the harvesting of size-structured batches of fish (Forsberg, 1999). The growth model he uses is a function of feed type, fish size, and seawater temperature, and salmon weights in a batch were modeled with a spread. The results demonstrated that it is more profitable to size-grade fish before harvesting, compared to harvest a batch of fish with similar size distribution to that of the standing stock. The optimization model developed by Forsberg (1999) is frequently referred to in later literature and is to our knowledge among the more advanced optimization models regarding salmon harvesting.

Many of the optimization models developed in the 90s do not take risk into account or estimate risk as a constant discount rate. Pascoe et al. (2002) analyzed optimal harvesting from an optimization model and compared the results to the real world (Pascoe et al., 2002). They stated that salmon farmers either operate in a sub-optimal manner, else the optimization model does not capture the full range of factors that need to be considered when planning for optimal harvesting, especially regarding risk and uncertainties. Uncertainty is, to a more considerable extent, included in more recent literature.

The literature presented thus far study salmon farming strategies based on analysis of a specific batch or production site. A salmon farming company, however, operates multiple production sites, and these sites are subject to regulatory control and restrictions. Furthermore, salmon farming production is structured in several consecutive phases, whereby seawater production follows after freshwater production and prior to slaughter and post-growth processing, as we described in Section 2.1. Until the last decade, there has been given little attention to production planning over multiple production sites as well as multiple parts of the value chain in the literature. Stikholmen (2010) analyzed the MAB system's impact on productivity and efficiency in Norwegian salmon farming (Stikholmen, 2010). He found a tendency of higher average productivity in the industry in the period after the MAB system was introduced compared to the period before. Langan and Toftøy (2011) also considered the MAB system, and they developed a stochastic optimization model to assist salmon farmers in tactical planning regarding smolt deployments and harvesting. The model objective is a maximization of profit, and growth and mortality are treated as uncertain parameters in the model. Their results indicate that it is beneficial to harvest salmon at lower average weights than practice in the industry. They implemented the model with the regulatory MAB restrictions. Rynning-Tønnesen and Øveraas (2012) extended and improved the work of Langan and Toftøy (2011) in order to better reflect reality. They additionally implemented the freshwater limitations that affect the production phase in seawater and thoroughly modelled the decision process of the point in time when smolt are ordered, delivered, and deployed. They found that average harvest weight should be adjusted in correlation to seasonal temperatures in order to maximize profit. They also indicate that freshwater production is not so limiting for seawater production. Hæreid et al. (2013) present a multi-stage stochastic programming formulation for a long-term production planning (Hæreid et al., 2013). The focus is on modelling growth and biomass development. The model objective is to maximize expected profits from salmon farming, with the main decisions regarding timing and the quantity of releasing smolt and selling salmon. Bravo et al. present two mixed-integer linear programming models, one for the freshwater phase and the other for the seawater phase, to obtain better coordination and well integrated and efficient production planning of the farm operators' freshwater and seawater units (Bravo et al., 2013). The model for the seawater phase seeks to maximize harvested biomass, takes the biomass demand at the production site as input, and decides timing and length of harvesting cycles. The model accounts for mortality data and the results for growth projection models, while also satisfying various economic and health constraints peculiar to salmon culture. The results indicate larger amounts of harvesting compared to reality, due to more optimal use of net pens, as well as ensuring optimal harvest weight when sent to slaughter. Denstad et al. (2015) developed a stochastic optimization model inspired by Hæreid (2011), but address more aspects of the value chain (Denstad, Lillevand, and Ulsund, 2015). The model is used for production planning and sales allocation in the salmon farming industry. The model scope includes the processing phase subsequent to farming in seawater and inventory management, in addition to global operations, and offers detailed modelling of

contract and transport decisions.

3.4 Our contribution

The work in this thesis is inspired by the work of Rynning-Tønnesen (2012) and Hæreid (2013), however, we study some other and new aspects of production planning in salmon farming which have not been studied before. To our knowledge, there has been done no more studies on optimal production planning of a production system consisting of multiple production sites which also include the correlation between them into account, than the ones presented thus far. The operational requirements for production site management regarding e.g., MAB, fallowing, and reuse of sites have been adjusted over the last couple of years, and no model is developed with current regulations. Furthermore, only the requirements that cover larger groups of production sites are included in the previous studies. No studies have been done on how the regulatory framework is applied to the dynamic between single sites. Another topic of interest, which has not been previously studied, is the possible production gains of including new production opportunities in the industry such as gender-sorted smolt.

4. Model Introduction

This chapter introduces the optimization model in this thesis. First, the problem scope and the model aim are presented in Section 4.1 and Section 4.2, respectively. Thereafter, a description of the planning horizon is given in Section 4.3, followed by the representation of time and information structure in the model in Section 4.4. Then, we present the conceptual model with corresponding decisions and constraints in Section 4.5. In Section 4.6 we make some necessary simplifications from the real world, and we present our modelling choices in Section 4.7. Lastly, we discuss the application areas for the model in Section 4.8.

4.1 Problem scope

Our problem is limited to the seawater part of the aquaculture value chain, which is illustrated in Figure 4.1, and thus includes smolt ordering, smolt deployments, growth in seawater and harvesting of salmon. We omit freshwater production and the market part of the value chain from the problem scope, by assuming that smolt supplies are unlimited and that the market demand for salmon is always larger than the production.

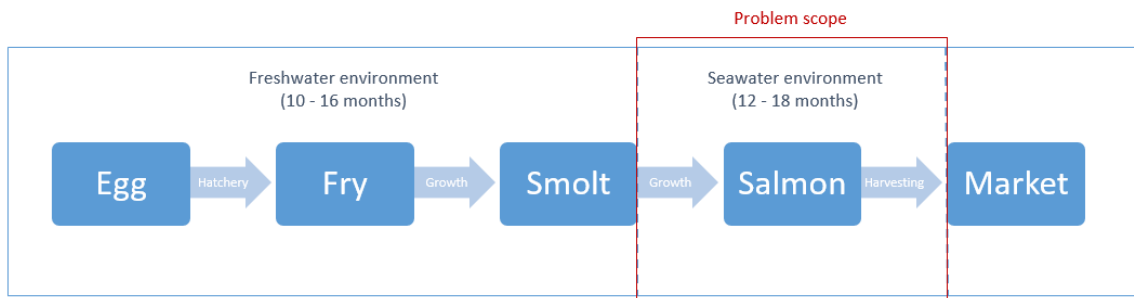


Figure 4.1: The part of the value chain included in the problem scope

Planning and controlling activities can be divided into three levels: Strategic planning, tactical planning, and operational planning (Bitran and Tirupati, 1993). The strategic level comprises the bigger picture, with large system boundaries and long planning horizons.

zon, and considers decisions such as location and sizing of new plants, acquisition of new equipment and design of logistic systems. Tactical planning is focused on the resource utilization process, with decisions regarding the allocation of capacity, accumulation of seasonal inventories, and distribution of resources. The planning horizon is of medium length. At the operational level, decisions deal with operational day to day scheduling problems. We consider our problem to be part of the tactical level. Decisions regarding smolt ordering, deployment, and harvesting of salmon concern resource allocation of fish at different production sites. These decisions are taken monthly, which is equivalent to a moderate time resolution, unlike a daily or annual time resolution. We choose the total planning horizon to be five years in our problem, which match the salmon farmer's practice of making five-year operation plans. This is a relatively long planning horizon when considered in the planning hierarchy, which is a more typical length for planning horizons at the strategic level. Due to the long production time of salmon, however, we consider five years as reasonable for the tactical level in salmon farming.

In Section 2.3 we described uncertainties present in seawater production. Growth uncertainty is a dominating uncertain parameter in salmon farming, and we discussed that temperature uncertainty causes growth uncertainty. Hence, we choose seawater temperature as the driver for growth uncertainty in our problem. Loss in production also includes uncertainty. The natural losses are relatively stable from one year to another, and these are thus considered to be constant in the problem. Unpredictable losses, due to e.g., disease outbreaks and sea lice treatment represent uncertainties in salmon farming. However, we choose to place these out of the problem scope due to our goal of analyzing biomass production, which can be done sufficiently without including these abnormalities.

4.2 Model aim

This thesis aims to analyze whether there is an untapped potential in the exploitation of the existing farming licenses in the salmon farming industry and thereby analyze the possibility of increase biomass production. We include the possibility of using gender sorted smolt, in addition to traditional mixed-gender smolt, and analyze the effects of including this option in salmon farming. Based on this aim and the problem scope, we have developed a stochastic optimization model. Stochastic optimization models can be used to provide decision support concerning production planning under uncertainty. Our model uses growth data and information about a production system as input, based on which the model optimizes a production plan, subject to regulatory requirements and restrictions regarding extensive production site management. The results provide decision support to the production planner regarding smolt ordering, smolt deployment, and salmon harvesting, and provide a basis for an analysis of biomass levels and exploitation of MAB.

4.3 Planning horizon

We have chosen the planning horizon in this problem to be five years with monthly time resolution, in order to match the length of the production plans made by salmon farmers in the industry. It is important that the planning horizon is of sufficient length to avoid sub-optimal and short-term solutions. Atlantic salmon are reared in seawater for up to two years, followed by a fallowing period which lasts 2 - 24 months, until a new generation of smolt is deployed. Thus, at least one rearing cycle at all production sites must be completed within a five-year planning horizon. A five-year planning horizon hence seems sufficiently long to avoid sub-optimal solutions.

Choosing a longer planning horizon leads to an explosion in the size of the computational problem to be solved, especially when uncertainty is included. Furthermore, production plans will be revised and re-planned for five new years at one or more points within the five-year planning horizon, as accurate information about uncertain parameters becomes available. Thus choosing a longer planning horizon will not provide any additional value, and is hence not necessary.

The model takes information about biomass levels at the production sites as input data to the very first period in the planning horizon. The inclusion of initial biomass levels in the model allows the decision makers to run the model over again with new and more accurate information about the biomass levels as input data, to revise and plan for five new years.

4.4 Representation of time and information structure

For simplicity, we omit processing times in the model. For example, the processing times for harvesting of salmon and releasing smolt are both omitted, although these processes last somewhere in between a few days up to over a month. Time is discretized in the model, and we assume that decisions are taken at the beginning of a time period. Hence, smolt deployment and harvesting are performed at the very beginning of a time period, and cannot be conducted e.g., in the middle of a time period. In the industry, salmon farmers plan for future smolt deployment and salmon harvesting on a monthly basis. Subsequently, they decide more specific which days the smolt ordering and harvesting of salmon is performed. However, we regard such decisions as part of the operational level in the production planning hierarchy, which is out of the model scope.

We define the information structure in the model, so that information about uncertain parameters is unknown to the salmon farmer prior to the first period in the planning horizon. New and accurate information about these parameters is revealed to the salmon farmer during the planning horizon. We categorize decisions into two groups, or stages,

based on the information available. In the first stage, decisions are taken with uncertain future information. In the second stage, accurate information has been revealed, and decisions are taken with this information available. In our case, growth is the only parameter which is considered to be uncertain, caused by uncertain seawater temperature. Then, accurate information about future seawater temperatures in all of the time periods in the planning horizon is revealed when entering the planning horizon, and all decisions taken within the planning horizon are done with accurate future information available. An illustration of the concept of how information is shown below.

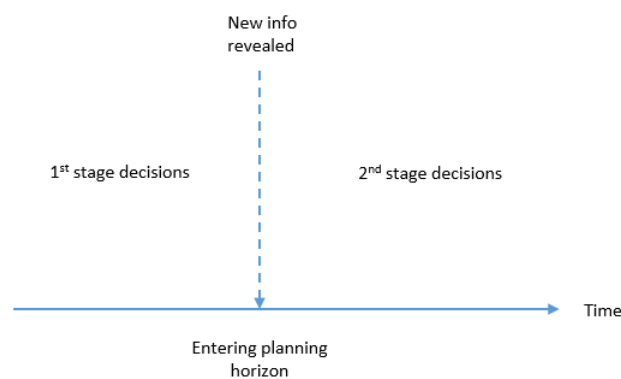


Figure 4.2: Illustration of the relation between decision-making and when information is revealed

4.5 Conceptual model

In this section, we present the conceptual model, which is shown in table 4.1. We introduce the model objective, the decisions, and the constraints which must be included due to our choice of problem scope.

Table 4.1: Conceptual model

Maximize	Harvested biomass
Subject to	Initial condition constrains
	Smolt deployment constraints
	Biomass development constraints
	Mass balance constraints
	MAB constraints
	Fallowing constraints
	Activity constraints
	Cycle duration constraints
	End-of-horizon constraints

4.5.1 Model objective

The main purpose of our problem is to maximize biomass and analyze the opportunity of increasing the biomass level produced by a salmon farmer operating in seawater. Hence, we choose the maximization of total harvested biomass as the model objective for the stochastic optimization model.

4.5.2 Decisions

There are three types of tactical decisions which must be taken within the problem scope. These decision types are smolt ordering, smolt deployment, and salmon harvesting. Regarding smolt ordering, we define that all decisions must be taken before entering the planning horizon. We define an order as all smolt which will be delivered and deployed among all production sites over a half-year period within the planning horizon. Thus, there must be decided a total of ten smolt orders, one for each half-year period in the five-year planning horizon. Furthermore, we define that each smolt order consists of a number of smolt, specified with the smolt type (weight and sorting). The previously ordered smolt must be distributed among the different production sites within the release windows in the planning horizon. We define this concern as the smolt deployment decision in the model. Regarding harvesting of salmon, the decision is defined as a number of salmon to harvest at every site, specified with the salmon type (size and sorting), and the month the harvesting is performed.

We define all smolt ordering decisions to be the first-stage decision in the model. These orders must be decided when future seawater temperatures, and thus growth is uncertain. All of the smolt orders thus must be decided prior to entering the planning horizon. Thereafter, information about seawater temperatures in every month throughout the planning horizon is revealed, and the smolt deployments and harvesting of salmon are decided in the second-stage. These decisions are thus taken with accurate information about future seawater temperatures available.

4.5.3 Constraints

Biomass constraints

Biomass development must be represented as a constraint in the model. Based on the seawater temperatures and the weight distribution in a certain time period, we calculate monthly growth rates for the period, and they are used as input to the biomass constraints. As fish grow, the weight distribution in a batch must be moved to higher weights from one month to the next. We do this by adding monthly growth to the weight distribution in one month, which causes an increase in salmon weight, and thus the weight distribution in the upcoming month is shifted towards higher weights. The mathematical method we have chosen to represent the biomass development in the optimization model

is presented in detail in Section 4.7. In the case of smolt deployment or harvesting in the period, the number of fish must be adjusted in the batch, before adding growth and calculating new weight distribution. Otherwise, the number of fish is only adjusted by constant monthly losses from one month to another.

MAB restrictions limit biomass levels. MAB restrictions function as upper limits for the biomass levels, which are specified both at site and company level. The sum of all the production site MABs is not equal to the overall company MAB. Thus the company MAB and the production site MAB alternately limit the model. The MAB limitations are hard constraints, meaning that they cannot be exceeded in any circumstances.

Regulatory constraints

There are several regulatory constraints present in aquaculture, which must be accounted for in the model. In the real world, the number of smolt in a deployment is regulated at net pen level by an upper limit, denoted net pen capacity. Net pens are placed out of the problem scope; however, the aggregated net pen capacity from all net pens at a site gives a site capacity which must be included as a boundary constraint for the number of smolt in the smolt deployment decisions. Furthermore, smolt deployments are restricted to take place in certain months a year, as described in Subsection 2.1.3.

Another regulatory requirement that must be accounted for in the model is fallowing. A production site must be completely fallowed for at least two subsequent months before a smolt deployment. Also, a production site cannot be completely fallowed for more than two years without being used.

4.6 Assumptions and simplifications

Precise modelling of the real world requires an overwhelming degree of details in order to be accurate. Complete accuracy implies more complexity and requires larger amounts of input data, compared to a simpler and equally useful model. Therefore we make some important simplifications and assumptions in the model scope, which we present in this section.

Smolt ordering and deployment

We assume that the smolt order quantity is unlimited, due to unlimited smolt supply from the smolt suppliers. Furthermore, we assume that the number of smolt in a specific order is fixed and cannot be adjusted subsequent to decision making. Thus, farmers must deploy exactly what they have ordered. We also restrict each rearing cycle to only have one time period with smolt deployment, in which all smolt in the rearing cycle must be deployed. We include a lower bound for the number of smolt in a deployment, to ensure that they are of a reasonable size. In reality, smolt comes in various weights, usually

within 60 - 150 grams. For computational simplicity in the model, however, we limit smolt types to be of specific points within this interval. We also define that all smolt in a deployment must be of the same smolt type (weight and sorting). Furthermore, we assume no lead-time in the smolt delivery process, meaning that all smolt are delivered and deployed at the beginning of the period it is planned.

Production system

The physical structures of the production system involved in the problem are a set of production sites. In the problem, we only regard each site as a large single net pen. We aggregate the capacity of each site as the sum of all the equivalent capacity yielding from all net pens independently. This approach serves our objective well enough, versus the more computational demanding alternative by assessing every single net pen separately. Each site is linked to a particular region, where a set of characteristic data is shared across the sites included in the same geographical region.

Harvesting and rearing cycles

In salmon farming, salmon must reach a certain weight before they are harvested. We define all salmon smaller than a certain weight as non-harvestable to ensure that salmon have reached a reasonable size when they are harvested. It is not allowed to harvest the non-harvestable salmon. We also include a lower bound on the number of harvested salmon each month, to avoid harvesting of very tiny portions of the batch. Harvesting of salmon can be done in all periods in a year; thus we assume that the slaughterhouses always have available slaughter capacity. Harvesting might be done by harvesting all salmon at a site at once in one single time period, or by harvesting smaller portions in multiple consecutive periods. In the case of the latter, the following period starts when the production site is empty of salmon. A rearing cycle of one generation of salmon usually lasts for 12 - 18 months. Thus, we include an upper limit on the cycle duration in the model, to avoid abnormally long rearing cycles.

Growth and uncertainties

Among the salmon characteristics, own weight, and gender composition in the batch are the two most essential factors in order to distinguish different salmon from each other in terms of growth performance. In addition to salmon characteristics, seawater temperature significantly affects growth. We also choose seawater temperature as the driver for uncertainty in salmon growth, as we pointed out in the problem scope. In total, we define growth rates, or growth performance, as dependent on salmon weight, seawater temperature and gender composition in the batch, whereby seawater temperature is an uncertain parameter. The process of defining growth rates for different salmon types is part of the pre-processing of input data to the model.

The model is implemented with production losses. The losses due to mortality, out-throws, and escapes are all functions of time, and there is a relatively stable loss rate from one month to another. Hence, these production losses are considered certain and taken as deterministic input to the biomass development in the optimization model. Losses due to the treatment of sea lice or disease outbreak represent a source of uncertainty in salmon farming. However, we choose to place these uncertainties out of the problem scope.

4.7 Modelling choices

In addition to the constraints and simplifications presented thus far, we choose to implement the model with an initial condition and an end-of-horizon condition. Our modelling choices in the implementation of these constraints are presented in this section, in addition to the way of implementing uncertainty, and the mathematical method we use to model biomass development.

4.7.1 Initial condition

We want the model to represent reality as good as possible at the beginning of the planning horizon. Thus we start the planning horizon with the production system in operation. Then some of the production sites are in use, while others are fallowed. To simulate that, we pre-generate biomass levels over several months at a random sample of the production sites, which is used as input data to the first period in the planning horizon. In the pre-generation process, we vary the number of months with biomass development at different production sites. In reality, some production sites are at the beginning and others at the end of a rearing cycle. The resulting initial biomass levels from the pre-generation process are implemented as a constraint in the optimization model.

4.7.2 End-of-horizon condition

Similar to the initial condition, we want the end-of-horizon condition to represent reality as good as possible. If not having any restriction on the end-of-horizon condition, it would be preferred to empty all of the production sites in order to maximize harvested biomass. However, in reality, a salmon farmer does not want to end his production at the end of a plan period. Therefore, we include a restriction that requires the MAB utilization to be at a certain level at the end of the last time period. In addition, to require a certain biomass level measured in kilograms, we implement a requirement concerning the number of fish. We demand that the number of fish among all production sites at the end of the last period must be equal to the number of fish, and roughly have the same weight distribution, as at the beginning of the first period. This ensures a size variation in small, medium, and large sizes, respectively. We include this additional constraint to ensure an acceptable weight distribution in the last period.

4.7.3 Scenarios

In order to model uncertainty, we develop a two-stage stochastic optimization model. In a stochastic optimization model, new information is made available by including split nodes in a scenario tree, as shown in Figure 4.3. In such a tree, information relevant to future decisions is revealed immediately after the decisions represented by a split node are made. The optimization model in this thesis is two-stage stochastic model, meaning that the decision process is divided into two stages. In the first stage, the decision maker must commit to decisions without having information about the outcome of future uncertainties. There are several possible scenarios for how the future will be, represented by the different scenario branches in the figure; however, the first-stage decision must be made without knowing which one. Subsequent to the first-stage decisions, a random event occurs and reveals new information to the decision maker. This event most likely affects the outcome of the first-stage decision. Afterward, new decisions can be taken in the second stage, in order to adjust the first-stage decisions according to new information. In our case, smolt ordering represents the first-stage decisions, while smolt deployment and salmon harvesting represent the second-stage decisions.

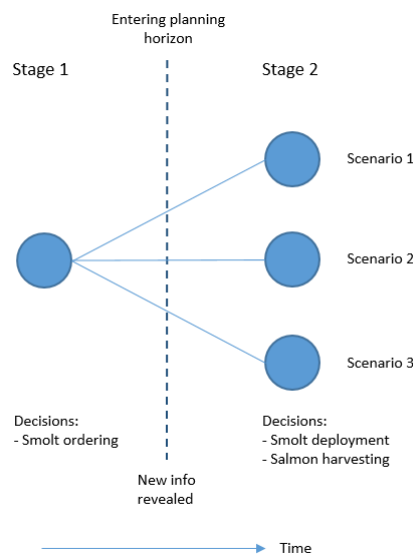


Figure 4.3: Illustration of decision-making in a two-stage stochastic optimization model, and how the decisions in our problem

4.7.4 Biomass development

We need a mathematical method of representing biomass development in our optimization model. Hæreid (2011) developed such a method, which was further developed and

corrected for an error by Denstad et al. (2015). We use this mathematical method in our model and describe the characteristics of it in this subsection.

Classification of fish

In order to simplify growth modelling, and to avoid modelling the weight of every individual fish in a batch, we discretize weight into different classes, called fish classes. Each salmon is part of a particular fish class f in the set of all fish classes \mathcal{F} , and each fish class f represents an interval. A specific weight V_f defines the interval and represents the average weight of all fish in the fish class. V_f is defined so that $V_f < V_{f+1}$. Upper and lower bounds limit the length of each fish class. These bounds are calculated by $\frac{V_f+V_{f+1}}{2}$ and $\frac{V_f+V_{f-1}}{2}$, respectively. All fish falling within these two bounds belong to fish class f .

Growth modelling in seawater

In short, we model growth by moving fish to new and higher fish classes from one period to another. Hence, we define an input growth rate parameter which describes the growth in kilograms of a fish in a given fish class and time period. We use different values depending on the batch of salmon being of mixed-gender or monosex type. This parameter is also dependent upon location, due to local variations regarding seawater temperatures. We define this parameter as stochastic, meaning that it is defined for each branch in the scenario tree. Summarized, we denote the growth rate as σ_{fgit}^s , for a fish class f , sorting type g , production site i , time period t and scenario s . For the same sets, we also define a survival rate of fish, which describes the survival in kilograms after adjusting for losses in the time period, denoted as φ_{fgit}^s .

We must define a stock-keeping variable to keep track of the growth from one period to another. Hence, we denote n_{fgit}^s as the number of fish in fish class f , of sorting type g , at production site i , in time period t , in scenario s . At the beginning of each time period, the number of fish from the previous time period is updated with growth and losses from the previous time period. In the case of smolt release or salmon harvesting, the number of fish being released or harvested in the period is thereafter added or subtracted. The resulting sum gives the number of fish at the beginning of a time period.

We must connect growth rates to the fish classes. The method we use to update the distribution of fish among fish classes with growth takes initial weights in period $t - 1$, given by the average for each interval V_f , and adds the growth during period $t - 1$, provided by σ_{fgit}^s . The new salmon weights in period t consequently fall between the average weights of two predefined fish classes, as represented below. Thus, we must perform further calculations to place salmon correctly into new fish classes.

$$V_{\underline{f}} \leq (V_f + \sigma_{fgit}^s) \leq V_{\bar{f}}.$$

If new salmon weights in period t , after adding growth in period $t - 1$, fall in between two fish classes \underline{f} and \bar{f} , we handle it by splitting the fish into two fractions which are distributed into \underline{f} and \bar{f} , respectively. The equations we use to calculate these fractions for salmon starting in fish class f and time period t are given below. We also illustrate the concept in Figure 4.4. The first illustration shows how fish are split into two fractions when growing from one period to another, while the second illustration shows how several fractions from fish in lower fish classes sum up to the number of fish in a higher fish class from one period to another.

$$\gamma_{\underline{f}fgit}^s = \frac{V_{\bar{f}} - (V_f + \sigma_{fgit}^s)}{V_{\bar{f}} - V_{\underline{f}}}$$

$$\gamma_{\bar{f}fgit}^s = \frac{(V_f + \sigma_{fgit}^s) - V_{\underline{f}}}{V_{\bar{f}} - V_{\underline{f}}}$$

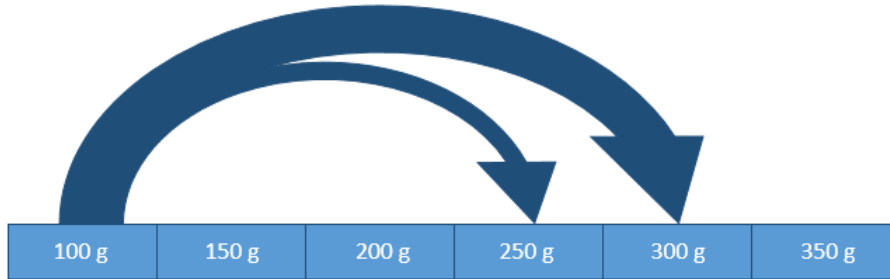


Figure 4.4: Illustration of how fish in one fish class are split into two fractions when growing from one period to another.

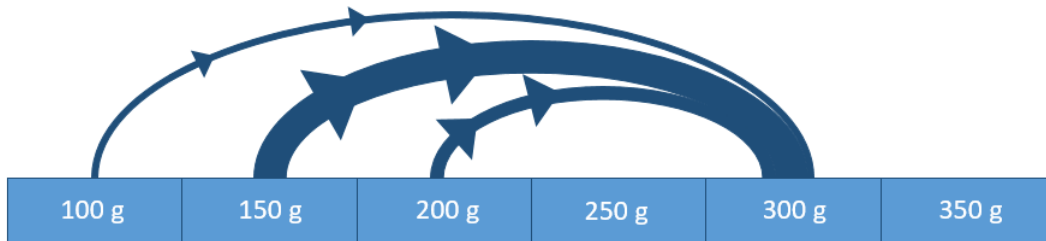


Figure 4.5: Illustration of how several fish classes contribute with a fraction each to the number of fish in a higher fish class when growing from one period to another.

The fish class intervals must be small enough, and the time intervals must be large enough to ensure that fish move to higher classes from one time period to the next. If growth in

one time period is such that $\underline{f} = f$, where f is the original fish class, and \underline{f} is the fish class to which the lower fraction is placed, some of the salmon will remain in the original fish class. If this is repeated in every time period, some salmon will never grow out of their original fish class, which is unacceptable behavior. Therefore, the width of each fish class must be small enough so that all fish of fish class f will grow out of their original fish class during one time period. Alternatively, time periods must be long enough, for the same reason. More extended time periods imply more growth and hence require a less detailed partitioning of fish classes than shorter time periods.

4.8 Use of model

The main area of application for the model is to give decision support to a production planner, which plans for salmon production in seawater. The output results from the model indicate which production sites to use in different time periods, and thus decision support regarding smolt ordering, smolt deployment, and salmon harvesting. The model can be run over again multiple times during a planning period so that the decision maker can update the initial conditions with correct information about biomass levels as time passes by. We have developed the model with a relatively moderate size salmon farming company in mind, only operating in the seawater part of the value chain. Both larger and more integrated companies, as well as smaller companies, can also benefit from the model because the model is supposed to function on different types of companies and give decision support in production planning under extensive production site management.

In addition, to give decision support, the model can be used as a starting point for different analyzes of biomass development, MAB utilization, and distribution of biomass levels among different production sites. The available smolt might be of just the traditional mixed-gender type, or additionally, contain the option of using monosex type. Choosing different input data for different model runs gives a starting point for performing analyzes on how different smolt types cause differences in biomass development, and thereby analyze the potential for increased production as a result of using different smolt types. Similarly, one can study how different smolt causes differences in the length and quantity of rearing cycles over a planning period.

5. Mathematical Model

In this chapter, we present the linear stochastic two-stage optimization model. Firstly, we present the formal definitions of sets, indices, constants, stochastic parameters and decision variables in Section 5.1. Thereafter, the model is presented with objective function and constraints in Section 5.2. An overview of the complete model is given in Section 5.3, and lastly a compact formulation of the model is presented in Section 5.4.

5.1 Formal definitions

In this section, we define the sets, indices, constants, stochastic parameters and decision variables we use in the model formulation. We formulate sets in capital calligraphic letters and corresponding indices in small, italic letters. Deterministic data is denoted in capital letters, both Greek and Latin, while stochastic data is denoted in small Greek letters. For the continuous decision variables we use small letters, while the binary decision variables is denoted by small Greek letters.

Table 5.1: Definition of sets, indices, parameters and variables

Sets	
\mathcal{F}	Set of all fish classes
\mathcal{G}	Set of all sorting types (gender composition)
\mathcal{F}^S	Set of all fish classes available for smolt release, $\mathcal{F}^S \subset \mathcal{F}$
\mathcal{F}^H	Set of all harvestable fish classes, $\mathcal{F}^H \subset \mathcal{F}$
\mathcal{F}_a	Set of all fish classes in end-of-horizon group a , $\mathcal{F}_a \subset \mathcal{F}$
\mathcal{I}	Set of all production sites
\mathcal{R}	Set of all regions
\mathcal{I}_r	Set of all sites in region r , $\mathcal{I}_r \subset \mathcal{I}$
\mathcal{S}	Set of all scenarios
\mathcal{Y}	Set of all years
\mathcal{T}	Set of all time periods
\mathcal{Z}	Set of all half years
\mathcal{T}^S	Set of all release windows $\mathcal{T}^S \subset \mathcal{T}$
\mathcal{T}_y^S	Set of all release windows in year $y \in \mathcal{Y}$, $\mathcal{T}_y^S \subset \mathcal{T}^S \subset \mathcal{T}$
\mathcal{T}_z^S	Set of all release windows in half year $z \in \mathcal{Z}$, $\mathcal{T}_z^S \subset \mathcal{T}^S \subset \mathcal{T}$
\mathcal{A}	Set of all end-of-horizon groups
Indices	
f, \hat{f}	Index of fish class f
g	Index of sorting type g
i	Index for site i
r	Index for region r
s, s'	Index for scenario s
t, τ	Index for time period t
y	Index for year y
z	Index for half year z
a	Index for end-of-horizon group a

Deterministic Data	
I_{fgi}^{BIO}	Initial number of fish of sorting type g , in fish class f , at site i
V_f	Weight of a fish in fish class f (kilograms)
MAB_i	Production site MAB in tonnes capacity at site i
MAB^{COMP}	Company MAB in tonnes capacity
K^{EOH}	Percentage of company MAB utilized at end-of-horizon
Λ	Minimum number of months with complete fallowing of a site
Γ	Maximum number of consecutive months with no activity at a site
Δ	Maximum number of months in a rearing cycle
Ψ_{fgit}	Survival rate of fish in fish class f of sorting type g , at site i , at time t
L_i^{DEP}	Lower bound for number of smolt in a deployment at site i (number of fish)
U_i^{DEP}	Upper bound for number of smolt in a deployment at site i (number of fish)
L^{HARV}	Lower bound for harvesting quantity (number of fish)
U^{HARV}	Upper bound for harvesting quantity (number of fish)
Stochastic Data	
π^s	Probability of scenario s
$\gamma_{\hat{f}fgrt}^s$	The share of fish of fish class \hat{f} and sorting type g which has grown to become part of fish class f due to growth in time period t , in region r , in scenario s
σ_{fgrt}^s	The growth in kilograms for fish in fish class f of sorting type g , in region r , in scenario s , in time period t
Decision Variables	
n_{fgit}^s	Number of fish in fish class f , sorting type g , at site i , in scenario s , in time period t
o_{fgz}	Number of fish ordered of fish class f , sorting type g in half year z , only defined for $f \in \mathcal{F}^S$
y_{fgit}^s	Number of fish released of fish class f , sorting type g , from site i , in scenario s , at time t , only defined for $f \in \mathcal{F}^S$ and $t \in \mathcal{T}^S$
w_{fgit}^s	Number of harvested fish in fish class f , sorting type g , at site i , in scenario s , at time t . Only defined for $f \in \mathcal{F}^H$
δ_{fgit}^s	Binary variable, 1 if a batch of smolt of fish class f , sorting type g is released at site i , for scenario s , in year y , at time t , 0 otherwise, only defined for $f \in \mathcal{F}^S$ and $t \in \mathcal{T}^S$
θ_{it}^s	Binary variable, 1 if site i , in scenario s at time t is allowed for smolt release, 0 otherwise, $t \in \mathcal{T}^S$
ω_{it}^s	Binary variable, 1 if site i , in scenario s at time t is in a period of harvesting, 0 otherwise
β_{it}^s	Binary variable, 1 if site i , in scenario s at time t is in use, 0 otherwise

5.2 Model formulation

In this section we present the model in detail. First, we present the objective function, followed by the constraints. Lastly, we have included an alternative way of formulating the model.

5.2.1 Objective function

The objective of the model is to maximize total harvested biomass throughout the planning horizon. Maximization of total harvested biomass can be represented by a sum consisting of one single term, shown in Equation 5.1.

$$\max \sum_{s \in \mathcal{S}} \pi^s \sum_{f \in \mathcal{F}^H} \sum_{g \in \mathcal{G}} \sum_{i \in \mathcal{I}} \sum_{t \in \mathcal{T}} V_f w_{fgit}^s \quad (5.1)$$

In each scenario, the number of harvested fish w_{fgit}^s is multiplied with the unit weight V_f , in order to obtain harvested biomass measured in kilograms. Then these amounts of harvested biomass are added together for all fish classes f , sorting types g , production sites i and time periods t , in order to obtain total harvested biomass for a scenario. In the objective function, π_s represents the probability for scenario s . Total harvested biomass for each scenario is multiplied with this probability, and eventually these products are added together to give the objective value.

5.2.2 Constraints

Smolt ordering constraint

The smolt ordering constraint ensures consistency between the number of smolt which is ordered and deployed.

$$\sum_{i \in \mathcal{I}} \sum_{t \in \mathcal{T}_z^s} y_{fgit}^s = o_{fgz} \quad f \in \mathcal{F}^S, g \in \mathcal{G}, z \in \mathcal{Z}, s \in \mathcal{S} \quad (5.2)$$

The smolt order quantities must be decided in the first stage with uncertain information about future seawater temperatures, while the smolt deployment quantities are decided in the second stage with precise information about seawater temperatures in all future periods in the planning horizon. Thus, the smolt order variable o_{fgz} is not indexed on scenarios, and must take the same value for all scenarios. The smolt deployment variable y_{fgit}^s , however, is defined and decided uniquely for each scenario s .

The variables are defined for different lengths of time. The smolt order quantity is defined for a half year z at company level, while the smolt deployment quantity is defined for a month t at site level. In order to obtain a half year time resolution on smolt deployments at company level, we sum all of the smolt deployment quantities deployed at all production sites i within the release windows \mathcal{T}^S in a given half year z . This number must be equal to the number of smolt ordered in the same half-year period. This constraint must apply to all half year periods z in the planning horizon. Furthermore, both the smolt order quantity and the smolt deployment quantity are defined uniquely for each smolt class $f \in \mathcal{F}^S$ and sorting type $g \in \mathcal{G}$, thus the smolt ordering constraint must be defined for all smolt classes and sorting types.

Smolt deployment constraints

We define the binary variable δ_{fgit}^s in order to keep track of the number smolt deployments, and to denote whether a smolt deployment is performed in a certain time period or not. δ_{fgit}^s takes the value 1 if smolt deployment of smolt type f and sorting type g is performed at site i , for scenario s , in year y , in time period t . We must ensure that there is only one smolt deployment per rearing cycle, and thus avoid numerous small deployments within the same cycle. This is taken care of by allowing a maximum of one rearing cycle per year, and the constraint is formulated as follows:

$$\sum_{f \in \mathcal{F}^S} \sum_{g \in \mathcal{G}} \sum_{t \in \mathcal{T}_y^S} \delta_{fgit}^s \leq 1 \quad i \in \mathcal{I}, y \in \mathcal{Y}, s \in \mathcal{S} \quad (5.3)$$

Equation 5.3 sums the number of smolt deployments over all smolt classes f , sorting types g and release windows t in year y . That means that it is allowed to deploy a maximum of one type of smolt (weight and sorting type) in maximum one time period in a year. This applies to all production sites i , in all years y and scenarios s . Equation 5.3 in combination with constraint 5.9 are sufficiently strict in order to avoid multiple smolt deployments. A possible second smolt deployment in the following year in a rearing cycle will not be able to grow fast enough to both reach harvestable weight and at the same time not break with the maximal cycle length. The values of the smolt deployment variables must be within the range of upper and lower bounds. The constraints that control this are formulated as follows:

$$y_{fgit}^s \leq U_i^{DEP} \delta_{fgit}^s \quad f \in \mathcal{F}^S, g \in \mathcal{G}, i \in \mathcal{I}, y \in \mathcal{Y}, t \in \mathcal{T}_y^S, s \in \mathcal{S} \quad (5.4)$$

$$y_{fgit}^s \geq L_i^{DEP} \delta_{fgit}^s \quad f \in \mathcal{F}^S, g \in \mathcal{G}, i \in \mathcal{I}, y \in \mathcal{Y}, t \in \mathcal{T}_y^S, s \in \mathcal{S} \quad (5.5)$$

Both inequalities are formulated in the same way, however, with opposite directed sign of inequality. In case of no deployment, the binary variable $\delta_{fgit}^s = 0$. In that case, the combination of 5.4 and 5.5 implies that $0 \leq y_{fgit}^s \leq 0$, so that $y_{fgit}^s = 0$. This relation ensures the obvious fact that the case of no smolt deployment must imply zero deployed smolt. In the cases when smolt deployment is performed, $\delta_{fgit}^s = 1$, and the combination of 5.4 and 5.5 gives $L_i^{DEP} \leq y_{fgit}^s \leq U_i^{DEP}$. This ensures that the number of deployed smolt stays within the upper and lower bounds. These inequalities are defined for all smolt types f and sorting types g at all production sites i , in all release windows t , in all years y , for all scenarios s .

It is not allowed to perform smolt deployments in all time periods in the planning horizon. Smolt deployments are restricted to the release windows, and they must comply with the following requirements. We ensure delimitation to the release windows by defining the smolt deployment variables y_{fgit}^s and δ_{fgit}^s only for the release windows $t \in \mathcal{T}^S$. The following requirement is implemented in constraint 5.7 in the following subsection.

In order to control whether it is allowed to perform a smolt deployment in a period or not, we define a binary variable θ_{it}^s . θ_{it}^s takes the value 1 if it is allowed to perform smolt deployment at site i , in time period t , in scenario s . θ_{it}^s is defined only for the release windows t in \mathcal{T}^S , just as the other smolt deployment variables y_{fgit}^s and δ_{fgit}^s . The connection between the two binary variables θ_{it}^s and δ_{fgit}^s is as follows:

$$\delta_{fgit}^s \leq \theta_{it}^s \quad f \in \mathcal{F}, g \in \mathcal{G}, i \in \mathcal{I}, t \in \mathcal{T}^S, s \in \mathcal{S} \quad (5.6)$$

Constraint 5.6 ensures that smolt deployment only can be performed in periods which is allowed for smolt deployment. If $\theta_{it}^s = 0$, it is not allowed to perform smolt deployment in period t , and then $\delta_{fgit}^s \leq 0$, meaning that the binary variable δ_{fgit}^s is forced to take the value 0. In the opposite case, if $\theta_{it}^s = 1$, it is allowed to perform smolt deployment in period t , and then $\delta_{fgit}^s \leq 1$, meaning that δ_{fgit}^s can be both 0 and 1, depending on whether smolt deployment is selected to be performed in the period or not.

Regulatory following constraints

A production site must be allowed for a minimum number of months after the last month of harvesting of the previous rearing cycle before a new batch of smolt can be deployed at the site. This condition is taken care of by the following constraint:

$$\Lambda \theta_{it}^s \leq \sum_{\tau=t-\Lambda}^{t-1} (1 - \beta_{i\tau}^s) \quad i \in \mathcal{I}, t \in \mathcal{T}^S \setminus \{1, \dots, \Lambda\}, s \in \mathcal{S} \quad (5.7)$$

The binary variable $\beta_{i\tau}^s$ takes the value 1 if a production site i is in use in time period τ , in scenario s , or $(1 - \beta_{i\tau}^s) = 1$ if a site is completely fallowed. Λ is a deterministic parameter which express the minimum number of consecutive time periods of fallowing. The right-hand side in the constraint above counts the number of fallowing periods over the Λ previous time periods. If the production site is fallowed for all these periods, so that $(1 - \beta_{i\tau}^s) = 1$ for all τ in the sum, then the number of fallowing periods will sum up to Λ . This implies that $\Lambda\theta_{it}^s \leq \Lambda$. Furthermore, this implies that θ_{it}^s can be both 1 or 0. In this case, the production site has been fallowed long enough so that smolt deployment can be performed. Otherwise, if at least one $(1 - \beta_{i\tau}^s) = 0$, then $\Lambda\theta_{it}^s < \Lambda$, meaning that θ_{it}^s is forced to be 0. In that case, the site does not fulfill the fallowing requirement, hence smolt deployment cannot take place.

Activity constraint

In addition to the minimum number of fallowing months between two rearing cycles, there is also a maximum number of fallowing months, until a production site must be reused. We include this requirement by demanding that at least one smolt deployment or harvesting period must take place over a period equal to the maximum length of fallowing plus one month. This requirement also holds for the situations where sites are in use, because the maximum cycle length is shorter than maximum fallowing length. The constraint is formulated as follows:

$$\sum_{\tau=t-\Gamma}^t \left(\left(\sum_{f \in \mathcal{F}^s} \sum_{g \in \mathcal{G}} \delta_{fgi\tau}^s \right) + \omega_{i\tau}^s \right) \geq 1 \quad i \in \mathcal{I}, t \in \mathcal{T} \setminus \{1, \dots, \Gamma\}, s \in \mathcal{S} \quad (5.8)$$

The binary variable ω_{it}^s takes the value 1 if harvesting is performed at site i , in time period t , in scenario s . Γ is a deterministic parameter representing the maximum length of the fallowing period. The left-hand site in constraint 5.8 sums all ω_{it}^s and δ_{fgit}^s over a time period equal to maximum length of the fallowing period plus one month. In this period, at least one smolt deployment or harvesting must be performed, meaning that at least one ω_{it}^s or δ_{fgit}^s must take the value 1. Thus, the right-hand site is set to 1. This constraint applies to all sites i , in all scenarios s . Since the constraint looks back at the Γ previous time periods, we define the constraint to apply for all $t \in \mathcal{T} \setminus \{1, \dots, \Gamma\}$.

Duration constraint

We choose to restrict the maximum length of each rearing cycle in the model, and denote the maximum length as Δ . Thus, in any sequence of Δ consecutive time periods plus one month, there must be at least one period with complete fallowing at a production site. This constraint is formulated as follows:

$$\sum_{t=\tau-\Delta}^{\tau} (1 - \beta_{it}^s) \geq 1 \quad i \in \mathcal{I}, \tau \in \mathcal{T} \setminus \{1, \dots, \Delta\}, s \in \mathcal{S} \quad (5.9)$$

The left-hand side sums $1 - \beta_{it}^s$ over a period of $\Delta + 1$ months. If a site is fallowed, $1 - \beta_{it}^s = 1$, so at least one of the periods must be fallowed in order to fulfill the inequality.

Harvesting constraints

We need a link between the binary harvesting variable ω_{it}^s , and the number of harvested fish w_{fgit}^s , in the same way as we connect binary smolt deployment variable to quantity variable. Thus, we define lower and upper bounds for the number of harvested salmon. These harvesting constraints are formulated as follows:

$$\sum_{f \in \mathcal{F}^H} \sum_{g \in \mathcal{G}} w_{fgit}^s \geq L^{HARV} \omega_{it}^s \quad i \in \mathcal{I}, t \in \mathcal{T}, s \in \mathcal{S} \quad (5.10)$$

$$\sum_{f \in \mathcal{F}^H} \sum_{g \in \mathcal{G}} w_{fgit}^s \leq U^{HARV} \omega_{it}^s \quad i \in \mathcal{I}, t \in \mathcal{T}, s \in \mathcal{S} \quad (5.11)$$

If harvesting is performed at a site, the binary variable ω_{it}^s takes the value 1. Then $w_{fgit}^s \geq L^{HARV}$ and $w_{fgit}^s \leq U^{HARV}$. In total, $L^{HARV} \leq w_{fgit}^s \leq U^{HARV}$, summed over all $f \in \mathcal{F}^H$ and $g \in \mathcal{G}$. This means that the number of harvested salmon is in the range of the upper and lower bounds. In the opposite case, when there is no harvesting, ω_{it}^s takes the value 0. Then $w_{fgit}^s \geq 0$ and $w_{fgit}^s \leq 0$, so in total $w_{fgit}^s = 0$,

Balancing constraint - Biomass

In previous chapter, in Section 4.7, we described the mathematical method we use for biomass development in the model. We must make some further simplifications from reality, in order to be able to formulate the method as a constraint in the model. Firstly, we assume that all fish within a fish class have the same growth during a time period, meaning that we omit growth variations within a fish class. Inclusion of growth variations requires a high level of detail in the information about growth rates, which is not available to us. Thus, this simplification is necessary. Secondly, we make a simplification regarding the number of fish, n_{fgit}^s . In reality, updating this variable is an integer-programming problem. However, in order to avoid the complexity of integer-programming, we let this variable be a floating variable. Due to its large magnitude, this is a reasonable simplification.

In order to keep track on biomass development at each site i , we use the variable n_{fgit}^s to register the number of salmon in fish class f , of sorting type g , at site i , in time period t , in scenario s . This variable must be updated with growth and survival rates in each time period, in order to obtain its new value in the upcoming period. Furthermore, smolt deployment quantities must be added to the number of fish in the fish classes $f \in \mathcal{F}^S$, and harvesting quantities must be subtracted from the number of fish in fish classes $f \in \mathcal{F}^H$. This implies a total of three constraints which apply to these separate subsets of the fish classes. The biomass development constraints are formulated as follows:

$$n_{fgit}^s = \sum_{\hat{f} \leq f} (\gamma_{\hat{f}fg_r(t-1)}^s n_{\hat{f}gi(t-1)}^s \Psi_{\hat{f}gi(t-1)}) + y_{fgit}^s \quad (5.12)$$

$$f \in \mathcal{F}^S, g \in \mathcal{G}, r \in \mathcal{R}, i \in \mathcal{I}_r, t \in \mathcal{T} \setminus \{1\}, s \in \mathcal{S}$$

$$n_{fgit}^s = \sum_{\hat{f} \leq f} (\gamma_{\hat{f}fg_r(t-1)}^s n_{\hat{f}gi(t-1)}^s \Psi_{\hat{f}gi(t-1)}) \quad (5.13)$$

$$f \in \mathcal{F} \setminus \{\mathcal{F}^S \cup \mathcal{F}^H\}, g \in \mathcal{G}, r \in \mathcal{R}, i \in \mathcal{I}_r, t \in \mathcal{T} \setminus \{1\}, s \in \mathcal{S}$$

$$n_{fgit}^s = \sum_{\hat{f} \leq f} (\gamma_{\hat{f}fg_r(t-1)}^s n_{\hat{f}gi(t-1)}^s \Psi_{\hat{f}gi(t-1)}) - w_{fgit}^s \quad (5.14)$$

$$f \in \mathcal{F}^H, g \in \mathcal{G}, r \in \mathcal{R}, i \in \mathcal{I}_r, t \in \mathcal{T} \setminus \{1\}, s \in \mathcal{S}$$

In each constraint above, the number of fish from the in time period $t - 1$, $n_{\hat{f}gi(t-1)}^s$, is multiplied with the survival rate $\Psi_{\hat{f}gi(t-1)}$ and the growth share of fish which grow from fish class \hat{f} to f , $\gamma_{\hat{f}fg_r(t-1)}^s$. This product is summed over all fish classes $\hat{f} \leq f$, because the contributions from all of the fish classes $\hat{f} \leq f$ sum up to give the number of fish in fish class f in time period t . In addition, the number of deployed smolt, y_{fgit}^s , is added in constraint 5.12, and the number of harvested salmon, w_{fgit}^s , is subtracted in constraint 5.14.

Maximal allowed biomass (MAB) constraints

We implement the regulatory restrictions in terms of production site MAB and company MAB as two separate constraints in the model. The constraint representing the production site MAB is given as follows:

$$\sum_{f \in \mathcal{F}} \sum_{g \in \mathcal{G}} ((V_f + \sigma_{fgt}^s) n_{fgit}^s \Psi_{fgit}^s) \leq MAB_i \beta_{it}^s \quad r \in \mathcal{R}, i \in \mathcal{I}_r, t \in \mathcal{T}, s \in \mathcal{S} \quad (5.15)$$

The stochastic parameter σ_{fgt}^s denotes the growth in kilograms for a fish in fish class f , of sorting g , in region r , in time period t . Thus, the sum $V_f + \sigma_{fgt}^s$ gives the new weight of V_f in kilograms after adding growth in period t . This sum is multiplied with all fish n_{fgit}^s , as well as the survival rate Ψ_{fgit}^s , to obtain the total biomass of all fish at a site in kilograms, after adding growth and adjusting for losses. This amount must be less than, or equal to MAB_i for all sites i . The binary variable β_{it}^s on the right-hand side is equal to 0 in case of no operation at site i , and thus ensures that n_{fgit}^s is forced to be zero in case of no operation. The constraint regarding company MAB is formulated the exact same way, however we sum the total biomass over all sites in all regions, instead of making a separate constraint for each site, as we do for the site MAB constraint. The company MAB constraint is formulated as followed:

$$\sum_{f \in \mathcal{F}} \sum_{g \in \mathcal{G}} \sum_{r \in \mathcal{R}} \sum_{i \in \mathcal{I}_r} (V_f + \sigma_{fgt}^s) n_{fgit}^s \Psi_{fgit}^s \leq MAB^{COMP} \quad t \in \mathcal{T}, s \in \mathcal{S} \quad (5.16)$$

Initial condition

We choose to model the production system as to be in operation when entering the planning horizon, meaning that the system contains biomass at some of the sites in the first time period t . We pre-generate these biomass levels and use them as input data to the optimization model, by giving values to the stock-keeping variable n_{fgi1}^s for the number of fish in fish class f , of sorting type g , at production site i , in time period $t = 1$, in scenario s . The deterministic parameter I_{fgi}^{BIO} represent the input biomass levels. The constraint is formulated as follows:

$$n_{fgi1}^s = I_{fgi}^{BIO} \quad f \in \mathcal{F}, g \in \mathcal{G}, i \in \mathcal{I}, s \in \mathcal{S} \quad (5.17)$$

End of horizon

We define a requirement for minimum biomass level in the very last time period in the planning horizon. Such a requirement avoids that all production sites are emptied in the last period, which would have been the case without the requirement, due to the model objective of maximizing harvested biomass. Hence we choose a minimum biomass level as a percentage K^{EOH} of the total MAB^{COMP} . The sum of biomass at all of the production

production sites must be larger than this lower bound. The constraint is formulated as follows:

$$\sum_{f \in \mathcal{F}} \sum_{g \in \mathcal{G}} \sum_{r \in \mathcal{R}} \sum_{i \in \mathcal{I}_r} (V_f + \sigma_{fgr|\mathcal{T}|}^s) n_{fgi|\mathcal{T}|}^s \psi_{fgi|\mathcal{T}|}^s \geq K^{EOH} MAB^{COMP} \quad s \in \mathcal{S} \quad (5.18)$$

The constraint is formulated in the same way as the MAB constraints. The sum of all biomass at the beginning of the last period $t = |\mathcal{T}|$, adjusted with growth and survival rate in the period, must be larger than, or equal to the lower bound on a percentage K^{EOH} of MAB^{COMP} .

In addition to require a minimum biomass level, we will also ensure a spread to different fish classes in the last period. We model this by dividing the set of fish classes \mathcal{F} into smaller subsets $\mathcal{F}_a \subset \mathcal{F}$. Furthermore, we state that the sum of the number of fish within a subset \mathcal{F}_a must be equal to, or larger than, the number of fish in the corresponding subset at the beginning of the first time period. This prevents fish from spreading freely among all fish classes, instead they are forced to have some degree of spread to different parts of the set of fish classes. We do not require the same spread among sites, or that the salmon must be of the same sorting types in the first and the last period, respectively. Hence, we sum the number of fish over all sorting types $g \in \mathcal{G}$, $i \in \mathcal{I}$ and $f \in \mathcal{F}_a$. The mathematical formulation for the constraint is as follows:

$$\sum_{f \in \mathcal{F}_a} \sum_{g \in \mathcal{G}} \sum_{i \in \mathcal{I}} n_{fgi1}^s \leq \sum_{f \in \mathcal{F}_a} \sum_{g \in \mathcal{G}} \sum_{i \in \mathcal{I}} n_{fgi|\mathcal{T}|}^s \quad a \in \mathcal{A}, s \in \mathcal{S} \quad (5.19)$$

Variable constraints

Lastly, we define the non-negativity and the binary constraints for the variables in the model. The indices are omitted in the formulation.

$$n, o, y, w \geq 0 \quad (5.20)$$

$$\delta, \beta, \theta, \omega \in \{0, 1\} \quad (5.21)$$

5.3 The Complete Model

Finally, the complete model is presented.

$$\max \sum_{s \in \mathcal{S}} \pi_s \sum_{f \in \mathcal{F}^H} \sum_{g \in \mathcal{G}} \sum_{i \in \mathcal{I}} \sum_{t \in \mathcal{T}} V_f w_{fgit}^s \quad (5.22)$$

$$\sum_{i \in \mathcal{I}} \sum_{t \in \mathcal{T}_z^S} y_{fgit}^s = o_{fgz} \quad f \in \mathcal{F}^S, g \in \mathcal{G}, z \in \mathcal{Z}, s \in \mathcal{S} \quad (5.23)$$

$$\sum_{f \in \mathcal{F}^S} \sum_{g \in \mathcal{G}} \sum_{t \in \mathcal{T}_y^S} \delta_{fgit}^s \leq 1 \quad i \in \mathcal{I}, y \in \mathcal{Y}, s \in \mathcal{S} \quad (5.24)$$

$$y_{fgit}^s \leq U_i^{DEP} \delta_{fgit}^s \quad f \in \mathcal{F}^S, g \in \mathcal{G}, i \in \mathcal{I}, y \in \mathcal{Y}, t \in \mathcal{T}_y^S, s \in \mathcal{S} \quad (5.25)$$

$$y_{fgit}^s \geq L_i^{DEP} \delta_{fgit}^s \quad f \in \mathcal{F}^S, g \in \mathcal{G}, i \in \mathcal{I}, y \in \mathcal{Y}, t \in \mathcal{T}_y^S, s \in \mathcal{S} \quad (5.26)$$

$$\delta_{fgit}^s \leq \theta_{it}^s \quad f \in \mathcal{F}, g \in \mathcal{G}, i \in \mathcal{I}, t \in \mathcal{T}^S, s \in \mathcal{S} \quad (5.27)$$

$$\Lambda \theta_{it}^s \leq \sum_{\tau=t-\Lambda}^{t-1} (1 - \beta_{i\tau}^s) \quad i \in \mathcal{I}, t \in \mathcal{T}^S \setminus \{1, \dots, \Lambda\}, s \in \mathcal{S} \quad (5.28)$$

$$\sum_{\tau=t-\Gamma}^t \left(\sum_{f \in \mathcal{F}^S} \sum_{g \in \mathcal{G}} \delta_{fgi\tau}^s \right) + \omega_{i\tau}^s \geq 1 \quad i \in \mathcal{I}, t \in \mathcal{T} \setminus \{1, \dots, \Gamma\}, s \in \mathcal{S} \quad (5.29)$$

$$\sum_{t=\tau-\Delta}^{\tau} (1 - \beta_{it}^s) \geq 1 \quad i \in \mathcal{I}, \tau \in \mathcal{T} \setminus \{1, \dots, \Delta\}, s \in \mathcal{S} \quad (5.30)$$

$$\sum_{f \in \mathcal{F}^H} \sum_{g \in \mathcal{G}} w_{fgit}^s \geq L^{HARV} \omega_{it}^s \quad i \in \mathcal{I}, t \in \mathcal{T}, s \in \mathcal{S} \quad (5.31)$$

$$\sum_{f \in \mathcal{F}^H} \sum_{g \in \mathcal{G}} w_{fgit}^s \leq U^{HARV} \omega_{it}^s \quad i \in \mathcal{I}, t \in \mathcal{T}, s \in \mathcal{S} \quad (5.32)$$

$$n_{fgit}^s = \sum_{\hat{f} \leq f} (\gamma_{\hat{f}fgr(t-1)}^s n_{\hat{f}gi(t-1)}^s \Psi_{\hat{f}gi(t-1)}) + y_{fgit}^s \quad (5.33)$$

$$f \in \mathcal{F}^S, g \in \mathcal{G}, r \in \mathcal{R}, i \in \mathcal{I}_r, t \in \mathcal{T} \setminus \{1\}, s \in \mathcal{S}$$

$$n_{fgit}^s = \sum_{\hat{f} \leq f} (\gamma_{\hat{f}fgr(t-1)}^s n_{\hat{f}gi(t-1)}^s \Psi_{\hat{f}gi(t-1)}) \quad (5.34)$$

$$f \in \mathcal{F} \setminus \{\mathcal{F}^S \cup \mathcal{F}^H\}, g \in \mathcal{G}, r \in \mathcal{R}, i \in \mathcal{I}_r, t \in \mathcal{T} \setminus \{1\}, s \in \mathcal{S}$$

$$n_{fgit}^s = \sum_{\hat{f} \leq f} (\gamma_{\hat{f}fgr(t-1)}^s n_{\hat{f}gi(t-1)}^s \Psi_{\hat{f}gi(t-1)}) - w_{fgit}^s \quad (5.35)$$

$$f \in \mathcal{F}^H, g \in \mathcal{G}, r \in \mathcal{R}, i \in \mathcal{I}_r, t \in \mathcal{T} \setminus \{1\}, s \in \mathcal{S}$$

$$\sum_{f \in \mathcal{F}} \sum_{g \in \mathcal{G}} ((V_f + \sigma_{fgr}^s) n_{fgit}^s \Psi_{fgit}^s) \leq MAB_i \beta_{it}^s \quad r \in \mathcal{R}, i \in \mathcal{I}_r, t \in \mathcal{T}, s \in \mathcal{S} \quad (5.36)$$

$$\sum_{f \in \mathcal{F}} \sum_{g \in \mathcal{G}} \sum_{r \in \mathcal{R}} \sum_{i \in \mathcal{I}_r} (V_f + \sigma_{fgr}^s) n_{fgit}^s \Psi_{fgit}^s \leq MAB^{COMP} \quad t \in \mathcal{T}, s \in \mathcal{S} \quad (5.37)$$

$$n_{fgi1}^s = I_{fgi}^{BIO} \quad f \in \mathcal{F}, g \in \mathcal{G}, i \in \mathcal{I}, s \in \mathcal{S} \quad (5.38)$$

$$\sum_{f \in \mathcal{F}} \sum_{g \in \mathcal{G}} \sum_{r \in \mathcal{R}} \sum_{i \in \mathcal{I}_r} (V_f + \sigma_{fgr|\mathcal{T}}^s) n_{fgi|\mathcal{T}}^s \psi_{fgi|\mathcal{T}}^s \geq K^{EOH} MAB^{COMP} \quad s \in \mathcal{S} \quad (5.39)$$

$$\sum_{f \in \mathcal{F}_a} \sum_{g \in \mathcal{G}} \sum_{i \in \mathcal{I}} n_{fgi}^s \leq \sum_{f \in \mathcal{F}_a} \sum_{g \in \mathcal{G}} \sum_{i \in \mathcal{I}} n_{fgi|\mathcal{T}}^s \quad a \in \mathcal{A}, s \in \mathcal{S} \quad (5.40)$$

$$n, o, y, w \geq 0 \quad (5.41)$$

$$\delta, \beta, \theta, \omega \in \{0, 1\} \quad (5.42)$$

5.4 Compact model formulation

We also present a compact formulation of the optimization model as follows, which will be used later on in the Stochastic Study in section 7.4.4:

$$\max \sum_{s \in \mathcal{S}} \pi^s Q(\mathbf{o}, \xi^s). \quad (5.43)$$

subject to

$$\mathbf{o} \in \bar{\mathbf{O}} \subset \mathbb{R}_+ \quad (5.44)$$

$Q(\mathbf{o}, \xi^s)$ represent the solution of the following second-stage problem:

$$Q(\mathbf{o}, \xi^s) = \max \sum_{f \in \mathcal{F}^H} \sum_{g \in \mathcal{G}} \sum_{i \in \mathcal{I}} \sum_{t \in \mathcal{T}} V_f w_{fgit}^s \quad (5.45)$$

subject to constraint (5.23) - (5.42). ξ^s represent a specific realization of the uncertain parameters, while \mathbf{o} denotes the complete set of first-stage decision variables satisfying all constraints in the second-stage problem.

6. Case Study

The input data in the model and the case study are described in this chapter. First, we present the production system of Eidsfjord Sjøfarm in Section 6.1, before all the data sets used in the model in Section 6.2.

6.1 Production system



Figure 6.1: Map of Eidsfjord Sjøfarm’s production sites in Vesterålen (blue area), Senja (red area) and Nord-Troms (purple area)

The implemented model is tested on a case study using input data from the salmon farming company Eidsfjord Sjøfarm AS. Eidsfjord Sjøfarm AS operates a total of eleven salmon farming licenses distributed on production sites in 6 municipalities located in the counties Nordland and Troms (Holmøy Maritime, 2018). They have an annual salmon production of approximately 15 000 tonnes of salmon, with a mean harvesting weight slightly above four kilograms (Eidsfjord Sjøfarm, 2019). We implement 16 of Eidsfjord Sjøfarm’s production sites in the optimization model. An overview of these production sites with relevant associating data is listed in Table 6.1. Each site is located in one out of three regions: Vesterålen, Senja or Nord-Troms. A map of these three regions with associating production sites is shown in Figure 6.1. Production site 1 - 10 from Table 6.1

are located in Vesterålen, site 11 - 13 are located in Senja, and site 14 - 16 are located in Nord-Troms.

Table 6.1: An overview of the production sites

Site ID (i)	Site name	MAB _{i} (tonnes)	Smolt lower bound L_i^{DEP}	Smolt upper bound U_i^{DEP}
1	Bremnesøya	3 900	500	1 390
2	Daljorda	3 120	500	1 390
3	Innerbrokløysa	3 120	500	1 390
4	Kuneset	3 120	500	1 390
5	Langholmen	3 120	500	1 390
6	Pollneset	3 120	500	1 390
7	Reinsnesøya	3 120	500	1 390
8	Sandan SØ	2 340	500	1 040
9	Stretarneset	3 120	500	1 390
10	Trolløya	3 120	500	1 390
11	Flesen	2 700	500	1 200
12	Kvenbukta	2 700	500	1 200
13	Lavika	2 700	500	1 200
14	Hagebergan	3 600	500	1 600
15	Haukøya	3 600	500	1 600
16	Russelva	3 500	500	1 560

We represent each production site by a site ID, listed in the leftmost column, which is taken as input to \mathcal{I} . Each site has a corresponding site MAB capacity, also listed in the table, which is input to MAB _{i} for each site i . In addition to these site-specific MAB limits, Eidsfjord Sjøfarm in total is subject to a company MAB on 10 902 tonnes of salmon, which for simplicity is rounded to 11 000 tonnes and used as input for MAB^{COMP}. A company MAB on 11 000 tonnes is approximately one-fifth of the sum of all the production site MABs, meaning that the company MAB puts a harder restriction on the total production system than what each site MAB does by itself.

In addition to restrictions for the biomass levels, we restrict the number of salmon at a site by upper and lower bounds, shown in Table 6.1. The regulatory upper limit is given as a number of fish at net pen level, which aggregated over all net pens at a site gives the maximum number of fish at a site. However, Eidsfjord Sjøfarm rarely fills up the entire capacity in all of the net pens at a site. Thus, we set the value of the upper bound based on Eidsfjord Sjøfarm's historical data on smolt deployments over a five-year period. We use the largest smolt deployment as a benchmark for the upper bound, and use it to calculate upper bounds at the other production sites, by adjusting for the differences in MAB capacity. This equation thus calculates the upper bound at site i based on the benchmark site r :

$$U_i^{DEP} = MAB_i \frac{U_r^{DEP}}{MAB_r}$$

Similarly, we set the lower bound slightly lower than the number of fish in the smallest historical smolt deployment. We use the same lower bound at all production sites.

6.2 Data sets

6.2.1 Planning horizon and time resolution

The model uses several sets and subsets regarding time periods, which all are illustrated in Figure 6.2. We implement the model with a five-year planning horizon, with monthly time resolution. The first period in the model is set to January 2020, and the last period is December 2024, implying a planning horizon with a total of 60 months or periods. These time periods are defined by the elements t in \mathcal{T} . In addition to the set of all time periods, we have defined the release windows \mathcal{T}^S as a subset of \mathcal{T} , which only consists of the months April - September, as well as January, for all years in the planning horizon. Both these sets of time periods are shown in Figure 6.2, with their corresponding divisions into years and half years.

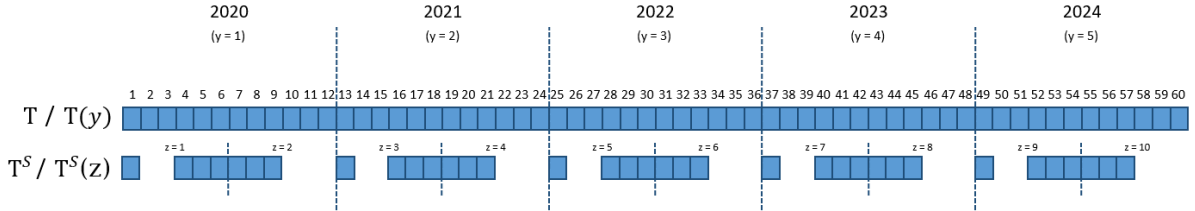


Figure 6.2: All time periods (upper row) and release windows (bottom row)

6.2.2 Biomass development

The division of salmon weights into fish classes is shown in Figure 6.3. The salmon weights, spanning from 0 to 7 kilograms, are discretized into a set of 79 fish classes f in \mathcal{F} . This range of fish weights is representative of the industry practice. The size of each weight class is 0.05 kilograms up to 2.00 kilograms, beyond which the size increases to 0.125 kilograms. The growth per month increases in line with increasing salmon weight, meaning that the requirement for fine resolution of fish classes diminish for higher weights. Hence, we choose larger weight intervals for the last half of the elements in \mathcal{F} . Fish class 51 - 79 represent all salmon larger than 3.5 kilograms, and they are elements in the subset \mathcal{F}^H . We have chosen 3.5 kilograms as a lower bound on harvesting weight, meaning that

the harvesting variable w_{fgit}^s is only defined for these fish classes. In terms of smolt types, we choose fish class 2 (150 grams), as the only element in the subset \mathcal{F}^S , representing the smolt classes. This means that all smolt deployments are simplified to solely consist of 150-gram smolt.

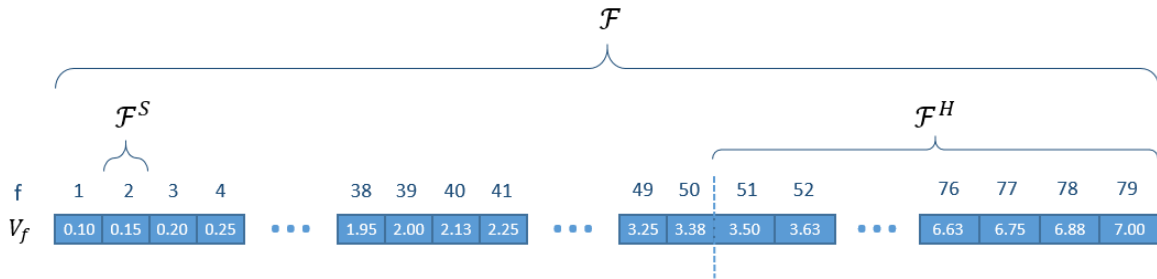


Figure 6.3: Fish classes, smolt class, and harvest classes

Mixed-gender growth

The method used for biomass development is the same as the one implemented by Hæreid (2011), and so is the input data for growth in the model. The growth data is based on data from Skretting (2011). Skretting presents a growth table with daily percentage salmon growth for Atlantic salmon, depending on salmon weight and seawater temperature (Skretting, 2011). The Skretting table is divided into 34 fish classes, with temperatures ranging from 1 to 20 °C, with 1 °C resolution. Hæreid extended the original table from 34 to 79 fish classes with 0.5 ° resolution by making use of interpolation. He also translated percentage growth to absolute growth and aggregated daily growth over a month to achieve monthly absolute growth. These data are input to the growth rate variable σ_{fgit}^s . A section of the resulting growth matrix is shown in Table 6.2. The last row in the matrix has a growth rate on 0 kilograms per month, to prevent that any fish grow out of the last fish class. The last fish class in the Skretting table is 5.25 kilograms, compared to 7.00 kilograms in our table. For simplicity, all rows in our table with weights larger than 5.25 kilograms take the same values as the 5.25 kilogram-row. A tiny portion of salmon grows into this area of the growth table, meaning that this is a sufficient simplification.

Monosex growth

The growth table described above is based on traditional mixed-gender batches of salmon. To develop an equivalent monosex growth table, we use growth data from the sorted batches of salmon AquaGen reared in 2017. For simplicity, we have only used growth data from one batch of monosex salmon to adjust the mixed-gender growth table. This batch consists of male salmon, meaning that no data from female salmon has been used in adjusting the growth table. This data consists of daily logging of the seawater temper-

Table 6.2: Absolute monthly growth (kg) for Atlantic salmon in different fish classes f , depending on weight and seawater temperature, developed by Skretting and adjusted by Hæreid (2011)

Fish class		Temperatures (°C)									
f	V_f (kg)	0.5	1.0		14.5	15.0		15.5	19.5	20.0	
1	0.10	0.00	0.00		0.10	0.10		0.11	0.08	0.08	
2	0.15	0.01	0.01	...	0.14	0.14		0.14	...	0.12	0.11
3	0.20	0.01	0.01		0.18	0.18		0.18		0.15	0.14
...			
56	4.13	0.04	0.04		0.74	0.74		0.74		0.59	0.56
57	4.25	0.04	0.04	...	0.75	0.76		0.75	...	0.60	0.57
58	4.38	0.04	0.04		0.76	0.77		0.76		0.60	0.57
...			
77	6.75	0.05	0.05		0.83	0.83		0.83		0.65	0.61
78	6.88	0.05	0.05	...	0.83	0.83		0.83	...	0.65	0.61
79	7.00	0.00	0.00		0.00	0.00		0.00		0.00	0.00

ature and average weight in the batch. By calculating the weight difference over a month, and additionally calculate the associating monthly mean seawater temperature, we get a monthly growth rate which is defined in the same way as the ones in the mixed-gender growth table. We calculate these growth rates for all the logging points in the data set, from which we get a few new growth rates that replace the old values from the mixed-gender growth table. Furthermore, we calculate ratios between old and new growth rates in the table cells where we have obtained values for monosex growth. We multiply these ratios with the mixed-gender growth rates in the remaining empty cells, in order to obtain monosex growth rates in the cells with no logging data. These calculations give us a complete growth table. A section of the resulting monosex growth matrix is shown in Table 6.3.

To illustrate the difference in growth behavior, we simulate the growth behavior of two separate populations under the same temperature. In the simulation, an arbitrarily chosen temperature profile is used, with a starting point in January. Both populations start as 0,15 kg smolt on the mean.

6.2.3 Seawater temperatures

Eidsfjord Sjøfarm operates across different geographical regions in Northern Norway. Production sites located in different regions are subject to different environmental conditions, and thereby different seawater temperatures. We use historical data from the three regions: Vesterålen, Senja, and Nord-Troms as a driver to generate the growth data from the growth tables presented above. The historical raw data on seawater temperatures

Table 6.3: Absolute monthly growth (kg) for Atlantic salmon of monosex type in different fish classes f , depending on weight and seawater temperature, calculated on basis from logging data from a batch of male salmon reared by AquaGen.

Fish class		Temperatures (°C)								
f	V_f (kg)	0.5	1.0	14.5	15.0	15.5	19.5	20.0		
1	0.10	0.01	0.01	0.16	0.17	0.17	0.17	0.16		
2	0.15	0.01	0.01	...	0.18	0.19	0.20	...	0.18	0.17
3	0.20	0.01	0.01		0.22	0.23	0.24		0.21	0.20
...		
56	4.13	0.07	0.07		1.13	1.14	1.17		1.08	1.01
57	4.25	0.07	0.07	...	1.08	1.10	1.13	...	1.02	1.00
58	4.38	0.06	0.06		1.01	1.02	1.05		0.90	0.90
...		
77	6.75	0.05	0.05		0.83	0.83	0.83		0.65	0.61
78	6.88	0.05	0.05	...	0.83	0.83	0.83	...	0.65	0.61
79	7.00	0.00	0.00		0.00	0.00	0.00		0.00	0.00

have been logged as daily seawater temperatures at all the production sites, at all days they have been in use over a five-year period. Thus, seawater temperatures have not been logged when a site has been fallowed. We aggregate the daily seawater temperatures for all sites in the same region, to obtain regional temperatures. The resulting plot of the historical seawater temperatures is shown in Figure 6.5. The seawater temperatures have been aggregated for all days each month to obtain monthly mean values, which are the values presented in the plot.

6.2.4 Initial biomass

We pre-generate biomass levels in a random selection of Eidsfjord Sjøfarm's production sites and use as input to the first period in the planning horizon. These sites are presented in Table 6.4, and taken as input data to $I_{f_{gi}}^{BIO}$. The number of months each site has been in operation prior to entering the planning horizon varies among the sites. We include production sites from all three regions in which Eidsfjord Sjøfarm operates in the selection.

Table 6.4: Initial biomass prior to planning horizon

Site r	Months in seawater	Number of smolt
Langholmen	11	432 000
Reinsnesøya	8	540 000
Trolløya	7	600 000
Flesen	6	420 000
Russelva	8	324 000

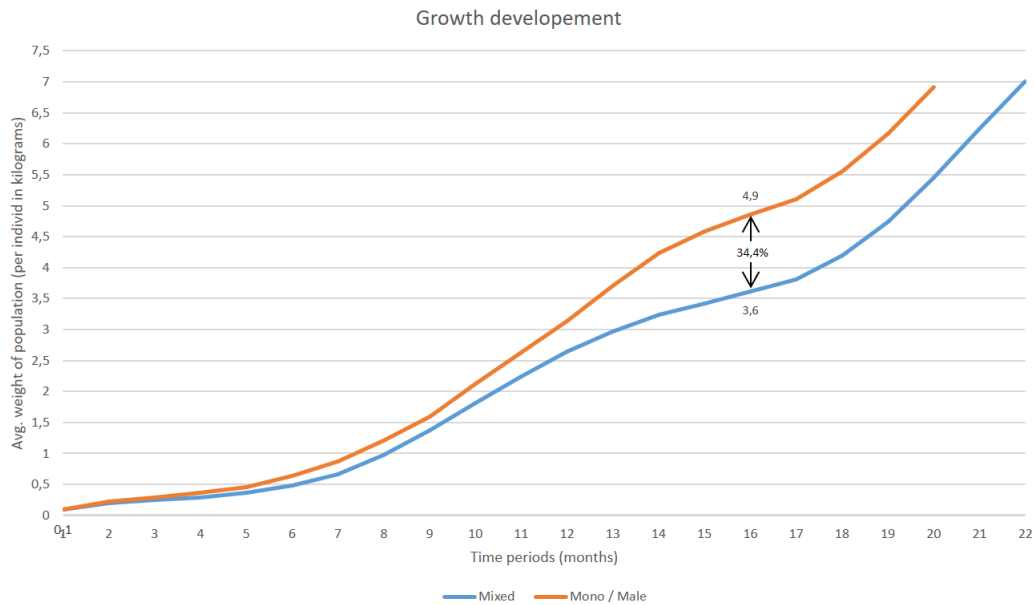


Figure 6.4: Simulated development in growth for two separate population, with start in January

6.2.5 Additional parameters

In addition to the data sets we have presented thus far, there are several deterministic parameters in the model, which must be defined. Regarding following, the minimum length on 2 months complete following, and the maximum length on 24 months complete following are input constants to Λ and Γ , respectively. Similarly, we set the maximum cycle duration on 19 months as input to Δ . Furthermore, we decide that the utilization of company MAB must be at least 60% by the end of the last period in the planning horizon, which is input to K^{EOH} . Regarding loss in production, we implement the model with a loss rate equal to the industry average on 15 % a year, which is equivalent to a survival rate of 85 % a year, yielding 98.7 % per month.

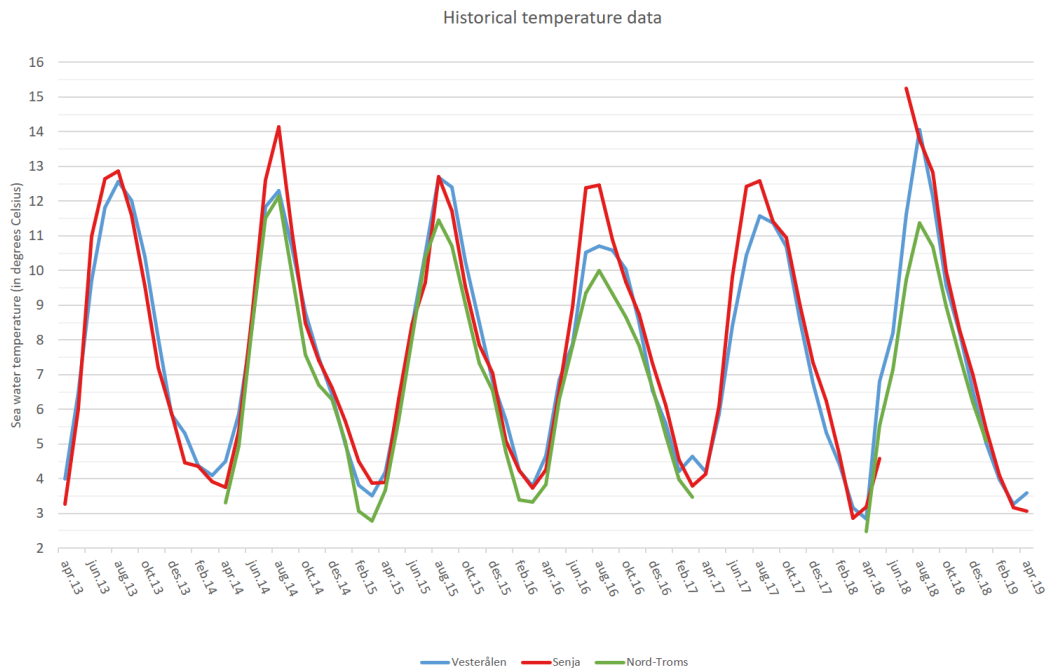


Figure 6.5: Logged temperature data for Eidsfjord Sjøfarm

Table 6.5: Summarizing table describing input parameters

Symbol	Description	Value
K^{EOH}	Utilization factor of MAB (company) at end-of-horizon	0,6
Λ	Min. number of months with complete following of a site	2
Γ	Max. number of consecutive months with no activity at a site	24
Δ	Max.number of months in a rearing cycle	20
Ψ_{fgit}	Survival rate per month	0,987
L_i^{DEP}	Lower bound for the number of deployed smolt at a specific site (in 1000)	500
L^{HARV}	Lower bound for the number of harvested salmon (in 1000)	25

7. Computational Study

7.1 Model implementation

We implement two versions of the stochastic optimization model presented in Chapter 5. These two versions are a deterministic version that omits uncertainty in biomass development, and a two-stage stochastic version which includes uncertainty in biomass development. In the deterministic model, we use expected values for the uncertain parameters, while for the stochastic model, information about uncertain parameters is revealed after making the first-stage decision.

Both models are written in Mosel and implemented in Xpress-IVE Version 1.24.24, 64 bit. The models are solved by Xpress Optimizer. All input data is pre-processed in Excel and MATLAB, and written to txt.-files which are used as input to Xpress. The output results are written to an output spreadsheet. The model runs were performed (at a computational) on a Linux-based computational cluster, named "Solstorm", owned by the Department of Industrial Economics and Technology Management at NTNU. The tests were performed on nodes from rack 1 with 4 x AMD Opteron 6274 2.4 GHz CPU and 128 Gb of installed RAM memory.

7.2 Base case study

In the introduction to the computational study, we present and analyze the results from a basis case instance, which approaches to Eidsfjord Sjøfarm's current production. We use this instance in order to compare the calculated production levels to current industry levels and control that the model behaves reasonably in line with industry practice. In addition, we use the base case to establish a benchmark for scoring the advantages of including the additional option of selecting monosex smolt from the smolt producer.

For all of the deterministic analyzes, we pre-generate a temperature profile for future seawater temperatures in all of the months in the five-year planning horizon, which is used as deterministic input to the model. This temperature profile is shown in Figure 7.1. The temperature profile is based on the historical temperature data presented in Subsection 6.2.3. We generated this temperature profile with the scenario generating algorithm we

describe later on in Subsection 7.4.1. We use the historical data to calculate an average value μ with corresponding standard deviation $\pm\sigma$ for the seawater temperature in each month of the year. Furthermore, we use these values to create confidence intervals for each month. For each year, we randomly pick a value $\gamma \in [-1, 1]$, which is continuously defined. We use γ to choose seawater temperature values from the confidence interval for all months in the year, to obtain a temperature profile for one year. We repeat this procedure five times, in order to generate five different temperature profiles, which in total give the temperature profile for the entire five-year planning horizon, shown in Figure 7.1.

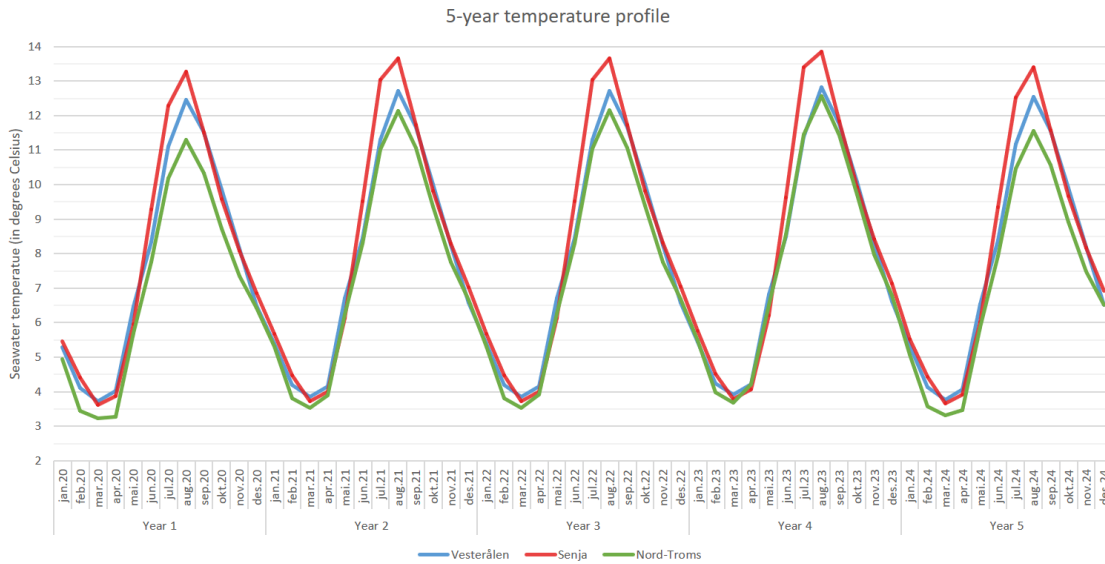


Figure 7.1: Seawater temperature profile used as input to the deterministic instances

7.2.1 Base case instance

The base case instance is presented in Table 7.1. In order to simulate Eidsfjord Sjøfarm's current production, we implement the model with all of the 16 production sites presented in Chapter 6 in the base case. The average harvesting weight for salmon produced by Eidsfjord Sjøfarm over the past five years is 4.1 kilograms, and Eidsfjord Sjøfarm rarely harvest salmon smaller than 3.5 kilograms. Thus we choose the lower bound for the harvesting weight to be 3.5 kilograms. Regarding smolt types, they solely use traditional mixed-gender smolt, and we set the maximum cycle length to be 19 months. We keep all other parameters in the model fixed to the values described in Chapter 6 for all instances.

Table 7.1: Deterministic base case instance

Instance	No. of sites	Harvest limit	Sorting types	Cycle length (max)
Base case	16	3.5 kg	Only mixed	19 mo.

7.2.2 Technical results from the base case run

The overall result from the base case run is shown in Table 7.2. Further details about the progression in number of solutions, objective value, run time and optimality gap during the run is shown in Figure 7.2.

Table 7.2: Deterministic base case result

Instance	Objective value	Optimality gap	Run time
Base case	79 162	1.94 %	7 h 9 min

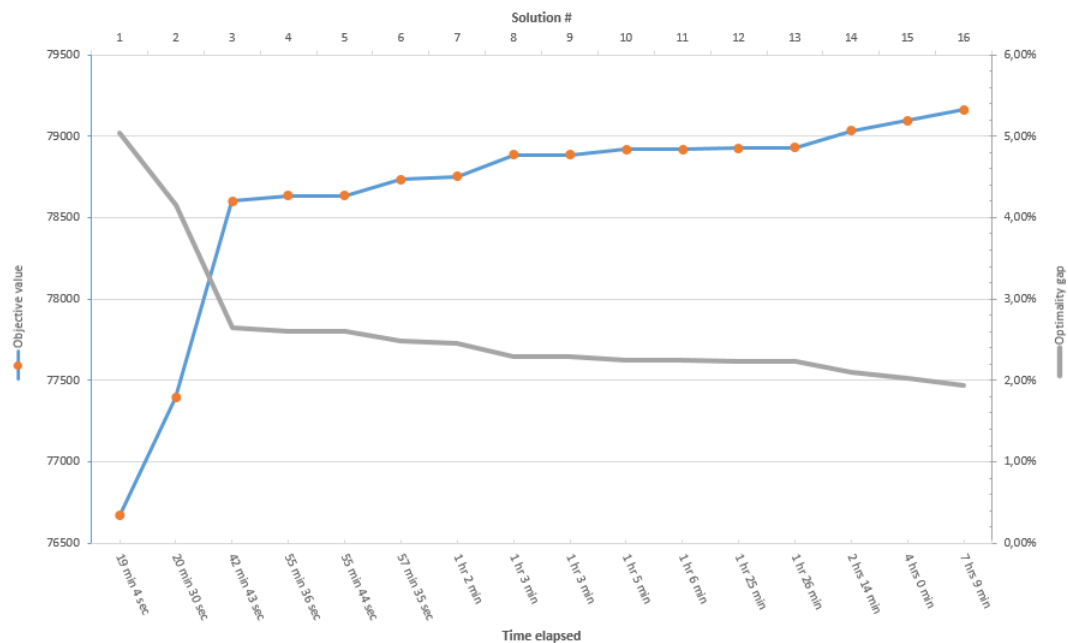


Figure 7.2: Optimality gap and objective value for each solution during base case model run

The overall result from the base case run is shown in Table 7.2. Further details about the progression in number of solutions, objective value, run time and optimality gap during the run is shown in Figure 7.2.

The model finds the first solution after 19 min with 5 % optimality gap. This solution

is significantly improved after 42 min in the third solution with 2.6 % optimality gap. Thereafter, the model gradually finds slightly better solutions until the sixteenth solution with objective value 79 162 is found after 7 h 9 min with 1.94 % optimality gap. The model does not find more solutions beyond the sixteenth, due to computer memory shortage. An optimality gap on 1.94 % is equivalent to a best bound for the objective value on 80 728, and thus a difference on 1 566 between best bound and best solution. This gap is sufficiently small to give a relatively accurate indication of the optimal objective value, due to the large magnitude of the objective value.

7.2.3 Total production level

We measure salmon production as the amount of harvested biomass, which is represented by the model objective in the optimization model. Annual and total production levels in the five-year planning horizon from the base case run, are shown in Figure 7.3. The base case results are here presented along with Eidsfjord Sjøfarm's historical production levels over a five-year period.

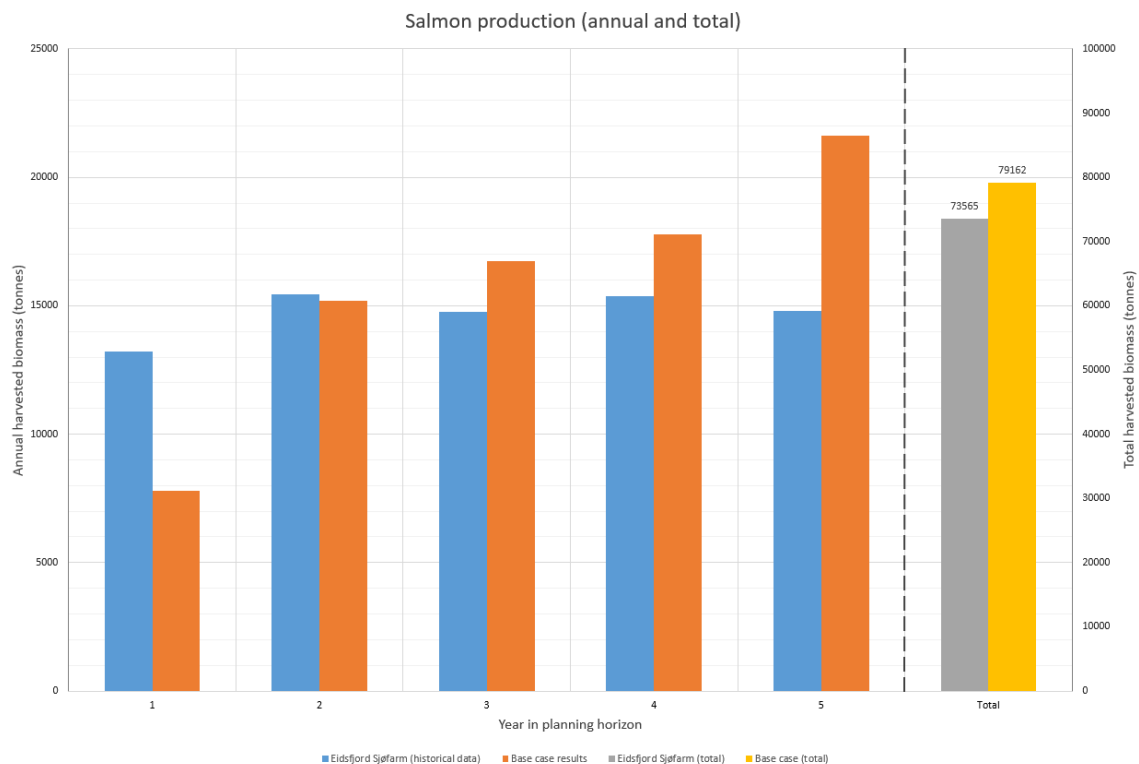


Figure 7.3: Annual and total salmon production from the base case run, compared to historical data from Eidsfjord Sjøfarm over a five-year period.

The rightmost yellow column shows the objective value, which is the total amount of harvested biomass from the base case run. The grey column shows Eidsfjord Sjøfarm's

actual salmon production. The objective value states 79 162 tonnes of harvested salmon, compared to an actual level of 73 565 tonnes. These levels are equivalent to annual averages on 15 832 tonnes and 14 713 tonnes, respectively. Thus there is a 7.1 % increase in production level from the real world in the base case result. The average harvesting weight is 4.12 kilograms in the base case result, compared to 4.18 kilograms for Eidsfjord Sjøfarm. These harvesting weights are approximately equal, and this indicates that the increased production in the base case result is due to a larger number of salmon being harvested within the planning horizon since the average harvesting weights are the same. The number of salmon planned for harvesting in the base case result is 19 198, compared to 17 681 in Eidsfjord Sjøfarm's historical data. This is an 8.6 % increase in the number of salmon sent to harvesting in a five-year planning horizon.

The orange and blue columns in Figure 7.3 show annual production levels from the base case results and Eidsfjord Sjøfarm's historical data, respectively. In the fifth year, the base case result is 43 % higher than Eidsfjord Sjøfarm's production level. We use a lower bound on the company MAB on 60 %; however, in reality, Eidsfjord Sjøfarm usually has 70 - 90 % exploitation of the company MAB (Eidsfjord Sjøfarm, 2018). The lower bound on 60 % allows for a larger amount of harvested salmon in the last period than what Eidsfjord Sjøfarm does in practice. We performed a test run with an increased lower bound of 80 % MAB exploitation for the end-of-horizon condition, in order to analyze this effect. This resulted in a production level of 21 003 tonnes in the last period, which is just a 2.3 % decrease compared to the result from the 60 % run. Hence, the lowered requirement on 60 % MAB exploitation has little effect on the production level.

In the first year, the base case result is 41.0 % lower than Eidsfjord Sjøfarm's production level. We do not account for the months the initial biomass has been in seawater prior to the first time period so that these rearing cycles can exceed the activity limit. Thus, a portion of the salmon that in reality would have been harvested in the first production year due to reaching the activity limit in the first year is shifted to the second year as a consequence. The years in the middle of the planning horizon (2 - 4) are more stable and unaffected by boundary conditions. Thus, the production in these years is similar to real-world situations. Overall, the model gives slightly higher harvest levels than current practice.

7.2.4 Production plan

The distribution of salmon on different rearing cycles among the 16 production sites is shown in Figure 7.4. The green dots represent smolt deployments, while the orange dots represent time periods with harvesting. The green and orange dots are connected with a dotted line which indicates that a production site is in operation.

The base case result consists of 25 complete rearing cycles. A complete cycle is defined such that both smolt deployment and harvesting are performed within the planning horizon. The rearing cycles have different lengths, and we define a cycle length to be

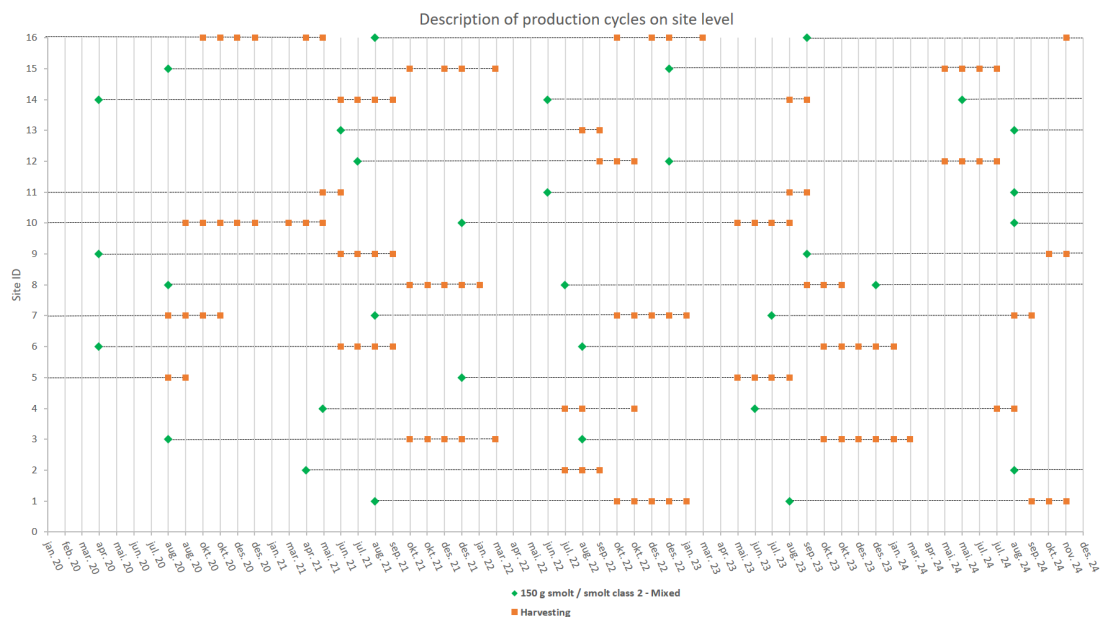


Figure 7.4: Production plan of all smolt deployments and salmon harvesting periods at all production sites from the deterministic base case run

the number of periods from smolt deployment to the last period of harvesting prior to following at a site.

The rearing cycles shown in Figure 7.4 is in the range of 15 - 19 months, and has an average cycle length of 17.3 months. For comparison, the length of Eidsfjord Sjøfarm's rearing cycles is in the range 18 - 23 months, with an average of 20 months (Eidsfjord Sjøfarm, 2019). The cycle lengths are thus shorter in the model results than current practice. This can be explained by our choice of upper bound for cycle length. We used 19 months as the upper bound for cycle length in the base case instance, which is shorter than Eidsfjord Sjøfarm's longest rearing cycle. Consequently, we get a smaller average cycle length in the model results compared to Eidsfjord Sjøfarm's practice.

Figure 7.4 shows when smolt deployments and harvests of salmon are performed, however not any sizes of the smolt deployment quantities or harvesting amounts. An illustration of the smolt deployment quantities and the amounts of harvested biomass at one specific site throughout the planning horizon is shown in Figure 7.5.

Two rearing cycles are completed within the planning horizon at production site 8, Sandan SØ. The number of smolt in the deployments are both below 700 000. These are both relatively small deployments seen in light of the upper and lower bounds on smolt deployments at Sandan SØ, which is 500 - 1 040 thousand smolt. The number of harvesting periods is five and three for the two rearing cycles, respectively. The harvesting amounts vary in each period. However, there are not any cases of one large harvesting

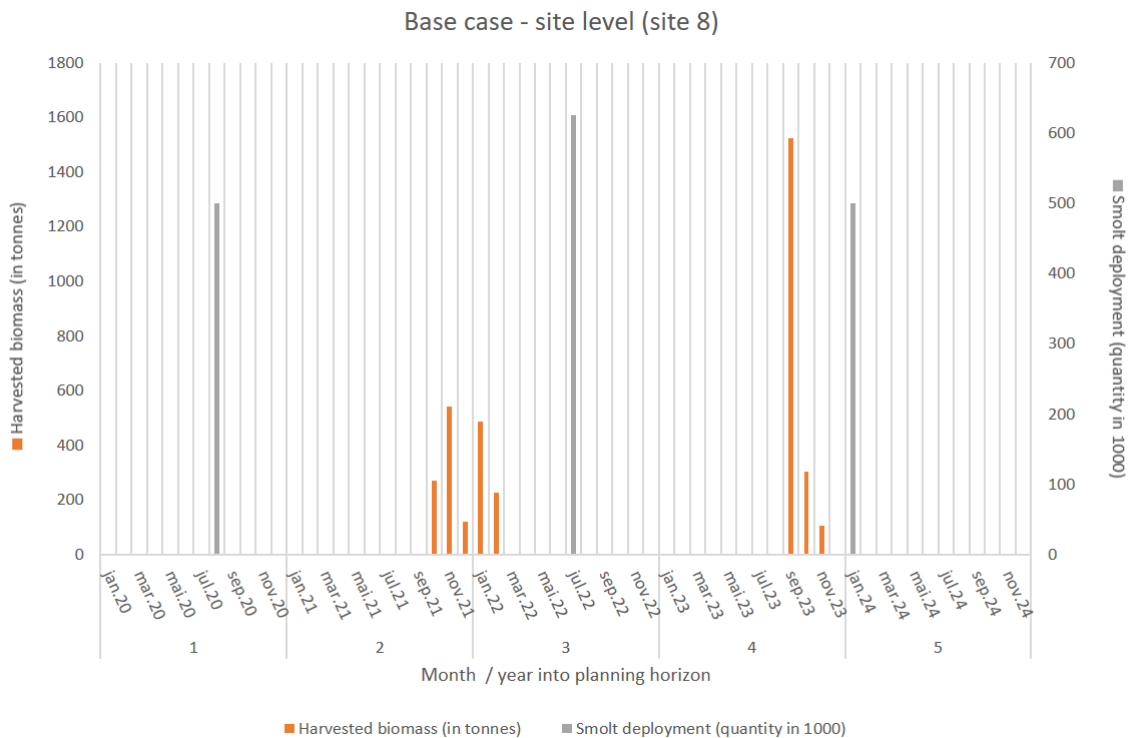


Figure 7.5: Overview of all smolt deployment quantities and harvest amounts in the planning horizon at production site 8, Sandan SØ.

amount in the last period, which is typical in current practice.

7.2.5 Smolt deployments

There is a total of 33 smolt deployments in the production plan shown in Figure 7.4. An illustration of the number of smolt in each smolt deployment is shown in Figure 7.6. Historical data on smolt deployments from Eidsfjord Sjøfarm over a five-year time horizon is listed together with the base case results in this illustration. The smolt deployments in the illustration are sorted by magnitude.

The base case result consists of 3 more smolt deployments than the number from Eidsfjord Sjøfarm's historical data, with 33 compared to 30 smolt deployments, respectively. The number of smolt per deployment span a wider range of numbers in the base case. The number of smolt per deployment ranges between 500 - 1 400 thousand and 570 - 1 113 thousand smolt for the base case and Eidsfjord Sjøfarm, respectively. The wide range in the base case results is related to the choices of upper and lower bounds on smolt deployments, which we set slightly higher and lower than the historical data.

The average number of smolt in a deployment is indicated for both the base case and

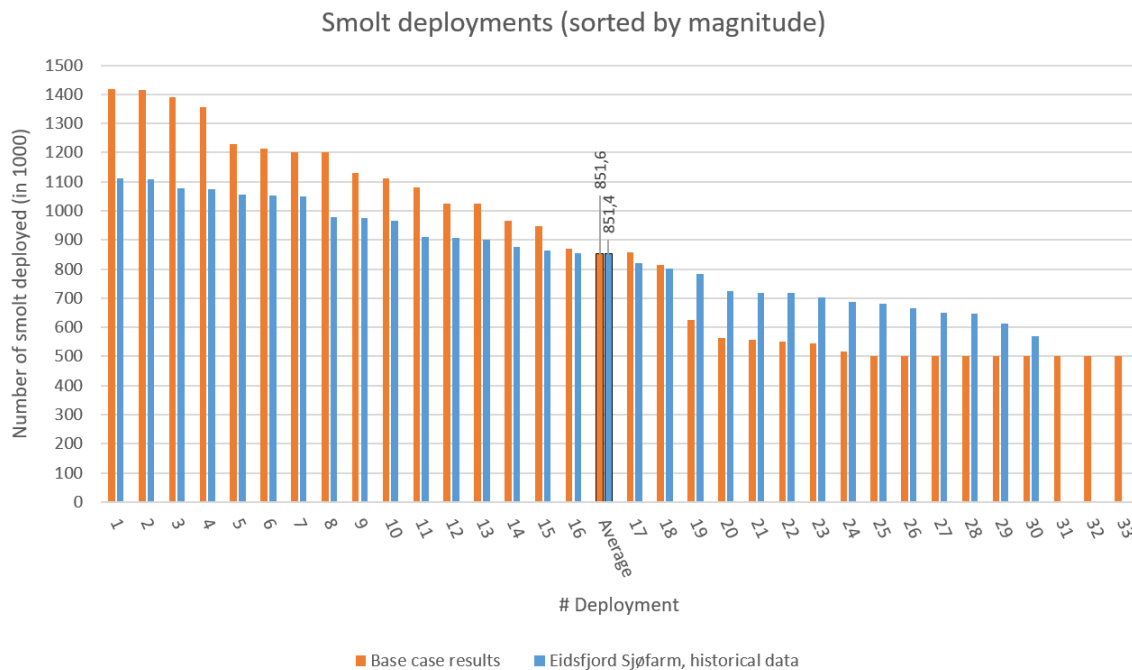


Figure 7.6: Comparison of all smolt deployments in the base case run and in Eidsfjord Sjøfarm's historical data, sorted by magnitude.

Eidsfjord Sjøfarm in Figure 7.6. These numbers are almost exactly the same, with 851.6 and 851.4 thousand, respectively. The base case result consists of a higher total number of deployed smolt, since the base case result includes three more smolt deployments, and the average number of smolt in each deployment is the same. The total number of smolt deployed in the base case result is 28.1 million, while the total number of smolt deployed by Eidsfjord Sjøfarm is 25.5 million. The base case result thus suggests 10.2 % more smolt for deployment than current practice for Eidsfjord Sjøfarm. This percentage increase is close to the 8.6 % increase in the number of harvested salmon.

In Figure 7.7, the collection of smolt deployments are listed chronologically over the planning horizon. As in Figure 7.6, each column represents a single smolt deployment at a specific site, which explains the occurrence of several columns in the same month. The figure shows that there are similarities between the model result and the historical data from Eidsfjord Sjøfarm, and that the model result thus fits the real world relatively well. The smolt deployments are in both cases relatively evenly outspread among all half-year periods in the planning horizon. Furthermore, by looking at which months the smolt deployments occur, one can see that the smolt deployments tend to occur more often in the warmer months in the year in both cases (late spring or early autumn).

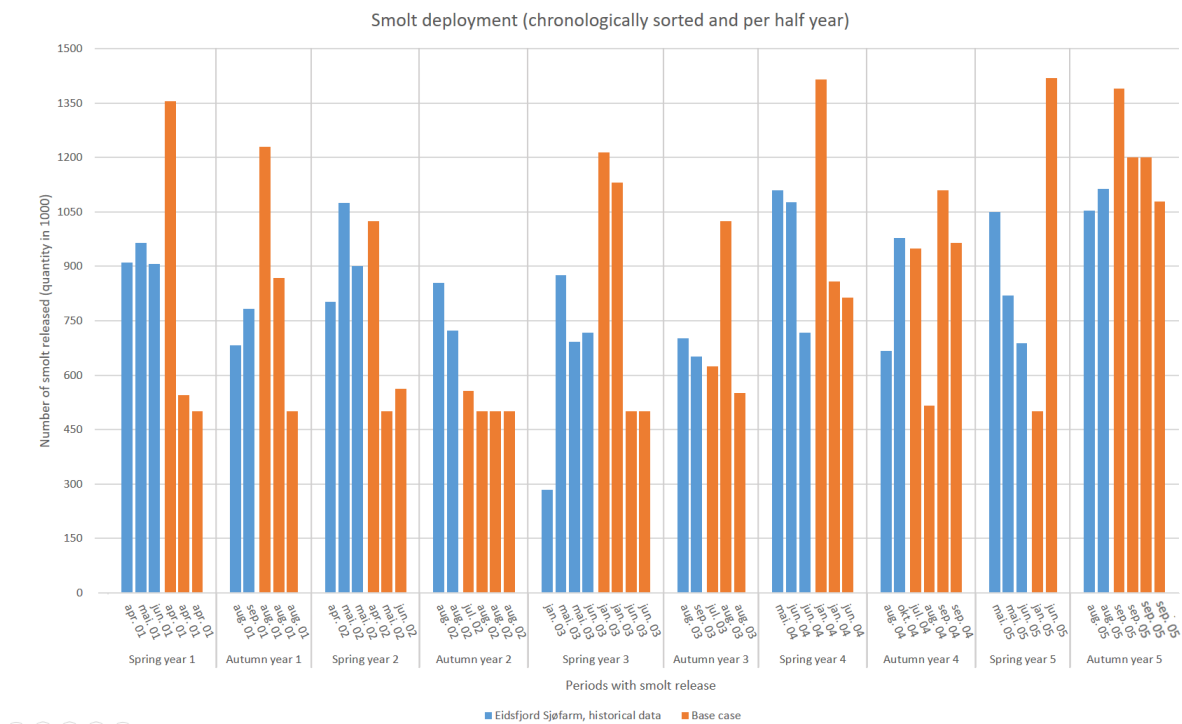


Figure 7.7: Comparison of all smolt deployments. on site level, in the base case run and in Eidsfjord Sjøfarm’s historical data, sorted chronological and per half year.

7.2.6 Contributions to increased production

Overall, the base case results indicate a slight increase in salmon production compared to the real world. The main source of increased production in the base case is the increased number of deployed and harvested salmon. During the five-year planning horizon, the base case results include 10.2 % more deployed smolt and 8.6 % more harvested salmon than current practice. The average harvesting weight is approximately equal to the real world situation, so there is an increased production of salmon due to a larger number of salmon reared over the five-year period.

7.3 Deterministic case study

In this section, we present and discuss the results of a deterministic case study. We implement the deterministic version of the model with four deterministic instances to analyze how different harvesting limits and the option of including monosex smolt affect the production level.

7.3.1 Instances

The four deterministic instances are listed in Table 7.3. Instance 2 is equal to the base case instance, except that the set of smolt types is extended from solely include mixed-gender smolt in the base case to include the monosex option in Instance 2. The effects of including monosex smolt can thus be analyzed by comparing the results from these two model runs. Instance 1 - 4 all include the option of both monosex and mixed-gender smolt; however, the harvest limits varies from 3.0 - 4.5 kilograms. Thus, we can compare the results from these four model runs to analyze the effects of using different lower bounds for harvesting weight.

Additionally, we increase the maximum cycle length from 19 months to 21 months, for Instance 3 and 4. Instance 3 and 4 have higher lower bounds for the harvesting weight, which require longer rearing cycles in order to obtain feasible solutions from the model. We must ensure that all fish in a batch reaches the lower harvesting bound before reaching the maximum cycle length. It is reasonable to increase this upper bound by 2 months, because the constraint represents a modelling choice we have implemented, and hence not a rigid regulatory practice. The constraint is included in the model to prevent abnormally long rearing cycles, and 21 months is also a reasonable upper bound for this purpose.

Table 7.3: Deterministic instances

Instance	No. of sites	Harvest limit	Sorting	Cycle length upper bound
Base case	16	3.5 kg	Only mixed	19 months
Instance 1	16	3.0 kg	Mono + Mixed	19 months
Instance 2	16	3.5 kg	Mono + Mixed	19 months
Instance 3	16	4.0 kg	Mono + Mixed	21 months
Instance 4	16	4.5 kg	Mono + Mixed	21 months

7.3.2 Computational results from deterministic instances

We ran the model for each instance until it found solutions with optimality gaps smaller than the base case solution. The solutions found are listed in Table 7.4 with objective value, optimality gap and run time. The correlation between run time and the optimality gap shows that longer run time leads to a smaller better optimality gap. The objective value decreases in line with increasing harvest limits. An explanation might be that the solution space narrows as the harvest limit increases. We discuss the objective value and the underlying results in more detail in the two upcoming subsections.

Table 7.4: Computational results from the deterministic runs

Instance	Objective value	Optimality gap	Run time
Base case	79 162	1.94 %	7 h 9 min
Instance 1	98 647	0.18 %	3 h 42 min
Instance 2	96 013	0.26 %	1 h 33 min
Instance 3	92 319	1.39 %	38 min
Instance 4	89 079	1.40 %	1 h 13 min

7.3.3 Effects of monosex growth

Total production level

The results for total salmon production from the base case, and Instance 2 are shown in Figure 7.8. The overall level of harvested biomass is higher in Instance 2, regarded both annually and in total over the planning horizon. The total harvested biomass in Instance 2 is 96 013 tonnes, while the total harvested biomass in the base case is 79 162 tonnes, which are equivalent to average annual production on 19 203 tonnes and 15 832 tonnes, respectively. This implies a 21.3 % increase in total salmon production when we include the option of using monosex smolt in addition to mixed-gender smolt. The annual variations within the planning horizon follow the same trend as the base case result; however, the production level is considerably higher.

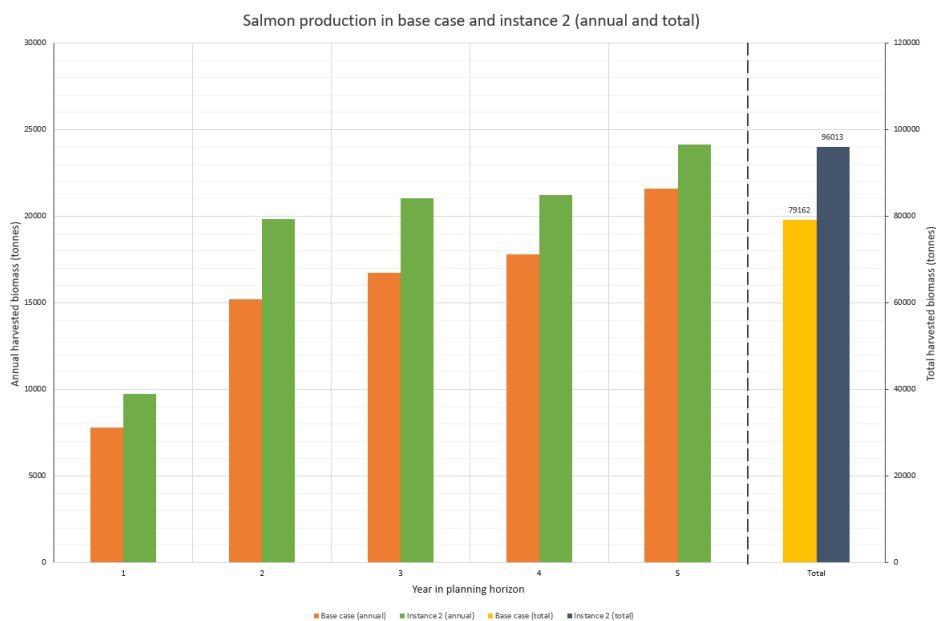


Figure 7.8: Annual and total salmon production from base case and the Instance 2.

The results for the number of harvested salmon during the planning horizon are 22.8 million, in Instance 2, compared to 19.2 million in the base case. The average harvesting weights are 4.2 and 4.1 kilograms, respectively. Hence, the harvesting weights are approximately the same in both cases, but the number of harvested salmon is 18.8 % higher, for Instance 2.

Production plan

The corresponding production plan with all smolt deployments, harvesting periods, and rearing cycles from the results from Instance 2 is shown in Figure 7.9. This figure is similar to the production plan from the base case presented in Figure 7.4. There are two smolt types available for deployment in Instance 2, both monosex and mixed-gender. It can, however, be seen from the black dots in Figure 7.9 that all smolt deployments are chosen to be of monosex smolt type. This is most likely due to the faster growth for the monosex smolt type, which makes it more beneficial to use over mixed-gender smolt. The number of complete rearing cycles within the five-year period is slightly higher than the number in the base case results, with 29 compared to 26 rearing cycles. Furthermore, the average cycle length is shorter, with 15.1 months compared to 17.3 months. The range of the cycle lengths is approximately the same as in the base case, with 15 - 18 months, compared to 15 - 19 months in the base case.

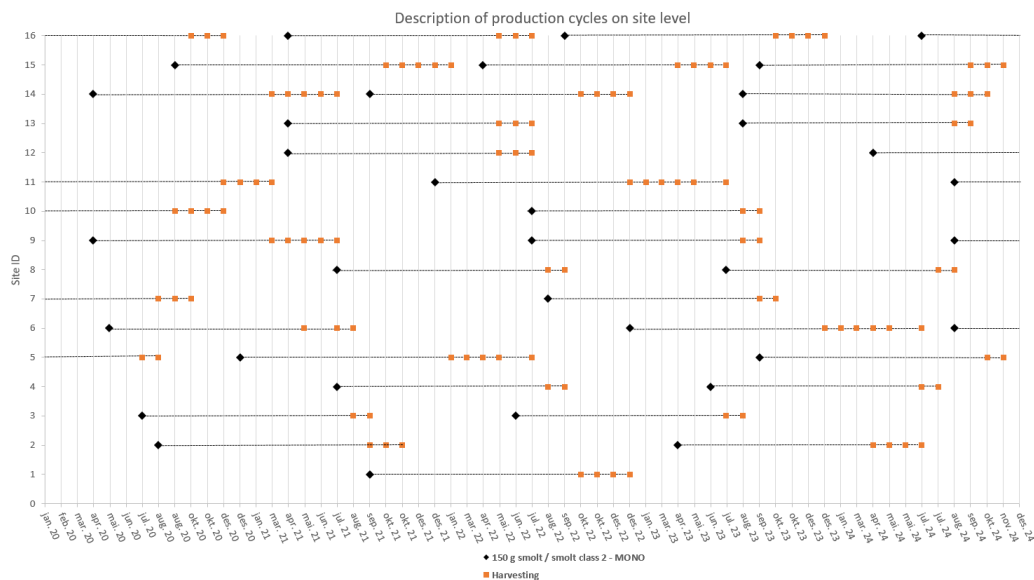


Figure 7.9: Production plan of all smolt deployments and salmon harvesting periods at all production sites from the model run of Instance 2

Contributions to increased production

Overall, the total production level in combination with the length and number of rearing cycles indicates that monosex smolt reaches the same harvesting weight as the mixed-gender smolt over a shorter time period, which causes a shortened length of the rearing cycles. This also leads to more rearing cycles being completed within the planning horizon, and thus a larger amount of salmon is harvested over the five-year period.

7.3.4 Effects of different harvest limits

An overview of the results when using different harvesting weights, meaning Instance 1 - 4, is shown in Table 7.5 and Figure 7.10.

Table 7.5: Computational results from the instances with different harvesting limits

Instance	Harvested biomass (tonnes)	Average weight	Cycle length (average)	Cycle length (min)	Cycle length (max)	No. of rearing cycles
Base case	79 162	4.1 kg	17.3 mo.	15 mo.	19 mo.	25
Instance 1	98 647	3.7 kg	14.7 mo.	13 mo.	19 mo.	29
Instance 2	96 013	4.2 kg	15.1 mo.	14 mo.	18 mo.	29
Instance 3	92 319	4.7 kg	17.4 mo.	15 mo.	21 mo.	26
Instance 4	89 079	5.1 kg	17.3 mo.	15 mo.	21 mo.	25

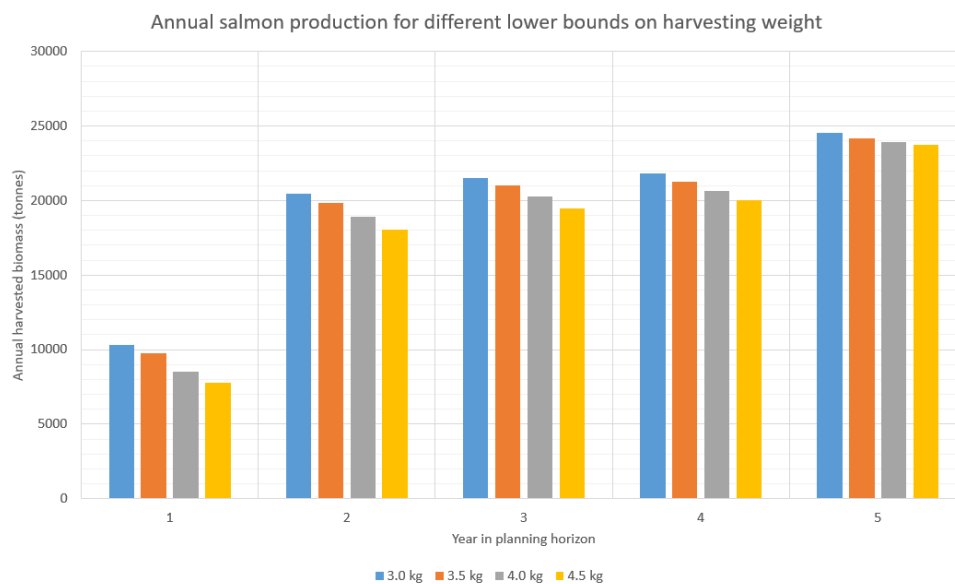


Figure 7.10: Annual salmon production for different lower bounds on harvesting weights.

The objective values for all of the instances are significantly higher than the base case result, due to the option of choosing monosex smolt. Within Instance 1 - 4, however, the amount of harvested biomass decreases in line with the increased lower bound for the harvesting weight. The solution space for the model is getting more limited when the lower bound for harvesting weight increases, which can be a reason for the reduction in harvested biomass. Otherwise, this result suggests that harvesting salmon at lower harvesting weights than current practice is more beneficial in order to maximize harvested biomass. This trend can also be seen in the annual production levels, shown in Figure 7.10. The change in production level from one year to another follows the same annual pattern for all instances, however the size of the columns decreases in line with increased lower bound on harvesting weight.

Table 7.5 shows that the average harvesting weight increases in line with the increase for the lower bound. Furthermore, the total number of harvested salmon decrease from 26.7 million in Instance 1 to 17.4 million in Instance 4. A lower bound for the harvesting weight on 3.0 kilograms enables for harvesting of a large number of small fish, compared to a lower bound on 4.5 kilograms.

The cycle lengths also change in line with the harvesting limit. The cycle lengths are longest for the higher most harvesting limits, in which the fish obviously must grow over a longer time period in order to reach the harvesting limit. Instance 3 and 4 also have the opportunity of having longer cycle lengths due to the increased upper bound for cycle length in these instances. The number of complete rearing cycles within the planning horizon, for Instance 1 and 2 are higher than for Instance 3 and 4, which is related to the shortened cycle length.

7.4 Stochastic study

In this section, we analyze the results from the stochastic version of the model. Firstly, we present how the scenarios are generated, followed by the stochastic instance and the stochastic analysis.

7.4.1 Scenario generation

Calculation of Confidence Interval

When handling an uncertain parameter in stochastic optimization, we need a distribution to draw from, in order to generate scenarios. Due to the limited accessible amount of data, it is necessary to make some assumptions related to the statistical distribution of the seawater temperature. We have chosen to approximate the monthly mean temperature as a normally distributed parameter, as well as applying the central limit theorem (CLT), even though the historical data represents a sample of small size. We calculate the statistical properties, average and variance, of the seawater temperature for each month m and each region r , denoted $\bar{t}_{m,r}$ and $\sigma_{m,r}^2$ as follows

$$\bar{t}_{m,r} = \frac{1}{N_{m,r}} \sum_{i=1}^{N_{m,r}} t_{m,r,i} \quad \sigma_{m,r}^2 = \frac{1}{N_{m,r} - 1} \sum_{i=1}^{N_{m,r}} (t_{m,r,i} - \bar{t}_{m,r})^2$$

Based on this approach, we calculate a confidence interval of varying size from month to month throughout the year, for each region separately. The value of α is for all practical measures set to 0.05. with $z_\alpha := \Phi^{-1}(1 - \alpha) = 1.96$. Further on the confidence interval is calculated as

$$\bar{t}_{m,r} \pm z_\alpha \frac{\sqrt{\sigma_{m,r}^2}}{N_{m,r}}$$

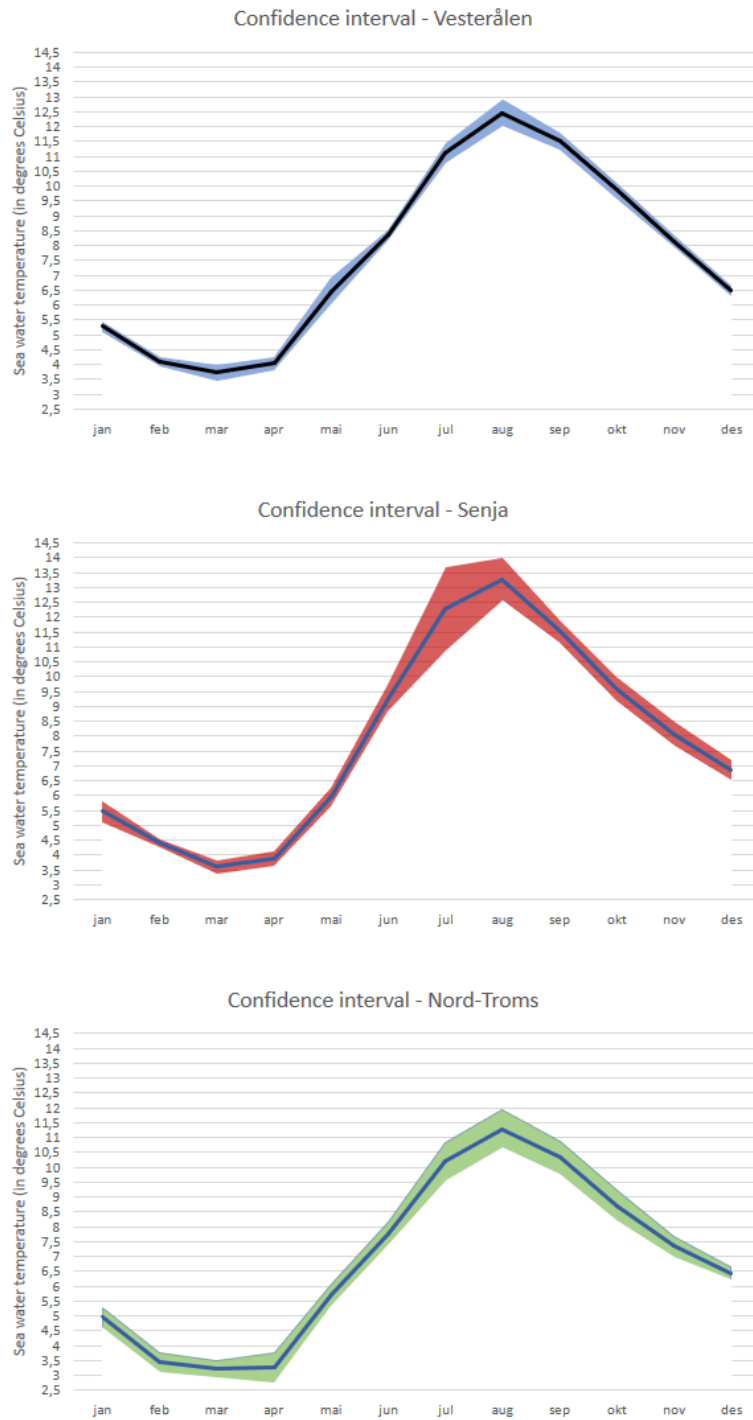


Figure 7.11: Confidence interval of monthly mean temperature for each region, with $\alpha = 0.05$

Method

The plots presented in Figure 7.11 illustrate the variations in seawater temperature for each region, where the calculated confidence intervals are the basis for the scenario generation. The illustrations of the confidence intervals are shown in larger format in Appendix B. The aim of scenario generation is to create a tree structure of scenarios, which is input in the stochastic model (Sutiene and Pranevicius, 2007).

Algorithm 1 Generating temperature scenarios

```

1: function TEMPSCENGEN( $\mu_{r,t}, \sigma_{r,t}, \gamma_y^s$ )
2:   Estimate a norm. dist. CI with  $\alpha = 0.05$ , of avg. temp for region  $r$ , month  $t$ 
3:   for each scenario  $s$  do
4:     for each year  $y$  do
5:       Draw a uniformly distributed number  $\gamma \in [-1.1]$  of type float
6:       for each month  $t$ , each region  $r$  do
7:         Use  $\gamma$  to generate values along the CI for each month  $m$  in year  $y$ , ...
8:         where  $\gamma$  equals 0 correspond to the mean
9:       end for
10:    end for
11:  end for
12: end function

```

In order to initialize the scenario generation, we use a uniform random number generator to simulate random behavior. E.g., in MATLAB the "rand"-function generates a uniform random number in this way. In the algorithm shown above γ represents this random number.

7.4.2 Stochastic instances

The stochastic version of the model is implemented with a set of scenarios $s \in \mathcal{S}$, in which each element s is generated by the method presented above. We must choose the number of scenarios to be sufficiently large in order to obtain a reasonable representation of uncertainty in the model. Thus we plan to use 20 scenarios in the set \mathcal{S} .

The stochastic optimization model is very complex to solve, due to a large number of binary variables in the second-stage decision. When implementing the stochastic model for the full-scale original production system with 16 sites, we see the challenges of obtaining sufficient results after a few test runs. Due to a large number of binary variables placed in the second-stage problem, the model increases in complexity when including scenarios.

In order to reduce the computational strain, we chose to run the stochastic model on a scaled-down production system consisting of 3 production sites, shown in Figure 7.12. In the salmon farming industry, there exist small salmon farming companies which operate

as few as 3 production sites, so this scaled-down production system can also represent real-world case (Fiskeridirektoratet, 2019a). Further down-scaling to less than 3 sites gives a production system that is too small to represent any production system from reality and is thus not very appropriate. In the scaled-down production system, we use all three regions in which Eidsfjord Sjøfarm operates are represented. One of the sites in the selection, Flesen, initially contains biomass in the first period. Thus, we take the initial biomass level at Flesen as input data to the model.

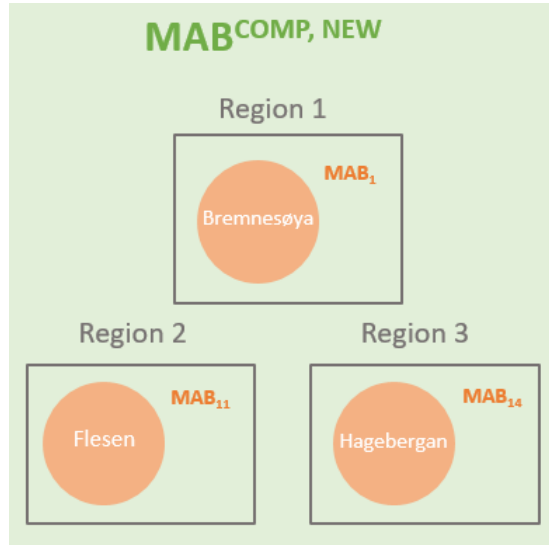


Figure 7.12: Scaled-down production system

For the other parameters in the model, we implement the scaled-down production system with the same parameter settings as in Instance 2, with a lower bound for the harvesting weight on 3.5 kilograms and the option of using monosex smolt included. The only parameter we need to adjust is MAB^{COMP} , which must be down-scaled according to the number of production sites. We set $MAB^{COMP, NEW}$ equal to 2 222 tonnes, which corresponds to the scaling factor of the sum of all the site MABs for the scaled-down system over the sum of the site MABs for each site of the full-scale system.

$$MAB^{COMP, NEW} = MAB^{COMP} \frac{MAB_1 + MAB_{11} + MAB_{14}}{\sum_{i=1}^{16} MAB_i}$$

7.4.3 Deterministic benchmark

We run the deterministic version of the model with the scaled-down instance, in order to obtain a benchmark result for comparison to the results from the stochastic version. The

pre-generated temperature profile for the deterministic instance is randomly generated in the same approach as for the large production system, discussed in Section 7.2. The overall deterministic result is shown in Table 7.6.

Table 7.6: Computational results from the small deterministic instance

Instance	Harvested biomass (tonnes)	Optimality gap	Run time
Small deterministic instance	18 351	1.7 %	43 min

Total harvested biomass is 18 351 tonnes, which corresponds to a decrease of 80.9 % relative to the result from Instance 2. This decrease matches the decrease in company MAB which, for comparison, was reduced with 79.8 %. The distribution of biomass among different rearing cycles, with corresponding smolt deployments and harvesting periods, is shown in Figure 7.13. The number of smolt deployments and complete rearing cycles for each production site over the planning horizon is approximately the same as for the large production system. Hence it seems that the model behaves reasonably relative to industry practice, also for small production systems.

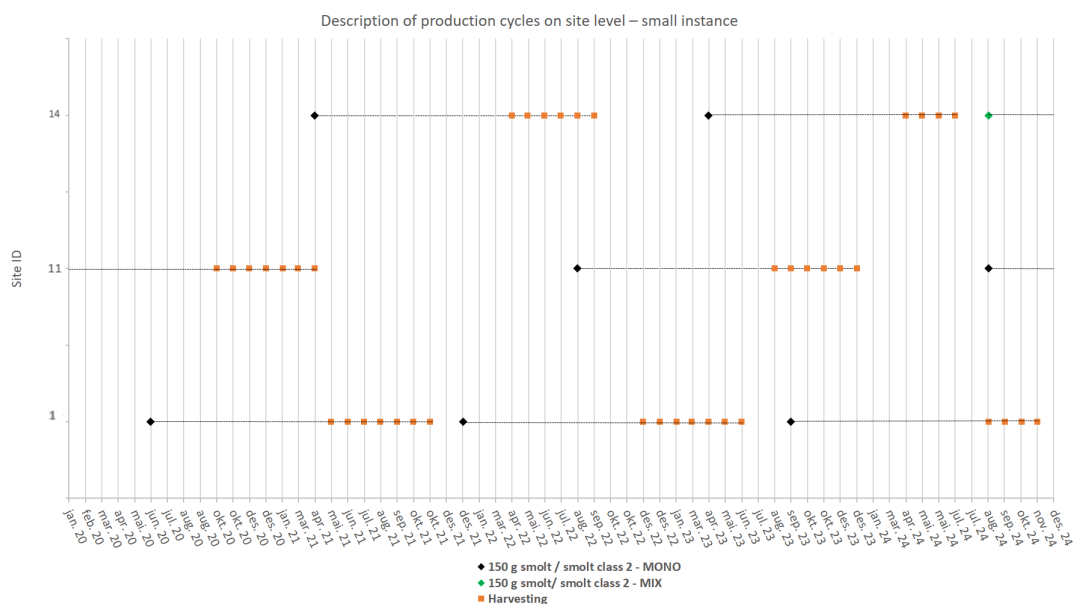


Figure 7.13: Production plan of all smolt deployments and salmon harvesting periods at all production sites from the model run for the down-scaled instance.

7.4.4 Sample Average Approximation

Even when reducing the size of the problem by down-scaling the production system, the two-stage implementation of the model with a sufficient number of scenarios struggles to generate feasible integer solutions due to computational strain. Thus, we use sample average approximation in order to enhance the solvability of the two-stage stochastic implementation of the model. With SAA, we are able to reduce the size of the original problem by sequentially solving it for a smaller set of scenarios (Schütz et al., 2009). In this section, we briefly outline the Sample Average Approximation technique. For a more detailed description of the step-wise procedure, we refer to Santoso (Santoso et al., 2005).

The SAA method

Sample Average Approximation is based on generating samples of size $N < |\mathcal{S}|$ of the uncertain parameters, and subsequently, solve M numbers of SAA problems of the selected sample size N . The SAA problem is based on the sample average function, which is denoted $\frac{1}{N} \sum_{n=1}^N Q(\mathbf{o}, \xi^n)$, whereby $Q(\mathbf{o}, \xi^n)$ represents the solution of the second-stage problem, as we presented in the compact model formulation in Section 5.4. Then, the original problem (5.22)-(5.42) is approximated by the following SAA problem:

$$\max_{\mathbf{o}} \left\{ \hat{f}(\mathbf{o}) = \frac{1}{N} \sum_{n=1}^N Q(\mathbf{o}, \xi^n) \right\}. \quad (7.1)$$

All samples of scenarios $m = 1 \dots M$, each with sample size N , are sampled independently. The expected value for the objective value in sample m is denoted v_N^m . When calculating the average \bar{v}_N^m of all v_N^m , $m = 1 \dots M$, we obtain a statistical upper bound for the original problem, 7.2. We will use this estimator later in the section, along with the corresponding sample variance $\frac{S_{N,M}^2}{M}$, when measuring the accuracy of the solutions later on.

$$\bar{v}_{N,M} = \frac{1}{M} \sum_{m=1}^M v_N^m. \quad (7.2)$$

From the M number of solutions obtained after solving the SAA problems we pick a feasible solution for (5.22)-(5.42), and use the set of first-stage decision variables from this solution for the estimation of the statistical lower bound. In our case, the first-stage decisions are the set of all smolt ordering variables o_{fgz} . We use the values from the first-stage decision variables in the candidate solution we picked, \hat{o} , to fix the first-stage

decision and solve N' number of the original problem. This problem is formulated as follows:

$$\tilde{f}_{N'}(\mathbf{o}) = \frac{1}{N'} \sum_{n=1}^{N'} Q(\mathbf{o}, \xi^n) \quad (7.3)$$

When the first-stage variables are fixed, we obtain reduced complexity, which allows us to solve a large number of single-scenario problems in sequence with relatively short run time. When handling a single realization of ξ^n separately, the problem 7.1 is deterministic and can be solved with appropriate optimization techniques (Santoso et al., 2005). When solving the N' number of the original problem with the fixed first-stage decision, the scenarios are generated independently from the first set of samples used when solving the set of SAA problems 7.1. Thus we generate N' number of scenarios, which will function as a reference sample in order to estimate the lower statistical bound. From the N' evaluations of the candidate solution, we estimate a lower statistical bound by calculating the average, along with the sample variance, $\frac{S_{N'}^2(\hat{o})}{N'}$, which is a part of the gap estimator introduced later on.

Solving the SAA Problems

We choose $N = 5$ and $M = 10$, meaning that we generating 10 independent samples consisting of 5 scenarios which is to be solved. From the model runs we obtain a set of first-stage solutions, \hat{o}^m , which are presented in Table 7.7.

From Table 7.7, we pick the 4th candidate solution ($m = 4$) as our candidate solution \hat{o} , in order to fix the first-stage variable. The statistical lower bound for the objective value of the original problem is estimated by solving problem 7.3. In our computations, we use $N' = 100$ for our reference sample.

Estimator analysis

Once completing the model runs we can, based on the reference sample N' , calculate values for estimators describing the optimality gap between the lower bound, $\tilde{f}_{N'}(\mathbf{o})$, and the true optimal value, denoted v^* , of the original stochastic problem. Due to the difficulties of obtaining v^* , we estimate this by using $\bar{v}_{N,M}$, which is calculated from equation 7.2. Hence, we get the estimator $\bar{v}_{N,M} - \tilde{f}_{N'}(\mathbf{o})$ of the optimality gap, $v^* - \tilde{f}_{N'}(\mathbf{o})$. In this section we analyze the performance and accuracy of the estimators calculated from the solutions of the SAA problems. Considering our max problem, the estimator $\bar{v}_{N,M}$ tends to have a positive bias to the true value v^* . Thus it follows that on average, the gap estimator $\bar{v}_{N,M} - \tilde{f}_{N'}(\mathbf{o})$ overestimates the optimality gap $v^* - \tilde{f}_{N'}(\mathbf{o})$ (Kleywegt et al., 2002). Kleywegt (2002) also refers to two other publications stating that it is possible to show that the bias of the estimator is monotonically decreasing in the sample size N .

Table 7.7: First-stage solutions, $\hat{\delta}^m$ for each of the SAA problem

Candidate solution, m										
Half Year	1		2		3		4		5	
	Mix	Mono	Mix	Mono	Mix	Mono	Mix	Mono	Mix	Mono
1	0	0	0	0	0	0	0	0	0	512.7
2	0	543.3	0	554.6	0	540.8	0	506.4	0	0
3	0	517.0	0	522.1	0	514.5	0	640.4	0	506.2
4	0	504.2	0	504.8	0	502.7	0	0	0	501.0
5	0	0	0	0	0	0	0	633.8	0	0
6	0	509.6	0	535.8	0	535.8	0	0	0	555.5
7	0	500.0	0	500.0	0	513.7	0	506.8	0	500.0
8	0	538.4	0	547.8	0	500.0	0	507.4	0	524.8
9	0	0	0	0	0	0	0	0	0	0
10	540.5	1200.0	540.5	1200.0	500.0	1096.5	500.0	1187.0	500.0	1159.0

Candidate solution, m										
Half Year	6		7		8		9		10	
	Mix	Mono	Mix	Mono	Mix	Mono	Mix	Mono	Mix	Mono
1	0	0	0	0	0	0	0	515.3	0	512.7
2	0	500.0	0	535.1	0	551.0	0	0	0	0
3	0	617.7	0	606.5	0	686.7	0	636.2	0	512.1
4	0	0	0	0	0	0	0	0	0	513.8
5	0	606.1	0	502.9	0	609.1	0	627.7	0	0
6	0	0	0	503.1	0	0	0	0	0	503.6
7	0	500.0	0	503.6	0	500.0	0	500.0	0	500.0
8	0	569.0	0	513.4	0	592.1	0	573.6	0	544.4
9	0	0	0	0	0	0	0	0	0	0
10	501.5	1200.0	858.7	975.8	635.8	1118.0	500.0	1199.9	582.4	1200.0

In addition, it is useful considering the accuracy of the estimators represented as a confidence interval for the gap estimator, $\bar{v}_{N,M} - \tilde{f}_{N'}(\mathbf{o})$. By ensuring that the two respectively set of samples, the M number of N realizations of the uncertain parameter ξ^1, \dots, ξ^N and the reference sample N , are generated independently, the variance of the gap estimator can be estimated by $\left(\frac{S_{N'}^2(\hat{\delta})}{N'} + \frac{S_{N,M}^2}{M}\right)$. Thus, to account for accuracy, we can add a multiple z_α of the estimated gap variance term to the gap estimator. Here, z_α is the value of the inverse cdf. of the standard normal distribution evaluated on $(1 - \alpha)$

$$(\bar{v}_{N,M} - \tilde{f}_{N'}(\mathbf{o})) + z_\alpha \left(\frac{S_{N'}^2(\hat{\delta})}{N'} + \frac{S_{N,M}^2}{M}\right)^{\frac{1}{2}}$$

Where the variance terms is calculated by:

$$\frac{S_{N,M}^2}{M} = \frac{1}{(M-1)M} \sum_{m=1}^M \left((v_N^m - \bar{v}_{N,M}) \right)^2 \quad \frac{S_{N'}^2(\hat{o})}{N'} = \frac{1}{(N'-1)N'} \sum_{n=1}^{N'} \left(Q(\hat{o}, \xi^n) - \tilde{f}_{N'}(\mathbf{o}) \right)^2$$

The results from the SAA is shown in Table 7.8. The statistical upper and lower bounds for the stochastic solution are 17 291 and 17 697, respectively, which implies that the value of the optimality gap estimator, $\bar{v}_{N,M} - \tilde{f}_{N'}(\mathbf{o})$, is 405.8. When including the accuracy term for the gap estimator, the results are presented as confidence intervals $\alpha = 0.05$ and $\alpha = 0.10$, in Table 7.9.

Table 7.8: Statistical lower bound and upper bound

M	N'	N	Lower bound		Upper bound	
			average	σ_{LB}	average	σ_{UB}
10	100	5	17291.66	18.25	17697.5	145.52

Table 7.9: Estimated optimality gap and confidence interval with $\alpha = 0.05$ and $\alpha = 0.10$

1 - α	Estimated optimality gap			Confidence Interval (CI)			
	Gap (abs)	Gap (%)	(σ_{gap})	min	%	max	%
95% CI	405.84	2.29%	146.65	118.39	0.67 %	693.29	3.92 %
90% CI	405.84	2.29%	146.65	164.60	0.93 %	647.07	3.66 %

Discussion of the SAA analysis

When running some tests on the down-scaled instance, described in Figure 7.12, we conclude with using $N = 5$ for our set of SAA problems. Compared to other cases of a similar size, for instance those described in (Schütz et al., 2009), using $N = 5$ is a small number. With this method the decided size of the SAA problems, picking $N = 5$ is a trade-off between how much computational effort needed, considering run time, on the one hand, and on the other hand, the quality of the solution obtained. Depending on the specific SAA problem, the computational complexity for solving the SAA problem increases at least linearly, and often exponentially, in the sample size N (Kleywegt et al., 2002). In addition it should be accounted, the perspective of decreasing bias for the estimator $\bar{v}_{N,M}$ in the sample size N .

However, the calculation of our optimality gap estimator, accounting for accuracy, points to the computations of our estimators of the objective value being with in an acceptable range of what we

For our specific case, when solving SAA problems in order to generate sets of feasible first-stage solutions \mathbf{o} , we encounter problems when evaluating the candidate solutions

$\hat{\delta}^m$ on the N' number of scenarios of the reference sample. None of the 10 candidate solutions fulfill the requirement of being feasible for the complete set of second-stage problem evaluated on a reference sample, N' . However, when evaluating the candidate solution $N = 4$, 91 runs out of 100 returned feasible. This is partly due to the nature of our model formulation, where rather soft requirements are considered less flexible. E.g., constraint 5.30-5.31, combined with 5.35-5.36 is rather strict, given the mechanisms where the maximum cycle length is imposed on a site where the smallest fish in the population are not yet considered as harvestable, for the given time period. This sequence of solutions is presented in Appendix, A.0.2.

In order to demonstrate, we computed the sequence of N' model runs on the same reference sample, given the first-stage variable fixed to the same candidate solution, with an increase in cycle length limit from 19 months to 21. The modification in cycle length limit reduce the number of infeasible cases returned from 9 to only 2. In addition due to the nature of our problem, solving the optimization model with the continuous first-stage variable \mathbf{o} fixed to $\hat{\delta}^m$ is numerical challenging for any State-of-the-art Solver, including Xpress Optimizer. In order to handle this, we approximate the fixation by allowing the decision variable to take values within a small interval of size ± 2 . E.g. given that the original decision variable was set to 436.09, the interval used would be [435, 438]. Considering the interval being sufficiently small, one can argue that the solution of both the problem being the same given the approximation of the first-stage fixing.

With the uncertain parameter of our problem being the seawater temperature for each region, the MAB constraint will function as a sort of risk constraint. For all samples, the ordered level of smolt, represented by the first-stage variable, must comply with the varying growth conditions across the scenario sample in order to stay on the allowed side of the MAB limit. With the sample size $N = 5$ being relatively small, the infeasibility issues that are encountered can be explained due to the limited set of scenarios comprising the SAA problem. One way of complying with these issues could, for instance, be a multi-objective approach or a chance-constraint formulation where a small fraction of second-stage evaluations is allowed to return infeasible.

7.4.5 Effects of uncertainty

The expected value of perfect information is defined as follows (Birge and Louveaux, 2011):

$$EVPI = WS - RP$$

We define the solution found by the two-stage stochastic model as the here-and-now solution, defined as the recourse problem (RP). In our case, the interval of upper and lower bounds for the objective value estimated with the sample average approximation

approach represents the value of the recourse problem. The wait and see solution (WS) is found by solving the model with perfect information available. We do this by implementing the stochastic model with only one scenario, which is similar to a deterministic implementation, and perform multiple sequential runs of the stochastic model using different realizations of the scenario. We calculate the average of all the resulting objective values, in order to obtain an expected value for the wait and see solution.

The objective value obtained with perfect information in the wait-and-see approach is 18 455 tonnes. The estimated upper and lower bounds for the objective value obtained from the SAA approach is 17 291 - 17 697 tonnes. This indicates that the value of perfect information (EVPI) is at least 758 tonnes, which corresponds to a decrease of 4.2 % in the difference from perfect information down to the upper bound for the stochastic approach.

Ideally, we would also have estimated the VSS in order to obtain the value of the stochastic solution of the model compared to the deterministic solution. We have not obtained any number to quantify this value, due to the struggle in finding a feasible first-stage solution $\hat{\delta}^m$ for all second-stage solutions. However, by studying the stochastic results we see that the objective value is significantly lower than the deterministic results. This indicates that the strict regulatory requirements, such as the MAB constraints, which cannot be broken under any circumstances, lead to a more risk-averse approach to the production level when planning with uncertainty, thereby smolt ordering and smolt deployments, in order to comply with the regulations.

8. Concluding Remarks

The purpose of this thesis is to analyze whether there is an opportunity to increase biomass production and thus obtain better exploitation of the existing salmon farming licenses, by including the option of deploying monosex smolt, in addition to traditional mixed-gender smolt. The problem scope embraces a five-year planning horizon, in which smolt ordering, smolt deployment, and harvesting of salmon must be planned for. We have developed a two-stage stochastic optimization model that considers a production system consisting of multiple production sites subject to regulatory requirements and capacity constraints. The model considers uncertainty in biomass development. A perfect representation of reality is impossible; hence we make some simplifications when developing the model. The model is implemented with Eidsfjord Sjøfarm's production system, and seawater temperature is used as a driver for uncertainty in biomass development. Other input parameters in the model are represented with deterministic values.

The model is implemented in two versions, a deterministic and a stochastic version, and the output results from both versions are analyzed. A comparison of the deterministic results to reality shows that the model gives reasonable results. The model results indicate an annual average production on 15 832 tonnes, which represents 7.1 % increase compared to reality. The increase is due to the production of a larger number of salmon over five years, and the results indicate that shorter cycle lengths (2-3 months) and a lowered harvesting weight is beneficial in order to increase biomass production. When the option for deploying monosex smolt is included, the average annual output is increased to 19 203 tonnes, which is 21.3 % more than the results from solely using mixed-gender smolt. The results indicate that it is beneficial to choose monosex smolts for all smolt deployments in order to maximize biomass production. The growth in output is due to faster growth for monosex smolt, which causes more rearing cycles of shorter lengths in average to be completed, and thus an increased number of salmon is harvested over a five-year period.

The results from the stochastic implementation of the model indicate that growth uncertainty has a significant impact on the production level. A sample average approach to the stochastic solution indicates 4.2 % lower production level compared to using a deterministic version. The strict regulatory requirements cannot be broken under any circumstances, which implies a more risk-averse approach to production planning when including uncertainty.

9. Future Research

Our modelling approach for the extensive site management of the production system causes a computational strain that exceeds the tolerance when implementing the stochastic version of the model for the full-scale instance. A domain for future work is improving the model, or develop a solution method, in order to make it solvable for larger instances. A decomposition-approach might be useful in order to maintain the portfolio aspect while solving several smaller problems in parallel. Additionally, the run time for the stochastic version is long, and shortening the run time, by applying a speed-up technique, is beneficial to make the model more useful.

The mathematical method we use to represent growth in our model is based on an algorithm firstly developed by Hæreid (2011) and use growth rates based on Skretting (2011) as input. In reality, salmon farming companies have their own methods for growth modelling, which are not publicly available. Implementing Eidsfjord Sjøfarm's method of growth modelling will make the model more reality-like.

The production systems are only considered at site level. An extension that includes net pens will provide a more accurate representation of the production system. Furthermore, smolt deployments are simplified to consist of just one smolt type, which might be extended to include the opportunity to deploy several smolt types per deployment (size and gender-sorting).

In this thesis, we analyze the production level and maximization of harvested biomass. Profit maximization and cost consideration is another approach that could be analyzed. We assume no additional restrictions or costs by using the monosex smolt type. In reality, however, producing the monosex smolt type is more resource-intensive than unsorted smolt.

Regarding the salmon farming value chain, the inclusion of the freshwater part of production or the slaughtering process could provide another perspective than solely studying seawater production. We account for growth uncertainty in this thesis. However, there also are sources to uncertainty present in terms of loss in production which could be implemented, for instance, the risk for a disease outbreak or treatment for sea lice.

Bibliography

- AquaGen (2018a). *Data recieved from AquaGen*. Contact: Ingun Næve.
- AquaGen (2018b). *Interview with Ingun Næve, Nina Santi, Roger Oddebug og Vibeke Emilsen*.
- Asche, F. and T. Bjørndal (2011). *The Economics of Salmon Aquaculture*. Wiley-Blackwell.
- Aunsmo, A. (2014). “Field validation of growth models used in Atlantic salmon farming”. In: *Aquaculture*.
- Birge, J. and F. Louveaux (2011). *Introduction to stochastic programming (second edition)*. Springer.
- Bitran, G. and D. Tirupati (1993). “Hierarchical Production Planning”. In: *Aquaculture*.
- Bjørndal, T. (1988). “Optimal Harvesting of Farmed Fish”. In: *Marine Resource Economics*, Vol 5: 139-159.
- Bravo, F. et al. (2013). “Mathematical models for optimizing production chain planning in salmon farming”. In: *International transactions in operational research*.
- Denstad, A., M. Lillevand, and E. Ulsund (2015). “Production planning and sales allocation in the salmon farming industry”. master’s thesis. NTNU.
- Eidsfjord Sjøfarm (2018). *Interview with Rolf-Arne Reinholdtsen*.
- Eidsfjord Sjøfarm (2019). *Data recieved from Eidsfjord Sjøfarm*. Contact: Rolf-Arne Reinholdtsen.
- Fiskeridirektoratet (2016). *Drift- og tilsyn av akvakultur*. URL: <https://www.fiskeridir.no/Akvakultur/Drift-og-tilsyn/Biomasse>.
- Fiskeridirektoratet (2017). *Lønnsomhetsundersøkelse for matfiskproduksjon*. URL: <https://www.fiskeridir.no/Akvakultur/Statistikk-akvakultur/Loennsomhetsundersoekelse-for-laks-og-regnbueoerret/Matfiskproduksjon-laks-og-regnbueoerret>.

- Fiskeridirektoratet (2018). *Settefisk*. URL: <https://www.fiskeridir.no/Akvakultur/Tildeling-og-tillatelser/Kommersielle-tillatelser/Laks-oerret-og-regnbueoerret/Settefisk>.
- Fiskeridirektoratet (2019a). *Akvakulturregisteret*. URL: <https://www.fiskeridir.no/Akvakultur/Registre-og-skjema/Akvakulturregisteret>.
- Fiskeridirektoratet (2019b). *Rømmingsstatistikk*. URL: <https://www.fiskeridir.no/Akvakultur/Statistikk-akvakultur/Roemmingsstatistikk>.
- Fiskeridirektoratet (2019c). *Tap i matfiskproduksjon 1997 - 2017*. URL: <https://www.fiskeridir.no/Akvakultur/Statistikk-akvakultur/Akvakulturstatistikk-tidsserier/Laks-regnbueoerret-og-oerret>.
- Food and Agriculture Organization of the United Nations (2018). *The state of the world fisheries and aquaculture 2018 - Meeting the sustainable development goals*. Rome.
- Food and Agriculture Organization of the United Nations (2019). *Salmo salar (Linnaeus, 1758)*. URL: http://www.fao.org/fishery/culturedspecies/Salmo_salar/en.
- Forsberg, O. (1999). "Optimal harvesting of farmed Atlantic salmon at two cohort management strategies and different harvest operation restriction". In: *Aquaculture Economics Management*, 3:2 (143-158).
- Hæreid, M. et al. (2013). "A Stochastic Programming Model for Optimizing the Production of Farmed Atlantic Salmon". In: *Stochastic programming - Applications in Finance, Energy, Planning and Logistics*.
- Hean, R. (1994). "An optimal management model for intensive aquaculture - An application in Atlantic salmon". In: *Australian Journal of Agricultural Economics*.
- Hjeltnes, B. et al. (2019). *The Health Situation in Norwegian Aquaculture 2018*. Norwegian Veterinary Institute 2019.
- Holmøy Maritime (2018). *Eidsfjord Sjøfarm AS*. URL: <http://prestfjord.no/selskaper/eidsfjord-sjofarm-as/>.
- Kleywegt, A. et al. (2002). "The Sample Average Approximation Method for Stochastic Discrete Optimization." In: *Siam Journal On Optimization* 12(2).
- Laird, L.M. (2001). "Salmonid Farming". In: *Encyclopedia of Ocean Sciences*.
- Lillestøl, J. (1986). "On the problem of optimal timing of slaughtering in fish farming". In: *Modeling, Identification and Control*, 7:199–207.

- Liu, Y. et al. (2010). “Wild and farmed salmon in Norway — A review”. In: *Marine Policy*.
- Marine Harvest (2018). *Salmon Farming Industry Handbook*.
- Nærings- og fiskeridepartementet (2018a). *Forskrift om bekjempelse av lakselus i akvakulturanlegg*. URL: <https://lovdata.no/dokument/SF/forskrift/2012-12-05-1140>.
- Nærings- og fiskeridepartementet (2018b). *Forskrift om drift av akvakulturanlegg*. URL: <https://lovdata.no/dokument/SF/forskrift/2008-06-17-822>.
- Nordgarden, U. et al. (2003). “Seasonally changing metabolism in Atlantic salmon (*salmo salar* L.) - Growth and feed conversion ratio”. In: *Aquaculture Nutrition*, pp. 9, 287–293.
- Pascoe, S. et al. (2002). *Optimal harvesting strategies: practice versus theory*. Centre for the Economics and Management of Aquatic Resources, University of Portsmouth.
- Santoso, T. et al. (2005). “A stochastic programming approach for supply chain network design under uncertainty”. In: *European Journal of Operational Research* 167.
- Schütz, P. et al. (2009). “Supply Chain Design under Uncertainty Using Sample Average Approximation and Dual Decomposition.” In: *European Journal of Operational Research* 199.2.
- Skretting (2011). *Fiskeføde*.
- Statistisk sentralbyrå (2017). *Akvakultur. Antall tillatelser i drift*. URL: <https://www.ssb.no/statbank/table/08967/>.
- Stikholmen, N. (2010). “Produktivitetsutvikling over tid i oppdrett av laks - En studie av perioden 2001 til 2008 med bruk av DEA og Malmquistindeks”. master’s thesis. Univeristy in Tromsø.
- Sutiene, H. and H. Pranevicius (2007). “Scenario Generation Employing Copulas”. In: *Proceedings of the World Congress on Engineering 2007 Vol II*.
- Thorarensen, H. and A. Farrell (2010). “The biological requirements for post-smolt atlantic salmon in closed-containment systems”. In: *Aquaculture*, 312(1-4):1-14.
- Torgersen, T. et al. (2009). “Hvordan takler laksen varierende merdmiljøforhold?” In: *Kyst og havbruk 2009*.

A. Appendix A - Results from the SAA analysis

A.0.1 SAA results

Table A.1: Objective value v_N^m with corresponding optimality gap and Run time for each solution of the SAA problems

m	N	Objective value, v_N^m	Optimality gap (%)	Run Time (s)
1	5	18079.78	1.0 %	391146
2	5	18151.06	1.1 %	303483
3	5	17718.82	8.2 %	234807
4	5	17190.62	9.9 %	128176
5	5	18177.28	1.0 %	445088
6	5	16999.62	12.7 %	128897
7	5	18088.8	3.2 %	519125
8	5	17424.54	3.9 %	256149
9	5	17172	15.6 %	134743
10	5	17972.48	3.8 %	123484

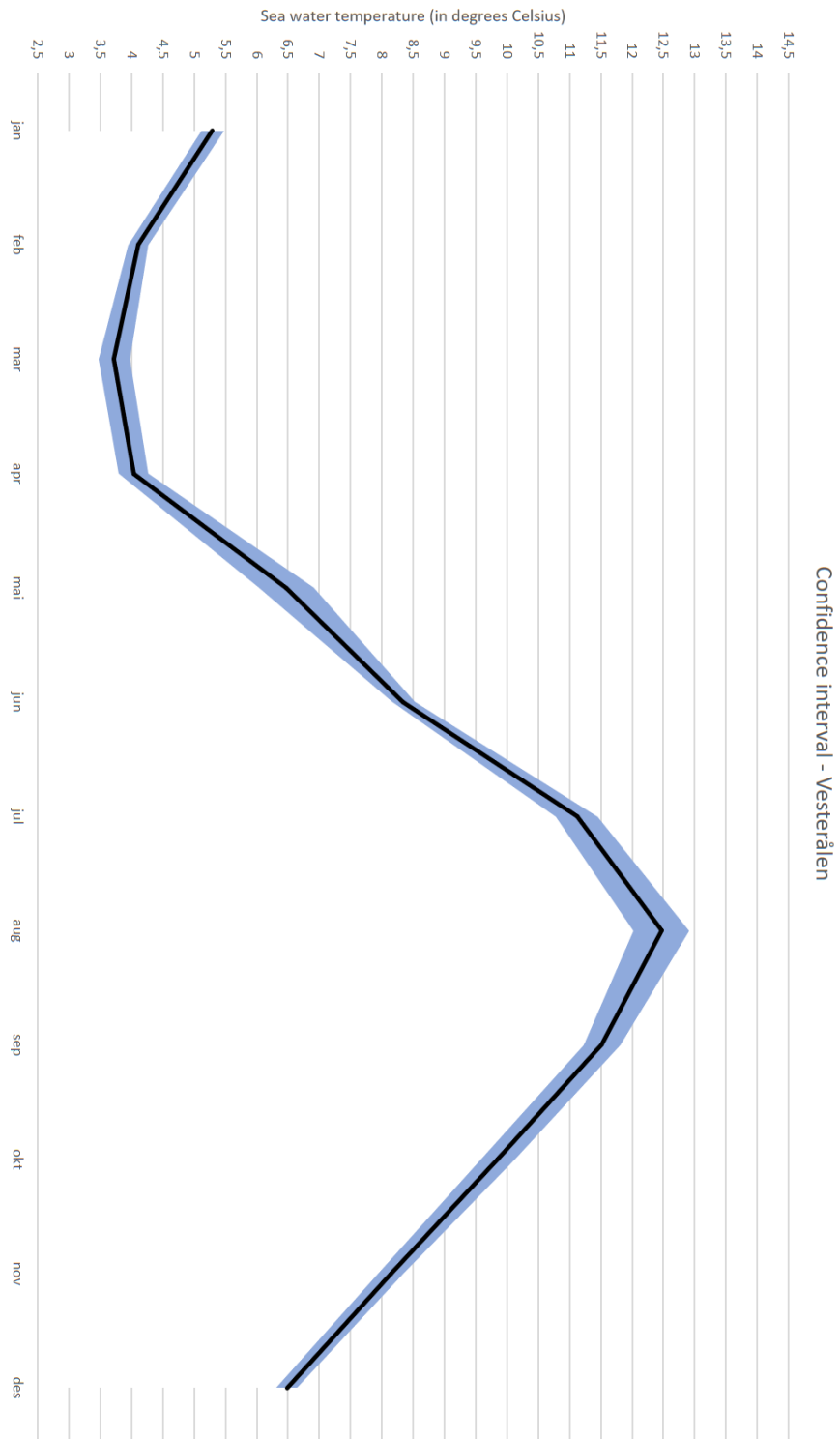
A.0.2 Evaluation results for candidate solution

Results from the model runs on the reference sample (N' = 100)
for estimating the lower bound in the SAA - analysis (Section 7.4.3)

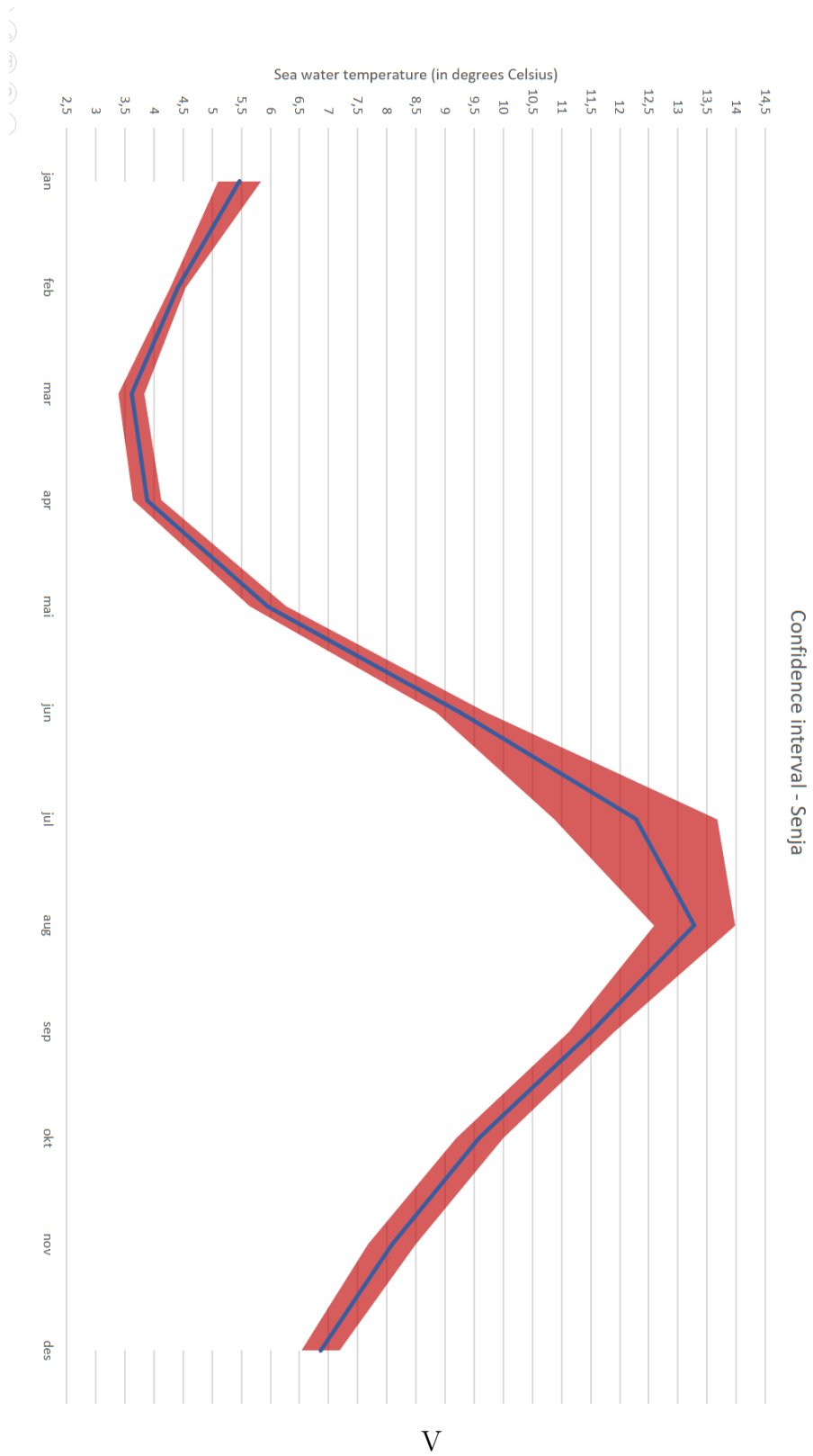
ID/ Scen #	OBJVAL	GAP	Probst	RUNTIME	ID / Scen #	OBJVAL	GAP	Probst	RUNTIME
1	17287,8	0,01695	2Optimum	100,479	55	17433,4	0,018548	2Optimum	137,903
2	17312,4	0,019998	2Optimum	146,153	56	16745,8	0,019597	2Optimum	113,238
3	17244,6	0,01006	2Optimum	138,95	57	17084,1	0,017251	2Optimum	111,02
4	17222,7	0,017701	2Optimum	173,966	59	16979	0,017578	2Optimum	143,831
5	17262,5	0,019362	2Optimum	133,686	60	17349,5	0,019213	2Optimum	124,384
6	17151,5	0,019837	2Optimum	115,935	61	17236,8	0,016916	2Optimum	81,232
7	17242,4	0,019369	2Optimum	125,967	62	17251,7	0,012633	2Optimum	129,902
8	17504	0,019034	2Optimum	113,761	63	17441,2	0,013615	2Optimum	101,946
9	17473,1	0,005067	2Optimum	98,066	64	17203,8	0,01994	2Optimum	129,394
10	17313,4	0,019366	2Optimum	104,926	65	17543,2	0,011015	2Optimum	88,593
11	17225	0,01951	2Optimum	124,904	66	17164,1	0,004813	2Optimum	115,792
13	17280,5	0,019717	2Optimum	87,151	67	17406,8	0,019057	2Optimum	57,98
14	16820,8	0,019636	2Optimum	119,091	68	17332,9	0,019712	2Optimum	83,947
15	17224,2	0,018543	2Optimum	130,932	69	17327,2	0,01335	2Optimum	77,945
16	17031,5	0,015589	2Optimum	113,889	70	17205,1	0,01971	2Optimum	121,836
17	16926,5	0,019763	2Optimum	384,818	71	17019,4	0,019732	2Optimum	91,025
19	17095,1	0,013743	2Optimum	102,339	72	17315,6	0,018471	2Optimum	104,944
20	17274,8	0,019464	2Optimum	72,658	74	17374,7	0,017899	2Optimum	134,688
21	17212,2	0,011294	2Optimum	103,854	75	17202,1	0,01939	2Optimum	94,315
22	17206,7	0,019524	2Optimum	109,673	76	17316,3	0,014734	2Optimum	131,998
23	17173,3	0,019855	2Optimum	98,273	77	17282,1	0,017324	2Optimum	77,751
24	17372,3	0,019922	2Optimum	162,411	79	17340,4	0,015704	2Optimum	124,781
25	17385,2	0,019695	2Optimum	132,224	80	17179,6	0,016917	2Optimum	100,979
27	17412,7	0,016913	2Optimum	153,474	81	17407,3	0,018458	2Optimum	108,566
28	17534,5	0,019391	2Optimum	90,36	82	17339,3	0,018627	2Optimum	91,674
29	17620,3	0,016351	2Optimum	98,552	83	17120,4	0,01995	2Optimum	106,526
30	17405,9	0,017241	2Optimum	110,255	84	17203,7	0,019543	2Optimum	86,434
31	17392,8	0,018813	2Optimum	103,985	86	17225,1	0,015171	2Optimum	118,956
32	17359,6	0,019814	2Optimum	92,69	87	17408,4	0,018853	2Optimum	142,785
33	17292,5	0,0193	2Optimum	139,571	89	17536,7	0,014516	2Optimum	100,119
34	17311,9	0,004111	2Optimum	125,135	90	17275,3	0,019355	2Optimum	90,312
35	17352,7	0,016606	2Optimum	97,919	91	16825,4	0,01954	2Optimum	134,373
36	17397,4	0,017343	2Optimum	120,402	92	17481	0,01579	2Optimum	139,072
37	17082,2	0,011555	2Optimum	102,179	93	17351,6	0,01983	2Optimum	87,996
38	17684,6	0,018558	2Optimum	88,177	94	17145,2	0,017306	2Optimum	112,757
39	17285,8	0,018461	2Optimum	125,2	95	17428,9	0,015582	2Optimum	66,072
40	17552,7	0,019269	2Optimum	107,851	96	17270,7	0,017389	2Optimum	105,576
41	17066,2	0,001022	2Optimum	138,788	97	16891,5	0,006418	2Optimum	133,084
42	17476,9	0,019166	2Optimum	95,335	98	17239,7	0,019892	2Optimum	112,11
44	17301,9	0,016776	2Optimum	133,861	99	17408,6	0,018257	2Optimum	70,717
45	17350,3	0,019235	2Optimum	99,016	100	17275,9	0,016699	2Optimum	117,335
46	17552,3	0,014168	2Optimum	78,795	12	-1,00E+40	0	6Infeasible	110,819
47	17401,4	0,009651	2Optimum	93,054	18	-1,00E+40	0	6Infeasible	108,684
48	17322,9	0,016555	2Optimum	141,36	26	-1,00E+40	0	6Infeasible	82,655
49	17380	0,019733	2Optimum	133,504	43	-1,00E+40	0	6Infeasible	223,263
50	17443,1	0,019677	2Optimum	75,301	58	-1,00E+40	0	6Infeasible	121,264
51	17509,7	0,018746	2Optimum	100,897	73	-1,00E+40	0	6Infeasible	144,677
52	17329,7	0,01446	2Optimum	80,646	78	-1,00E+40	0	6Infeasible	100,179
53	17464,7	0,019519	2Optimum	78,733	85	-1,00E+40	0	6Infeasible	70,307
54	17444,5	0,018994	2Optimum	83,006	88	-1,00E+40	0	6Infeasible	87,624

**B. Appendix B Confidence interval
in seawater temperature for each
region**

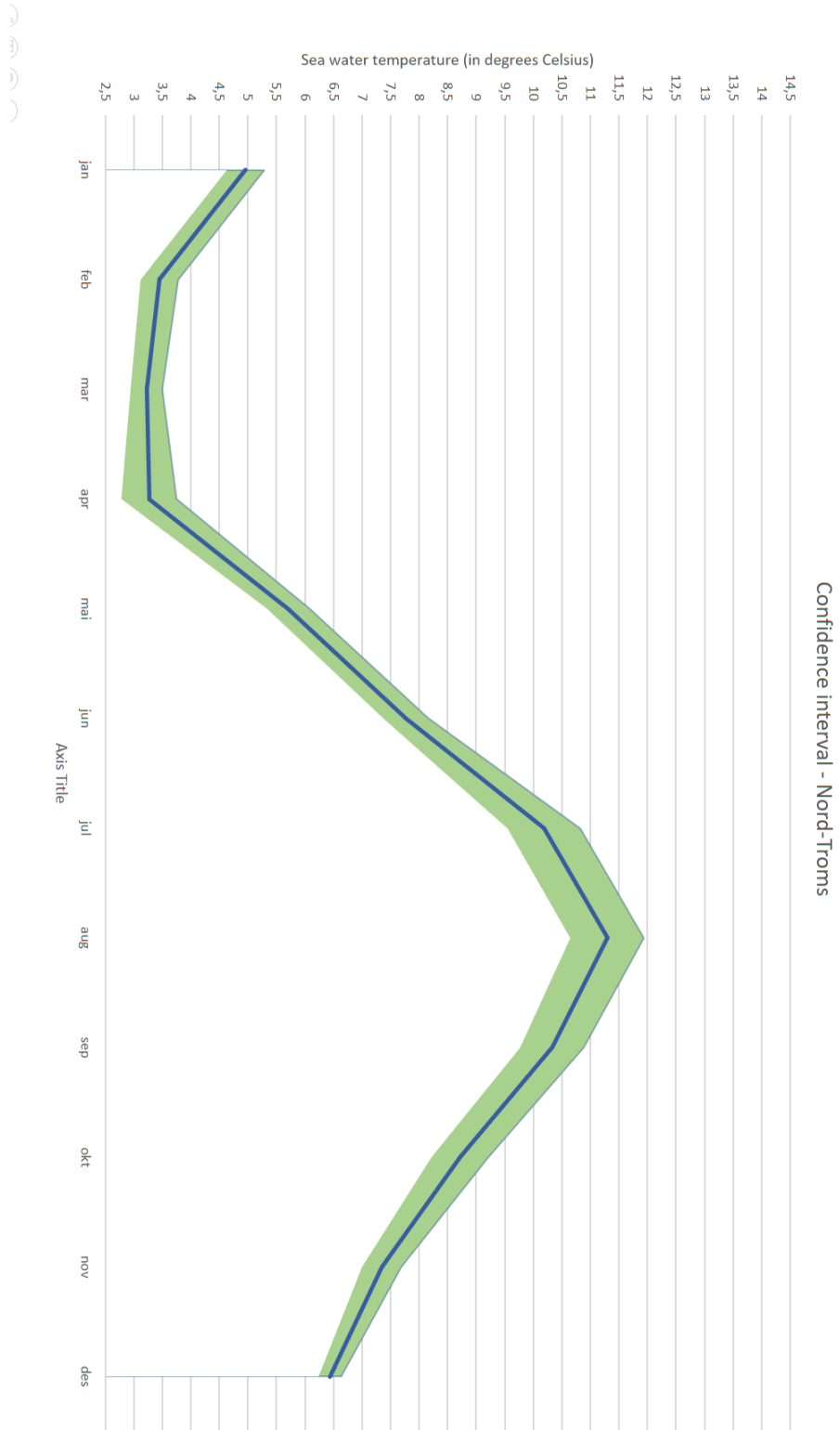
B.0.1 Vesterålen



B.0.2 Senja



B.0.3 Nord-Troms



C. Appendix C Growth Tables

C.0.1 Monthly growth rates for mixed-gender salmon

C.0.2 Monthly growth rates for monosex salmon

